HEINRICH HEINE
UNIVERSITÄT DÜSSELDORF

Novel insight into G-protein mediated cellular signaling in endothelial biology and chronobiology

Inaugural-Dissertation

zur Erlangung des Doktorgrades
der Mathematisch-Naturwissenschaftlichen Fakultät
der Heinrich-Heine Universität Düsseldorf
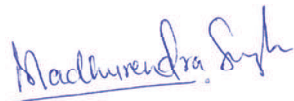
vorgelegt von
MADHURENDRA SINGH
aus Gorakhpur, Indien

aus dem Institut für

Biochemie und Molekularbiologie II

der Heinrich-Heine Universität Düsseldorf

Eidesstattliche Erklärung

Hiermit erkläre ich an Eides statt, dass ich die hier vorgelegte Dissertation eigenständig und ohne unerlaubte Hilfe angefertigt habe. Es wurden keinerlei andere Quellen und Hilfsmittel, außer den angegebenen, benutzt. Zitate aus anderen Arbeiten wurden kenntlich gemacht. Diese Dissertation wurde in der vorgelegten oder einer ähnlichen Form noch bei keiner anderen Institution eingereicht und es wurden bisher keine erfolglosen Promotionsversuche von mir unternommen.

Düsseldorf, Juni 2014

Madhurendra Singh

Table of Contents

Table of Figures

1. INTRODUCTION

1.1 Basic principles and mechanisms of signal transduction

Cells are the fundamental units of an organism. Multicellular organisms contain billions of cells arranged in a well structured manner, respond to various stimuli, and transduce and process the information in an orchestral manner. The nature of stimuli can be categorized into two groups: lipophilic stimuli, which cross the plasma membrane and bind directly to intracellular receptors, and hydrophilic stimuli, which bind to transmembrane receptors.
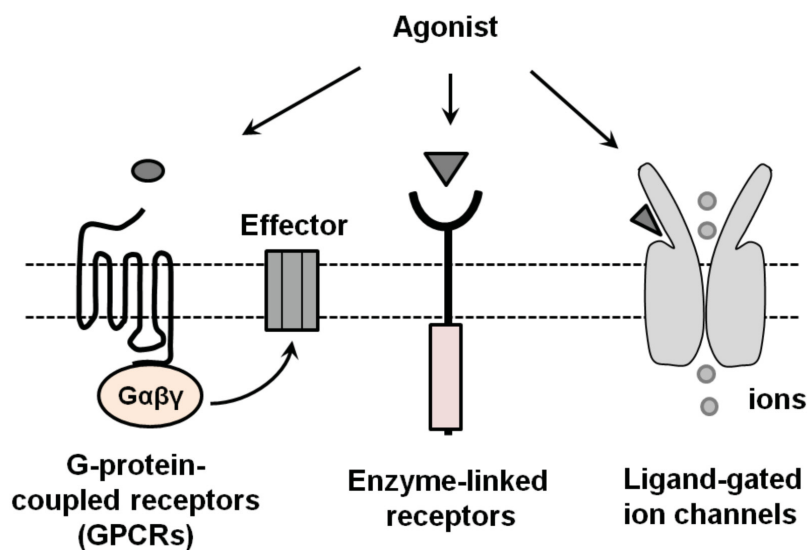
Figure 1: General principles of signal transduction through transmembrane receptors. Ligand binding to the extracellular domains of the receptors (G-protein coupled receptors, enzyme-coupled receptors, and ligand-gated ion channels) induces intracellular processes.

Transmembrane signaling requires two basic elements transmembrane receptors and effectors molecules. Transmembrane receptors bind to various extracellular stimuli like organic odorants, small molecules including amino acids, nucleosides, nucleotides, peptides, as well as proteins, lipids and fatty acid mediators and thereby transduce the signal into the cell using effector molecules (Hermans, 2003). Transmembrane receptors and effectors play an important role in cell communication and coordinate various physiological processes (Bockaert et al., 1999; Severin et al., 2011). On the basis of signal transduction, transmembrane receptors can be divided into (1) G-protein-coupled receptors, (2), enzyme-linked receptors (3), and ligand-gated ion channels (Figure 1).

(1) G-protein-coupled receptors (GPCRs) comprise the largest family of cell-surface receptors that are involved in multiple cellular processes in eukaryotes (Nürnberg, 2004;

Tadevosyan et al., 2012). Interestingly, more than 1000 GPCRs are encoded by mammalian genomes. The majority of GPCRs in mammals belongs to the group of olfactory, taste, and pheromone receptors (Wettschureck et al., 2005). GPCRs transduce extracellular signals *via* membrane-associated heterotrimeric G-proteins, which consists of a monomeric α-subunit and the dimeric βγ-subunit (Figure 2). Ligand binding induces receptor-dependent activation of G-proteins, leading to a replacement of GDP-bound Gαβγ (basal state) to Gα-GTP (active state) and free Gβγ dimer (Offermanns, 2003).
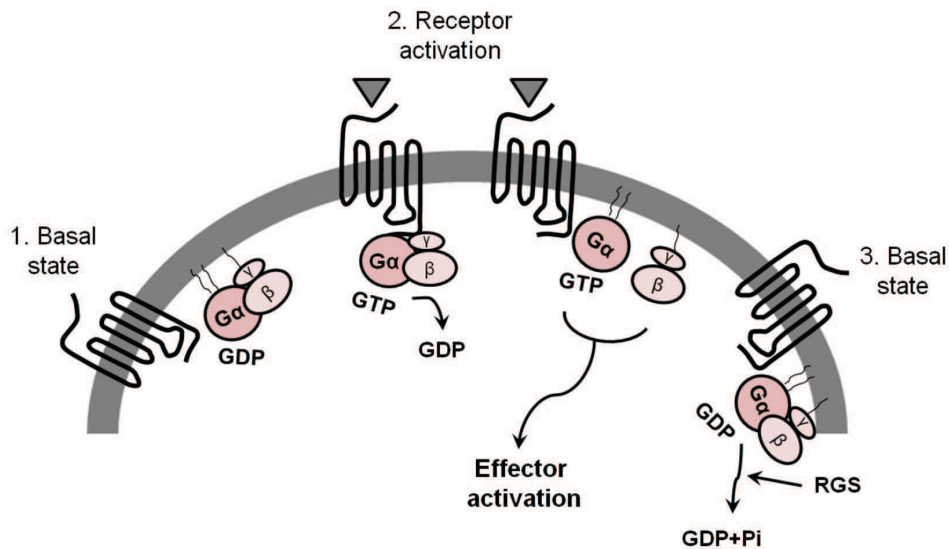
Figure 2: GTP-GDP cycle required for G-protein activity. Ligand dependent activation and deactivation of heterotrimeric G-proteins. The hydrolysis of GTP to GDP can be accelerated by various effectors as well as Regulators of G-protein Signaling (RGS) GTP, guanosine triphosphate; GDP, guanosine diphosphate.

The GTP-bound, active α-subunit and the βγ-complex interact with effector proteins (e.g. enzymes and ion-channels) and thereby regulate their functions. The signaling is terminated by hydrolysis of GTP into GDP and inorganic phosphate (P_i) by an intrinsic GTPase activity of Gα-proteins. The formed GDP remains bound to the α-subunit that now reassociates with the βγ-complex to form the inactive basal state (Figure 2) (Cabrera-Vera et al., 2003; Offermanns, 2003). In addition, a family of regulatory proteins, called Regulators of G-protein Signalling (RGS), are able to increase the GTPase activity of the Gα-subunit (Ross et al., 2000). RGSs play an important role in controlling the lifetime of the GPCR/G-protein-mediated signal transduction.

Enzyme-linked receptors: The family of enzyme-linked receptors is the second major transmembrane receptor family. Members of this receptor family are characterized by an agonist-binding domain on the outer surface of the plasma membrane and a cytoplasmic domain that either displays an intrinsic enzyme activity or is directly associated with an

enzyme. Enzyme-linked receptors play important roles in growth, proliferation, survival, cell cycle control and differentiation in response to extracellular stimuli. On the basis of cytoplasmic domain activity the enzyme-linked receptors are subdivided into the following classes: (a) Receptor Tyrosine Kinases (RTK), which autophosphorylate specific tyrosine residues (e.g. Fibroblast or epidermal growth factor receptors including the EGFR or ErbB families) (Lemmon et al., 2010); (b) receptor protein tyrosine phosphatases, which remove phosphate groups from tyrosines of various signaling proteins (e.g. CD45 or Src family members) (Fischer, 1999; Petrone et al., 2000); (c) receptor Serine/threonine kinases, which phosphorylate specific serines or threonines present in signaling proteins (e.g. transforming growth factor receptor, TGF-beta receptors, and activin A receptors) (ten Dijke et al., 2004); and lastly (d) receptor guanylyl cyclases, which catalyze the generation of the second messenger cGMP (Pyriochou et al., 2005).

Ligand-gated ion channels (LGIC): Ligand-gated ion channels are a group of multimeric transmembrane ion-channels which play a central role in intracellular communication within the nervous system. Ion channels represent receptors for neurotransmitters and are involved in fundamental neurophysiological processes such as attention, memory, and learning (Betz, 1990; Calimet et al., 2013). Receptors for serotonin (5-hydroxytryptamine), acetylcholine, and glutamate receptors are examples of cation-permeable LGIC (Changeux et al., 1992; Hoyer, 1990; Masu et al., 1993). The γ-aminobutyric acid receptor (GABA$_A$) and the glycine receptor (GlyR) are characterized as anion-permeable LGIC (Kozuska et al., 2012; Langosch et al., 1990).

1.2 The heterotrimeric G-protein family

GPCRs represent the biggest and most diverse receptor family in mammals and signal through heterotrimeric G-proteins. Heterotrimeric G-proteins are members of the GTP-binding superfamily which are fundamentally conserved from bacteria to mammals (Gilman, 1995; Oldham et al., 2008). Upon ligand binding, activated GPCRs stimulate members of several subgroups of heterotrimeric G-proteins, including G$_s$, G$_i$, and G$_q$ which are involved in many physiological and pathological processes (Beaulieu et al., 2011; Defea, 2008; Nürnberg et al., 1995). In response to various extracellular ligands binding to GPCR, the activated G-protein and the specificity of G-protein-effector interaction define the range of cellular responses. Thus, heterotrimeric G-proteins act as molecular switches which determine the fate of the downstream signaling pathway (Hooks et al., 2003; Neer, 1994).

There are additional factors besides GPCRs that are able to modulate G-protein-mediated signaling. Among those are receptor-independent regulators of G-protein signaling (RGSs) or activators of G-proteins signaling (AGSs) (Cismowski et al., 2001; Wettschureck et al., 2005) (for more details see Table 1).

Different tools have been used to study G-protein-mediated signaling pathways. Both mouse mutants of heterotrimeric G-proteins and bacterial toxins, i.e. pertussis toxin (PTX; from *Bordetella pertussis*) and cholera toxin (CTX; from *Vibrio cholerae*), have uncovered important cellular and pathobiological functions. Pertussis toxin catalyzes adenosine diphosphate (ADP) ribosylation of members of the $G_{i/o}$-protein family at a cysteine residue near the C-terminus resulting in an functional uncoupling of the GPCR - $G_{i/o}$-protein interaction (Offermanns, 2003). In contrast, cholera toxin ADP-ribosylates the G_s-family and thereby causes its constitutive activation by blocking the GTPase activity of G_s-proteins (Passador et al., 1994; Sanchez et al., 2008; Tubbs et al., 2009).

1.2.1 G-protein α-subunits: structure and function

G-proteins are composed of three different subunits, termed Gα, Gβ, and Gγ, with molecular masses of about 38-52 kDa, 35-39 kDa, and 6-8 kDa (Nürnberg et al., 1996; Oldham et al., 2008). Altogether, 23 different Gα-subunits have been described in the mammalian system, which share in average an amino acid identity of approximately 20%. Based on the amino acid sequence, structural and functional homologies of the α-subunits, heterotrimeric G-proteins are classified into four main families (Table 1): G_s (includes four splice variants of G_s, G_{XL}, and G_{olf}); G_i (includes G_{i1}, G_{i2}, G_{i3}, G_{o1}, G_{o2}, G_{o3}, $G_{t-r\ or\ t-c}$, G_{gust}, G_z), G_q (includes G_q, G_{11}, G_{14}, $G_{15/16}$), and G_{12} (contains G_{12} and G_{13}) (Milligan et al., 2006; Nürnberg et al., 1996; Simon et al., 1991). Recently, a new class of non-mammalian Gα-proteins (G_v; includes G_{v1} and G_{v2}) was identified (Table 1), but the function of G_v-proteins remains unclear (Oka et al., 2009).

Unlike GPCRs, Gα-subunits are not transmembrane proteins. Instead they are associated with the plasma membrane. For this, Gα-subunits undergo co-translational and/or post-translational modifications at their terminal glycine and cysteine residues, such as N-myristoylation and palmitoylation (Milligan et al., 2006).

Table 1: Gα-subunits and their modulators and effectors (Offermanns, 2003; Wettschureck et al., 2005)

Families	α-subunits	Gene	Expression	Effector(s)	RGS/AGS regulation
G_s	$G\alpha_s$	Gnas	ubiquitous	AC↑	RGS-PX1 (Heart)
	$G\alpha_{sXL}$	Gnasxl	neuroendrocrine	AC↑	
	$G\alpha_{olf}$	Gnal	olfactory epithelial, brain, pancreas, testis	AC↑	
G_i	$G\alpha_{i1}$	Gnai1	mainly neuronal	ACI,V,VI↓; (GIRK↑)*	RGS2-6, 8, 16, 17,20 and AGS1,3
	$G\alpha_{i2}$	Gnai2	ubiquitous	ACI,V,VI↓; (GIRK↓, PLCβ↑, PI3K↑)*	RGS1-5,7-14, 16-20 and AGS1,3
	$G\alpha_{i3}$	Gnai3	mainly non-neuronal	ACI,V,VI↓; (GIRK↑, PLCβ↑,)*	RGS1-5, 10-14, 16-20 and AGS1,3
	$G\alpha_o$	Gnao	neuronal, neuroendocrine	ACI↓; (VDCC↓, GIRK↑, PLCβ?)*	RGS6,7,10-12, 14
	$G\alpha_{t-r}$	Gnat1	retinal rods, taste cells	cGMP-PDE↑	RGS9
	$G\alpha_{t-c}$	Gnat2	retinal cones	cGMP-PDE↑	
	$G\alpha_{gust}$	Gnat3	taste cells, brush cells	PDE↑?	
	$G\alpha_z$	Gnaz	neuronal, endocrine, platelets	ACI,V,VI↓; Rap1GAP	RGS10, 17,20
G_q	$G\alpha_q$	Gnaq	ubiquitous	PLCβ1-4↑; Rho-GEF↑	RGS1-5, 16, 18, 19
	$G\alpha_{11}$	Gna11	almost ubiquitous (except thrombocytes)	PLCβ1-4↑; Rho-GEF↑	RGS1-5, 16, 18, 19
	$G\alpha_{14}$	Gna14	kidney, lung, spleen and testis	PLCβ1-4↑	
	$G\alpha_{15/16}$	Gna15	hematopoietic cells	PLCβ1-4↑	
G_{12}	$G\alpha_{12}$	Gna12	ubiquitous	Rho-GEF↑; Btk↑, Gap1^m↑; cadherin	
	$G\alpha_{13}$	Gna13	ubiquitous	Rho-GEF↑; radixin	
G_v[#]	$G\alpha_{v1}$	Gnav1	larva and adult zebrafish, teleost families	not known	
	$G\alpha_{v2}$	Gnav2	teleost families	not known	

[*]Regulation of these effectors occurs via Gβγ-dimers derived from activated Gα-subunits.

[#]Fifth class of Gα-proteins, present in some vertebrates, arthropods, mollusks, and annelids. However, these proteins are absent in human, mouse, fruit fly, and nematodes.

↑: stimulation; ↓: inhibition; AC, adenylyl cyclase; AGS, activators of G-protein-mediated signalling; Btk, Bruton's tyrosine kinase; cGMP-PDE, cGMP-dependent phosphodiesterase; Gap1^m, Ras GTPase-activating protein 2; GIRK, G-protein-regulated inward rectifier potassium channel; PI3K, phosphoinositide-3-kinase; PLC, phospholipase C; RGS, regulators of G-protein-mediated signaling; Rho-GEF, Rho guanine nucleotide exchange factor; VDCC, voltage-dependent calcium (Ca^{2+})-channel.

The G_s was the first G-protein identified and originally discovered in rabbit liver. It causes a receptor-dependent stimulation of all known adenylyl cyclases and thereby increases the intracellular cAMP concentration, a key secondary messenger (Krechowec et al., 2008; Mamillapalli et al., 2010; Northup et al., 1980). Members of the G_q family mediate the pertussis toxin-insensitive activation of phospholipase C-β (PLC-β) resulting in particular in the generation of the second messenger inositol 1,4,5 triphosphate (IP_3) and hence an elevation of intracellular [Ca^{2+}] levels (Gomez et al., 2013; Taylor et al., 1991). The members

of the G_{12} family, $G\alpha_{12}$ and $G\alpha_{13}$, are widely expressed, but their functions were initially not well understood (Morris et al., 1999). However, it could be shown later on that $G\alpha_{12}$ and $G\alpha_{13}$ activate Rho-GEFs and thereby play an important role in the regulation of actin cytoskeleton-dependent processes, such as adhesion, polarity and migration (Goulimari et al., 2005; Moers et al., 2008; Vogt et al., 2003; Wettschureck et al., 2005). The family of pertussis toxin-sensitive G_i-proteins and their known functions are described in section 1.3.

1.2.2 G-protein βγ-subunits: structure and function

Gβγ consists of Gβ- and Gγ-subunits, which form a tightly bound functional unit (Melien, 2007). At least six different β- and fourteen different γ-subunits have been described (Table 2).

Table 2: Gβ-and Gγ-subunits: classification, expression, and effectors (Wettschureck et al., 2005)

Isoform	Gene	Expression	Effectors
$G\beta_1$	Gnb1	widely, retinal rods	
$G\beta_2$	Gnb2	ubiquitous	
$G\beta_3$	Gnb3	widely, retinal cones	
$G\beta_4$	Gnb4	widely, brain, lung, placenta	
$G\beta_5$	Gnb5	neuronal, lung, germ cells, ovaries	
$G\beta_5$ (l)	Gnb5	retina	
			$ACI\downarrow$, ACII, IV, VII$\uparrow$, GIRK1-4$\uparrow$, PLCβ1-3$\uparrow$, PI3Kβ and γ$\uparrow$, receptor kinases (GRK2 and 3)$\uparrow$ Btk$\uparrow$, Tsk$\uparrow$, P-Rex1$\uparrow$, VDCC$\downarrow$, PLA_2, p140$^{Ras-GEF}$$\uparrow$, Raf-1$\uparrow$
$G\gamma_1$	Gngt1	brain, retinal rods	
$G\gamma_{14}$	Gngt2	brain, retinal cones	
$G\gamma_2$, $G\gamma_6$	Gng2	widely, neuronal	
$G\gamma_3$	Gng3	brain, blood	
$G\gamma_4$	Gng4	widely	
$G\gamma_5$	Gng5	widely, placenta, liver	
$G\gamma_7$	Gng7	widely, brain, thymus, eye	
$G\gamma_8$ ($G\gamma_{olf}$)	Gng8	neuronal, vomeronasal epithelium	
$G\gamma_9$	Gng9	retina, neuronal	
$G\gamma_{10}$	Gng10	widely, brain, placenta	
$G\gamma_{11}$	Gng11	widely, except neuronal	
$G\gamma_{12}$	Gng12	ubiquitous	
$G\gamma_{13}$	Gng13	widely, brain, taste buds	

The classification of Gβ- and Gγ-subunits is based on their DNA sequence homologies. (l) Denotes the long splice variants of $G\beta_5$. $\uparrow$: stimulation; $\downarrow$: inhibition; AC, adenylyl cyclase; Btk, Bruton's tyrosine kinase; GIRK, G-protein-regulated inward rectifier potassium channel; PI3K, phosphoinositide-3-kinase; PLA_2, phospholipase A_2; PLC, phospholipase C; P-Rex1, guanine nucleotide exchange factor of the Rac-GTPase; Raf-1, a member of Raf-subfamily of serine-threonin protein kinase; Tsk, interleukin-2 inducible tyrosine kinase; VDCC, voltage-dependent calcium (Ca^{2+})-channel.

The Gβ-subunits Gβ$_{1-4}$ share approximately 80% amino acid sequence identity as compared to only 50% identity with Gβ$_5$. There is significantly lower identity among Gγ-subunits (Downes et al., 1999), which undergo a lipid modification, i.e. isoprenylation, at their C-terminal CAAX motif (C is cysteine, A is any aliphatic amino acid, and X is any amino acid). Gγ isoprenylation is responsible for membrane association of the βγ-dimer (Milligan et al., 2006). Different Gβ$_{(1-5)}$ and Gγ$_{(1-14)}$ proteins can pair and form unique Gβ$_{(1-5)}$γ$_{(1-14)}$ combinations. However, the functional significance for this diversity is not well understood (Smrcka, 2008).

Unlike Gα-subunits, Gβγ-complexes possess no enzymatic activity. Nevertheless, they modulate the activity of several effectors, including GIRK channels, some members of the family of adenylyl cyclases (Gautam et al., 1998; Mirshahi et al., 2002; Sadja et al., 2002), or activation of class I$_B$ phosphoinositide 3-kinase (PI3K) (Shymanets et al., 2013).

1.3   G$_i$-protein family: isoform-specific and redundant biological roles

G$_i$-proteins (36-42 kDa) include several diverse subtypes as summarized in Table 1. G$_{i1}$, G$_{i2}$, G$_{i3}$, G$_o$, G$_z$, and G$_{gust}$ inhibit adenylyl cyclase, thereby decreasing cAMP production, whereas the retinal expressed subtypes G$_{t-r}$ and G$_{t-c}$ activate cGMP-specific phosphodiesterase (cGMP-PDE) (Hepler et al., 1992; Melien, 2007). G$_i$-proteins modulate the activity of various intracellular effector systems resulting in the regulation of a variety of cellular responses (Figure 3). Downstream effectors consist of enzymes (e.g. adenylyl cyclase, phospholipase C, and PI3K) and ion channels (e.g. potassium and calcium channels) (Hamm, 1998; Melien, 2007; Urano et al., 2013; Wettschureck et al., 2005), which take over a distinct spectrum of biological roles.

As an important characteristic, all members of the G$_i$-protein family (except G$_z$) are sensitive to pertussis toxin (PTX) (Codina et al., 1984; Katada, 2012; Murayama et al., 1983; Straub et al., 2012). G$_i$-proteins are together with G$_{q/11}$-proteins the most abundant G-protein family present in mammals. Interestingly, Gα$_o$ constitutes up to 1-2% of the total membrane protein in the brain (Melien, 2007).

The Gα$_i$ subfamily comprises three closely related members, Gα$_{i1}$, Gα$_{i2}$, and Gα$_{i3}$. These isoforms share an amino acid sequence identity of 85-95% (Wilkie et al., 1994) and a partially overlapping expression profile. Targeted loss-of-function mutations in mice have been produced for all Gα$_i$ genes (Jiang et al., 2002). Gα$_{i1}$, Gα$_{i2}$, and Gα$_{i3}$ knockout mice are viable and show a spectrum of phenotypes (Figure 4). In contrast, double deficiency for Gα$_{i2}$

and $G\alpha_{i3}$ causes an early embryonic lethality in mice suggesting redundant functions of both isoforms during development (Gohla et al., 2007). Moreover, $G\alpha_{i1}/G\alpha_{i3}$ double-deficient mice are viable (Plummer et al., 2012) indicating that the ubiquitously expressed $G\alpha_{i2}$ is the quantitatively and functionally predominant $G\alpha_i$ isoform. Since the cellular levels of the G_i-proteins (in particular $G\alpha_{i2}$) are relatively high, they also represent an important source of $G\beta\gamma$-complexes.
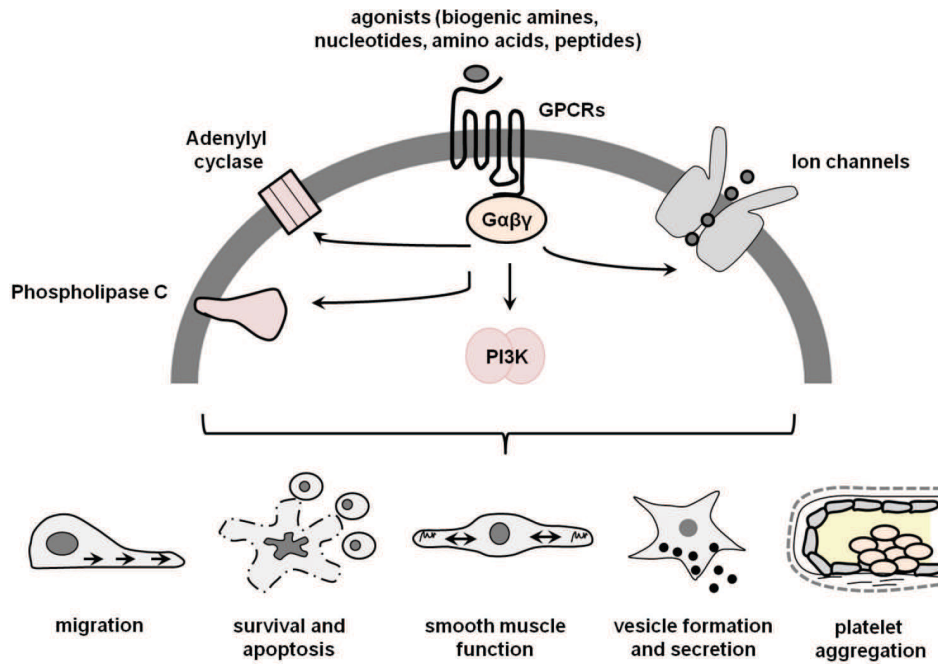
Figure 3: G-protein-regulated effector pathways in cellular processes and biological responses. Upon activation G-proteins regulate the activity of different effector molecules and thereby modulate cellular functions like migration of macrophages or vasotonous activity of smooth muscle cells. PI3K, phosphatidylinositol 3-kinase.

1.3.1 Tissue specific expression and functions of $G\alpha_{i1}$, $G\alpha_{i2}$, and $G\alpha_{i3}$

Quantitatively, $G\alpha_{i2}$ is the predominant $G\alpha_i$ isoform and it is ubiquitously expressed. $G\alpha_{i1}$ is the first discovered $G\alpha_i$ isoform and is expressed in the nervous system. $G\alpha_{i3}$, the closest homolog of $G\alpha_{i1}$, is hardly detectable in the nervous system, but is broadly expressed in peripheral tissues (Table 1). Targeted loss-of-function mutations of the respective $G\alpha_i$ isoforms have been generated in mice and the resulting phenotypes demonstrate isoform-specific as well as redundant functions (Figure 4). The loss of $G\alpha_{i1}$ affects long term memory by diminishing synapse-specific plasticity (Pineda et al., 2004). $G\alpha_{i2}$-deficient mice spontaneously develop ulcerative colitis (Rudolph et al., 1995) and display a defective macrophage and neutrophil migration (Wiege et al., 2013; Wiege et al., 2012). Moreover, they have an altered heart rate dynamics (Zuberi et al., 2008). $G\alpha_{i3}$ is essentially responsible

for the antiautophagic effects of insulin in the liver (Gohla et al., 2007) and plays a potent role in melanosome biogenesis (Young et al., 2008).
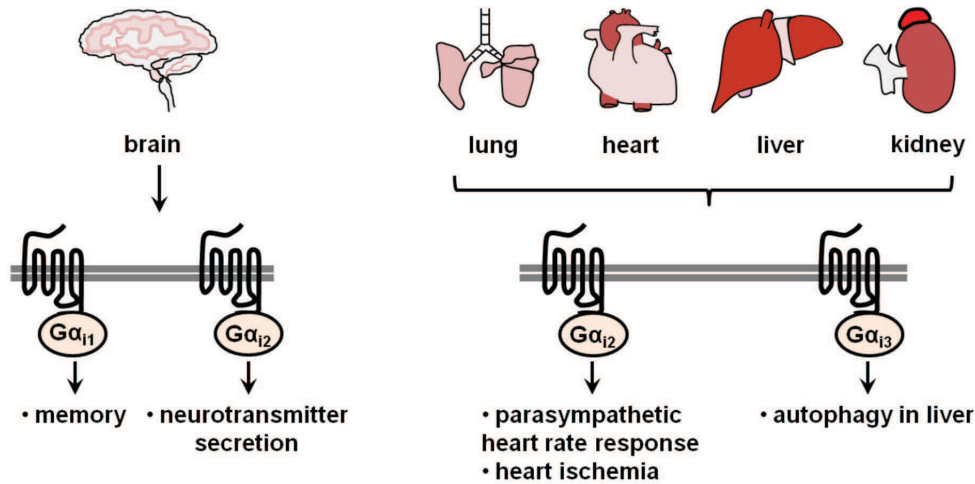
Figure 4: Organ- and cell-specific expression and function of Gα$_i$-protein family members. Isoform-specific expression and known functions of Gα$_{i1}$, Gα$_{i2}$, and Gα$_{i3}$ in central (brain) and peripheral organs.

1.4   G$_i$-proteins in the cardiovascular system

1.4.1   G$_i$-mediated signal transduction in cardiovascular homeostasis

Cardiovascular homeostasis and heart function are maintained through various extracellular signaling molecules like hormones, neurotransmitters, and growth factors which often act through GPCRs at the cell surface (Rockman et al., 2002). Heterotrimeric G$_i$-proteins, which are functionally coupled with many of these GPCRs, represent crucial components for cardiovascular homeostasis. In the cardiovascular system, Gα$_{i2}$ and Gα$_{i3}$, the two major Gα$_i$ isoforms expressed, display redundant as well as isoform-specific functions (Albarran-Juarez et al., 2009; Dizayee et al., 2011; Hippe et al., 2013) Commonly expressed GPCRs in the cardiovascular system are β1-adrenergic receptors (G$_s$-coupled), β2-adrenergic receptors (G$_s$/G$_i$-coupled), and M2-muscarinic receptors (G$_i$/G$_o$-coupled), the latter of which are responsible for autonomic control of heart function. Of note, the isoform G$_{i2}$ takes over an important cardioprotective role (DeGeorge et al., 2008; Foerster et al., 2003; Köhler et al., 2014; Offermanns, 2003; Waterson et al., 2011).

1.4.2   The role of G$_i$-proteins in the regulation of the vascular tone

The endothelium plays an important role in the regulation of the vasotonous (balance between vasoconstriction and vasodilatation). Endothelial cells represent the innermost layer

of blood and lymph vessels controlling the activity of smooth muscle cells by releasing various endothelium-derived vasoactive agents, i.e. vasoconstrictors and vasodilators. Various vascular GPCRs control and influence the vasotonus under physiological and pathological conditions (Breyer et al., 2001; Vanhoutte, 2009b). The function of pertussis toxin (PTX)-sensitive, heterotrimeric G_i-proteins ($G\alpha_i\beta\gamma$) in endothelium-dependent vasotonous regulation is poorly understood and rather based on the analysis of *in-vitro* and *in-vivo* effects of PTX. Initially, it was assumed that PTX-sensitive G_i-dependent signaling is required for both endothelium-dependent vasorelaxation and vasoconstriction, possibly dependent on the vessel and cell type analyzed (Flavahan et al., 1990; Komaru et al., 1997; van Meijeren et al., 2004a; van Meijeren et al., 2004b). At this, several studies described a PTX-dependent inhibition of NO- and EDHF-dependent relaxation (Boulanger et al., 1997; Day et al., 1995; Michel et al., 2010; Shibano et al., 1994). However, the PTX effects in these studies may have not only been limited to the endothelium, but may have influenced smooth muscle cells as well (Hohlfeld et al., 1990). Moreover, PTX displays also G_i-independent unspecific effects (Mangmool et al., 2011). Thus, these findings urge a genetic analysis of the role of $G\alpha_i$ isoforms in endothelial dependent vasotonus regulation by employing knockout mouse models.

As summarized in Figure 5 and outlined in the following, heterotrimeric G_i-proteins are involved in the production of vasoactive agents, i.e. Endothelium-Derived Constriction Factors (EDCF) and Endothelium-Derived Relaxation Factors (EDRF). EDCF comprise reactive oxygen species, prostanoids (e.g. PGE_2) generated by cyclooxygenases (COX), and the potent vasoconstrictor endothelin-1 (ET-1). In contrast, major EDRFs are nitric oxide (NO), prostanoids (PGI_2) generated by cyclooxygenases, and endothelium-derived hyperpolarizing factors (EDHF) (Giannarelli et al., 2010; Grosser et al., 2010; Vanhoutte, 2009a). Interestingly, several EDCF and EDRF can function as ligands for vascular GPCRs which signal and modulate the vasotonous activity of smooth muscle cells *via* endothelial cells.

Nitric oxide (NO) released by endothelial cells accounts for the relaxation of smooth muscle cells attributed to endothelium-derived relaxing factor (Bian et al., 2008; Pieper, 1998). NO is produced by the endothelial expressed isoform of nitric oxide synthase (eNOS). eNOS catalyzes the oxidation of L-arginine into L-citrulline and NO (Forstermann et al., 2006; Morlin et al., 2002; Palmer et al., 1988). NO serves as a "multi-tasking mediator" in mammals. It maintains the blood pressure (Stauss et al., 1999), modulates platelet activation,

and control leukocyte adhesion (Gkaliagkousi et al., 2009; Moncada et al., 1991; van Hinsbergh, 2012). Several studies indicate a role of G_i-proteins in endothelium-derived NO-production. E.g., PTX increased L-arginine uptake and thereby the NO-production in pulmonary endothelial cells (Zharikov et al., 2004). Furthermore, the HDL stimulated, G_i-coupled sphingosin-1-phosphate receptor S1P3 induces NO-production through activation of eNOS in endothelial cells (Nofer et al., 2004).
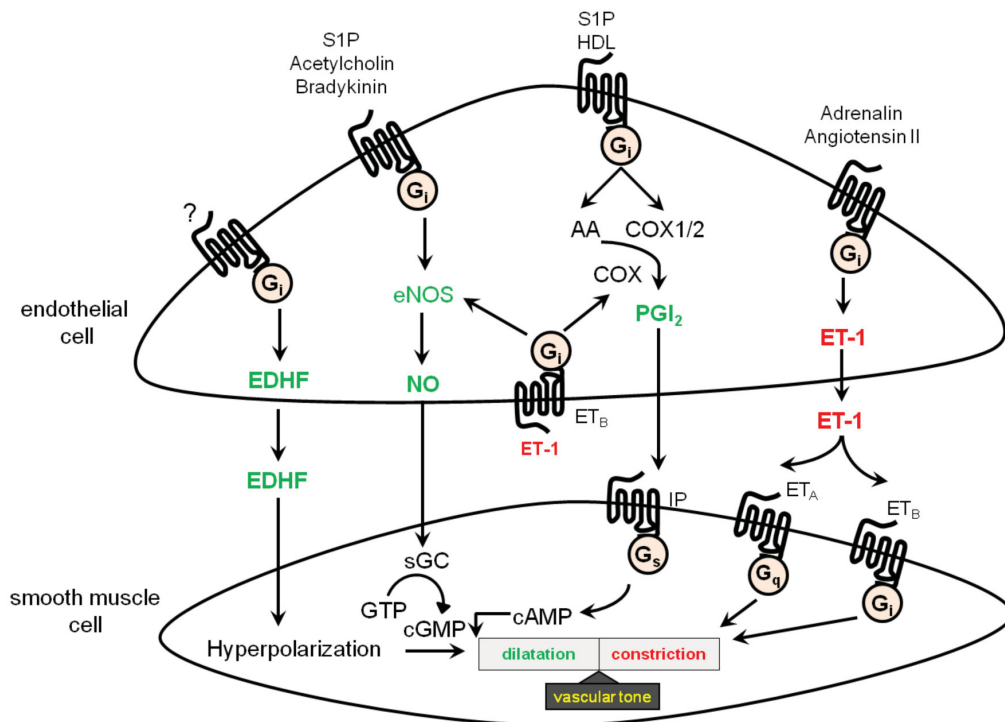
Figure 5: G_i-dependent intracellular signaling in the regulation of the vasotonous. Schematic presentation of G_i-dependent signaling pathways in endothelial cells (EC) related to the production and downstream effects of nitric oxide (NO), prostacyclin (PGI_2), and endothelin-1 (ET-1). AA, arachidonic acid; COX, cyclooxygenase; cAMP, cyclic adenosine monophosphate; cGMP, cyclic guanosine monophosphate; ET_A and ET_B, endothelin receptor A and B; eNOS, endothelial nitric oxide synthase; HDL, high density lipoprotein; IP, prostacyclin receptor; S1P, sphingosin-1-phosphate; sGC, soluble guanylate cyclase; TXA_2, thromboxane A_2; TP, thromboxane A_2 receptor. Model adapted and modified in part after (Pexa, 2012).

Further EDRF released by endothelial cells are EDHF and PGI_2. EDHF denotes a vasodilative agent that hyperpolarizes the underlying vascular smooth muscle cells (Figure 5). The entity of EDHF is not yet known with complete certainty, but an epoxide of arachidonic acid that is formed by a cytochrome P450–derived monooxygenase (Campbell et al., 1996) and hydrogen peroxide (Shimokawa et al., 2005) may work as EDHF. In fact, G_i-proteins seem to be involved in an EDHF-dependent relaxation of mesenteric vessels (Griffith et al., 2002; Vequaud et al., 2001). Interestingly, deficiency of RGS2 (regulator of G-protein signaling 2 that accelerates inactivation of G_i-proteins) enables an endothelial G_i

11

activity to inhibit EDHF-dependent relaxation, whereas RGS2 sufficiency facilitates EDHF-evoked relaxation by squelching endothelial G_i activity (Osei-Owusu et al., 2012).

The prostanoid prostacyclin (PGI_2) is the major vasodilator and prostaglandin produced by endothelial cells. PGI_2 is synthesized by cyclooxygenases (constitutively expressed COX-1 and inducible COX-2) and a subsequent PGI_2 synthase (Caughey et al., 2001; Grosser et al., 2010).

PGI_2 diffuses to the vascular smooth muscle layer and causes vasodilatation through activation of the G_s-coupled IP receptor (Figure 5). Interestingly, G_i-proteins induce the formation of PGI_2 in vascular smooth muscle cells which modulate the contraction of smooth muscle cells in an intracrine manner (Martinez-Gonzalez et al., 2004; Taurin et al., 2007). In this line, myofibroblasts isolated from the small intestine and colon of $G\alpha_{i2}$-deficient mice display a reduced arachidonic acid mobilization and a decrease in COX-1 and COX-2 expression as well as PGE_2 levels (Edwards et al., 2006). These findings indicate a critical role of $G\alpha_{i2}$ in the synthesis of prostaglandins that then affect vasodilatation and/or vasoconstriction. Of note, COX-1 and COX-2 deficient mice show several cardiovascular and stroke-related phenotypes as described in Table 3.

Lastly, endothelial cells produce a strong vasoconstrictor, Endothelin-1 (ET-1). Endothelial G_i-proteins seem to be involved in the regulation of ET-1 expression (Chua et al., 1993; Thorin et al., 1997; Yokokawa et al., 1991) (Figure 5). The vasoactive effects of ET-1 in smooth muscle cells are mediated through two GPCRs, ET_A ($G_{q/11}$) and ET_B (G_i) (Cramer et al., 2001; Eguchi et al., 1993) (Figure 5). Notably, ET_B (G_i) is also expressed on endothelial cells and functions there as "clearance" receptor for ET-1 thereby controlling serum ET-1 levels.

Overall, altered levels of ET-1, NO, and PGI_2 and hence their altered signaling pathways are causative for endothelial and vascular dysfunction and thereby associated with stroke pathologies and cerebral ischemia (Table 3). However, both the role of G_i-dependent signaling in the generation of these vasoactive agents as well as in their downstream effects has been mainly addressed by the use of PTX *in-vitro* and *in-vivo*. (Banquet et al., 2011; Vanhoutte, 2006, 2010). In addition, PTX represents a multifunctional toxin that displays both G_i-dependent and -independent effects (Mangmool et al., 2011). Genetic analysis of endothelial $G\alpha_i$ isoforms in vasotonus regulation by employing knockout mouse models is largely missing.

Table 3: Regulators of the vasotonous and their pathophysiological roles as analysed in knockout mouse models.

Genes	Genetic modification(s)	Surgical method(s) / stroke model	Phenotype of gene knockouts
eNOS	eNOS$^{-/-}$	middle cerebral artery occlusion (MCAO)	reduced blood flow and larger infarcted areas (Huang et al., 1996)
PGI$_2$ receptor	IP$^{-/-}$	bilateral occlusion of common carotid artery	cerebral ischemia (Wei et al., 2008)
COX-1	COX-1$^{-/-}$	MCAO	more susceptible to focal cerebral ischemia (Iadecola et al., 2001b)
COX-2	COX-2$^{-/-}$	MCAO & insertion of catheter into common carotid artery	reduced infarcted areas (Iadecola et al., 2001a)
ET-1	Tg ET-1 (↑)	MCAO	larger infarcted areas and volumes (Leung et al., 2004)

1.4.3 Role of G$_i$-proteins in thrombocyte activation

Thrombocytes or platelets are small cell fragments which are derived from megakaryocytes and are characterized by a discoid shape. Platelets circulate in an inactive state in the mammalian blood stream under normal physiological conditions. Upon vessel injury, platelets take over an important role in primary hemostasis through formation of blood clots (George, 2000). The vessel injury exposes subendothelial fibrils (which contains collagen and endothelial expressed von-Willebrand-factor) such that circulating platelets are able to adhere at the injured vessel wall *via* different surface membrane glycoproteins, including integrins and the fibrinogen receptor which mediate the initial platelet adhesion and activation (Jackson, 2011; Varga-Szabo et al., 2008). The interaction between platelets and subendothelial fibrils accounts for the activation of platelets, which is characterized by changes in the morphology of discoid platelets into a pseudopodia-like shape. Activated platelets secrete diffusible local mediators such as thromboxane A$_2$ (TXA$_2$) and ADP which function as positive amplification signals for the activation and aggregation of platelets (Nieswandt et al., 2011; Rivera et al., 2009). Accumulation of these mediators at the sites of injury recruits additional platelets into the growing thrombus. This positive amplifying feedback eventually results in stable thrombus formation. Physiological activators of platelets like ADP, TXA$_2$, and thrombin act through GPCRs which in turn activate G$_i$, G$_q$, G$_{12}$, and G$_{13}$ driven signaling cascades (Nieswandt et al., 2011; Offermanns, 2000, 2006; Stegner et al., 2011).

Most platelet activating stimuli function through several GPCRs. In particular, ADP can bind to two purogenic GPCRs, P2Y$_1$ and P2Y$_{12}$, which are functionally coupled with G$_q$, and G$_i$, respectively (Offermanns, 2000; Rivera et al., 2009; Savi et al., 1998).
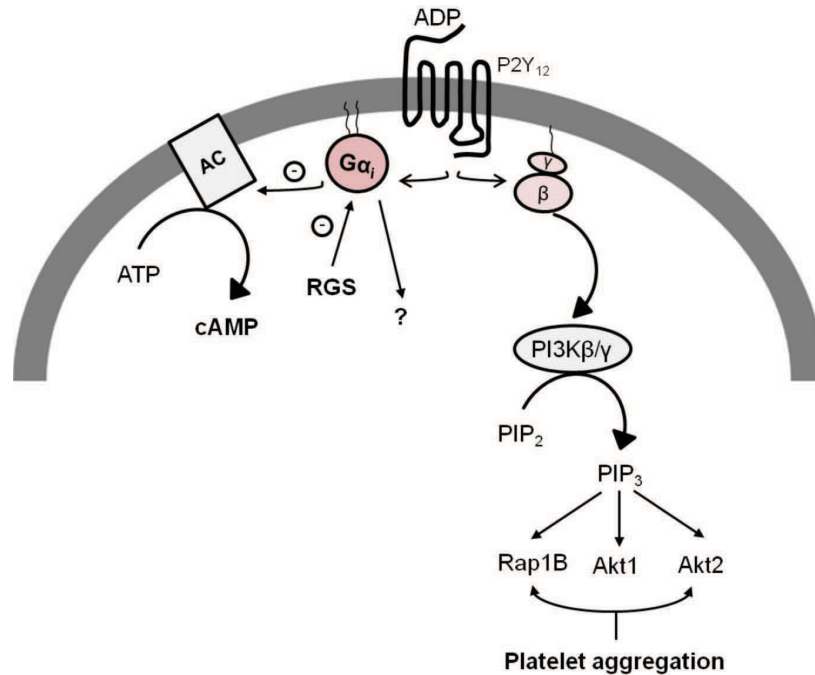
Figure 6: Involvement of G_i-proteins in platelet activation and aggregation. Several platelet stimuli agonists like ADP bind and activate GPCRs coupled to G_i-proteins, resulting in the activation of signaling pathways required for platelet aggregation. AC, Adenylyl cyclase; RGS, regulator of G-proteins; PI3K, phosphoinositide 3-kinase; PIP_2, Phosphatidylinositol-(4,5)-bisphosphate; PIP_3, phosphatidylinositol-(3, 4, 5)-trisphosphate.

$P2Y_1$ activates β-isoforms of phospholipase C (PLC) and is required for platelet functions like shape change, secretion, and aggregation. On the other hand, $P2Y_{12}$ inhibits adenylyl cyclase and co-activates PI3K-Akt1/Akt2 and Rap1B effector pathways via Gβγ required for platelet aggregation (Offermanns, 2003; Ohlmann et al., 1995; Woulfe, 2010) (Figure 6). Both G_q-coupled $P2Y_1$ and G_i-coupled $P2Y_{12}$ seem to be required for ADP-induced activation and aggregation of platelets (Rivera et al., 2009; Wettschureck et al., 2005). Although it has been shown *ex-vivo* that $G\alpha_{i2}$-deficient platelets display an aggregation defect (Jantzen et al., 2001; Offermanns, 2006), an in-depth *in-vivo* analysis of platelet function in hemostasis and thrombosis employing $G\alpha_i$ knockout mice is missing.

1.5 G-proteins and the peripheral circadian clock

1.5.1 Circadian rhythm and clock network

Circadian rhythms represent biological processes which are characterized by oscillations of approximately 24 h. These rhythms are driven by "clock genes", are internally generated and function to anticipate the environmental changes associated with the solar day (Ko et al.,

2006). In mammals, the circadian clock system has a hierarchical structure with a central/master clock (localized in the suprachiasmatic nuclei [SCN]) and peripheral oscillators (all tissues and cell types except the SCN).

Figure 7: Clock gene expression, synchronization, and regulation at the molecular level. The mammalian clock genes are ubiquitously expressed. Two major synchronizers of these molecular clocks are environmental light cues and food intake. In mammals, circadian clock mechanisms consists of transcriptional/translational feedback loops which drive 24 h body rhythms. B, brain and muscle aryl hydrocarbon receptor nuclear translocator-like; C, clock; CRY, cryptochrome; PER, period. ROR and REV, family of nuclear hormone receptors.

The central clock resides in the SCN which is part of the hypothalamus and is mainly synchronized by light cues (Reppert et al., 2001). The peripheral clock is expressed in every cell of an organism and synchronized by signals both from the SCN (Reppert et al., 2002) and e.g. by food intake (Stokkan et al., 2001). The circadian clock system contains three major components (Figure 7A): (1) an input pathway, where light directly falls on retinal photoreceptors and thereby signals are passed to the self-sustained master circadian pacemaker, i.e. SCN. Moreover, the feeding time seems to be a dominant "Zeitgeber" for peripheral oscillators, since restricting food access at the time, when mice usually do feed, causes a phase-reversal of peripheral clocks without affecting the phase of the central clock in the SCN; (2) a circadian pacemaker, i.e., core clock components, which generate autonomous self-sustaining oscillations and ensure a period length of approximately 24h; and (3) the output pathways by which the circadian pacemaker regulates overt rhythms in physiology and

behavior of organisms (Lowrey et al., 2004)(Figure 7A). The major output functions from the SCN in mammals are sustaining overall locomotor activity. In contrast, the output functions of the peripheral clock include e.g. the control of the detoxification system by the liver and urine production by the kidney. Importantly, all output functions are due to regulation by the core clock (e.g. Bmal1 and Per1, see below) or core clock-controlled genes (so-called output genes, e.g. Dbp, see below).

Core clock genes are defined as genes whose products are necessary components for the generation of the circadian rhythm within individual cells in an organism. The core clock genes in unicellular as well as multicellular organisms are characterized by interconnected positive and negative autoregulatory feedback loops at the level of transcription and translation (Lee et al., 2000; Richards et al., 2012; Shearman et al., 2000) (Figure 7B). Core clock gene products are involved in complex cycles of transcription, translation, protein-protein interaction, post-translational modification, and nuclear translocation which collectively generate and ensure daily rhythms in organisms. In mammals, the two key core clock genes, Clock and Bmal1, encode proteins of the helix-loop-helix (bHLH)-PAS (Period-Arnt-Single-minded) transcription factor family (Bunger et al., 2000). CLOCK and BMAL1 proteins form heterodimers and act as transcriptional activators in order to induce expression of many core clock and output clock genes (Figure 7). The other core clock genes, i.e. Period (Per1, Per2, and Per3), and Cryptochrome (Cry1 and Cry2), function as a negative loop in the circadian clock. PER and CRY proteins, when produced at a critical level, form a complex and thereby inhibit BMAL1/CLOCK-induced transcription. Other components, like ROR and REV (REV-ERB), can activate or inactivate the transcription of Bmal1, respectively (Figure 7B).

Lastly, the output clock genes, i.e. the PAR-domain basic leucine zipper (PAR bZip) transcription factors Dbp (albumin site D-box binding protein), Hlf (hepatocyte leukemia factor), and Tef (thyrotroph embryonic factor) accumulate in a highly circadian manner in the SCN and peripheral tissues (Fonjallaz et al., 1996; Mitsui et al., 2001). The circadian accumulation of Dbp is thereby mediated by the periodic binding of CLOCK/BMAL1 to the Dbp promoter (Figure 8) (Ripperger et al., 2006; Stratmann et al., 2012; Yamaguchi et al., 2000).

1.5.2 G_i-protein-dependent mechanisms in circadian clock regulation

So far, no studies have been published addressing a direct involvement of members of the G_i-protein family in the regulation of clock gene expression and function. As mentioned in the

previous section, the major Gα$_i$ isoforms, Gα$_{i2}$ and Gα$_{i3}$ are the isoforms, which are typically expressed in peripheral tissues (with a predominant expression of Gα$_{i2}$ as compared to Gα$_{i3}$) and display redundant and gene-specific functions.
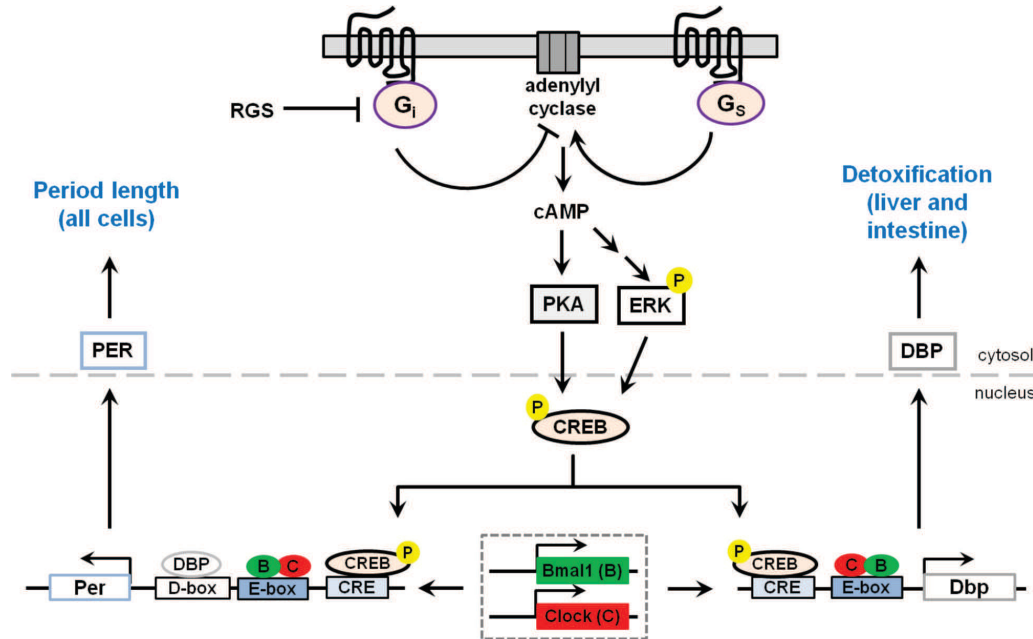
Figure 8: Model for G$_i$-dependent cellular signaling in regulation of clock gene expression and function. G$_i$-proteins inhibit adenylyl cyclase and thereby subsequent downstream signaling pathways. Here, G$_i$-dependent/PKA-mediated activation of the cAMP response element binding protein (CREB) at Ser133 regulates expression of Per and Dbp in mammals.

Gα$_i$-proteins inhibit adenylyl cyclase activity and thereby decrease the cAMP concentration in cells. Interestingly, the cAMP concentration follows a circadian accumulation both in the SCN (Yamazaki et al., 1994) and in peripheral tissues (Zhang et al., 2010). In this regard, increasing the cAMP levels in the SCN by treatment with PTX (i.e. by inactivation of G$_i$-proteins) lengthens the circadian period length (O'Neill et al., 2008), demonstrating that cAMP-dependent signaling represents a core component of the mammalian circadian pacemaker. However, the mechanism(s) by which PTX affects SCN chronobiology remain(s) unclear. Additionally, the regulator of G-protein signaling 16 (RGS16) functions as a GTPase-accelerating protein (GAP) for G$_i$-protein family members thereby accelerates the hydrolysis of GTP. Of note, the gene encoding RGS16 exhibits in the SCN and liver circadian variations in transcript levels (Huang et al., 2006). Consistent with this, Rgs16-deficient mice displays a loss of circadian production of cAMP in the SCN, which lastly results in a period lengthening of the locomotor activity rhythm (Doi et al., 2011). At the effector level, the cAMP-PKA (Protein Kinase A) and cAMP-pERK axes (Kawasaki et al., 2004) represent the major activators of the transcription factor CREB. Activated (i.e.

phosphorylated) CREB translocates then into the nucleus and functions as potent transcription factor for many clock and clock-controlled genes (Figure 8), including the clock output gene Dbp (Balsalobre et al., 2000; Haas et al., 1995; Tischkau et al., 2003).

The clock output genes Dbp, Hlf, and Tef (all members of the PAR bZip family of transcription factors) are involved in the regulation of expression of atleast two sets of important target genes (Figure 8). These include on one hand members of the cytochrome P450 family that are involved in metabolic pathways and xenobiotic detoxification processes in the liver (Gachon et al., 2006). On the other hand, DBP is required for normal, circadian expression of Per genes (Per1, Per2) (Yamajuku et al., 2011). In this regard, many genes like c-Fos, Fos-B, Per1, and Per2 are activated by serum stimulation in cultured fibroblasts as well as light-activated in the SCN (Balsalobre et al., 2000; Shearman et al., 1997). Several chemical and physical signals are thereby able to trigger the expression and circadian oscillation of the core clock genes Per1 and Per2 and of the output clock gene Dbp in cultured cells. These signals include besides cAMP, calcium, glucocorticoids (Dexamethason), or temperature changes (Brown et al., 2002; Li et al., 2014; Schneider et al., 2014; Yagita et al., 2000).

Taken together, the following questions remain to be addressed in regards to the role of G_i-proteins in the above described signaling pathways: (1) Are peripherally expressed $G\alpha_i$ isoforms involved in clock gene and/or clock output gene regulation *via* impacting on the cAMP/PKA-pCREB pathway? And (2), given that cAMP and pCREB take over major functions in the circadian SCN synchronization and mammalian physiology, the question arises to which extent $G\alpha_i$ isoforms are involved in clock gene expression and function in peripheral tissues, in particular in the liver.

2.   CHAPTER 1

The G-protein Gα$_{i3}$ regulates a sexual-dimorphic, circadian expression of the clock controlled gene DBP in murine liver

Singh M, Pexa K, Kuck F, Stibane D, Janke L, Lindecke A, Wiek C, Hanenberg H, Köhrer K, von Gall C, Reinke H, Piekorz RP. Manuscript in preparation.

The circadian clock is evolutionary conserved and found in all prokaryotes and unicellular and multicellular eukaryotes. In mammals, the circadian clock system is divided into the central (SCN) and peripheral clock (all tissue except SCN) thereby playing important regulatory roles in various physiological processes. Cells from peripheral tissues generate circadian rhythms in a central clock (i.e. light-driven)-independent manner, mainly triggered by the feeding time as "Zeitgeber" and controlled by the central regulators and transcription factors CLOCK and BMAL1. Interestingly, about 10% of all transcripts follow a cyclic expression in peripheral tissues. For example, numerous gene products in the liver are involved in metabolic and detoxification processes. They accumulate in a circadian manner based on the activity of clock output genes (e.g. Dbp, Hlf and Tef). The cAMP/PKA/pCREB signaling pathway has been implicated in the transcriptional control of Per1 (core clock component) and Dbp (clock output gene). However, the involvement of the GPCR-associated G$_i$ isoforms Gα$_{i2}$ and Gα$_{i3}$ in the regulation of these genes is undefined.

This study is based on an initial microarray-based, one-time-point gene expression profiling of aortic tissue from Gα$_{i2}$- and Gα$_{i3}$-deficient mice. Surprisingly, clock output genes (e.g. Dbp, Hlf, and Tef) and their transcriptional target genes (e.g. members of the cytochrome P450 family) are found at altered levels in Gα$_{i3}$-deficient mice, but not in Gα$_{i2}$$^{-/-}$ or wild-type control animals. To get insight into the relative contribution of the central *vs*. the peripheral clock in this phenotype, Gα$_{i3}$-deficient male and female mice and their respective wild-type controls were kept under "synchronized conditions" and thereby maintained in a strict 12 h light-dark cycle with free access to food and water. Liver tissue was collected "around the clock", i.e. every 6 h for up to 24 h, and further subjected to quantitative real-time PCR (qPCR) and immunoblotting analysis to validate and expand the microarray screen-based findings. Here, the expression of the majority of core clock (including Bmal, Per1/2, and Cry1/2) and clock output genes (Hlf, Tef) is greatly unchanged (i.e. not phase-shifted during the 12 h light-dark cycle). Consistent

with this finding, the Per1-driven period length of tail fibroblasts from $G\alpha_{i3}^{-/-}$ female mice (as measured by a Bmal1-Luciferase reporter construct) is comparable to the period length of wild-type control cells. In contrast, the clock output gene Dbp shows specifically an altered circadian (i.e. clearly phase-shifted) expression in female, but not male $G\alpha_{i3}^{-/-}$ animals. In line with this, an increased activation of CREB (pSer133-CREB) is detectable in liver nuclear extracts from $G\alpha_{i3}$-deficient female, but not male mice. Lastly, the transcript levels for the DBP target gene and cytochrome P450 family member Cyp3a11, which is in particular involved in xenobiotic metabolism, are significantly elevated in livers from $G\alpha_{i3}^{-/-}$ female mice. Taken together, the findings in this study uncover a novel isoform-specific role of $G\alpha_{i3}$ and thereby indicate that the G_{i3}-cAMP/PKA-pCREB signaling pathway functions -together with CLOCK/BMAL1- as a critical determinant in the sexual-dimorphic, circadian expression and function of DBP.

The author of this dissertation maintained the $G\alpha_{i2}$- and $G\alpha_{i3}$-deficient mouse strains and performed their overall *in-vivo* characterization. He isolated and analyzed primary tail fibroblasts and liver tissue and performed the qPCR and immunoblotting analysis. In addition, he has co-designed the concept of the manuscript, interpreted and discussed the data.

3. CHAPTER 2

Role of Gα$_{i2}$ in the endothelium-mediated regulation of vasoconstriction and vasodilatation

Singh M *et al*., manuscript in preparation.

Cardiovascular *in-vivo* phenotyping of Gα$_i$ knockout mouse lines revealed that lack of Gα$_{i2}$, but not Gα$_{i3}$ expression results in an increased susceptibility for cerebral ischemia (Pexa, 2012). Approximately 45% of Gα$_{i2}$ knockout animals develop a stroke phenotype upon unilateral carotid artery ligation, resulting in a lack of ipsilateral blood supply and severe cerebral ischemia. Anatomical defects in the brain vasculature, an increased neuronal sensitivity (i.e. glutamate toxicity), or thrombotic insults (see Chapter 3) could be largely excluded as possible reasons for the stroke phenotype associated with Gα$_{i2}$ deficiency (Pexa, 2012). However, this stroke phenotype could be based on an altered vasotonus leading to an increased vasoconstriction and/or impaired vasodilatation. In this regard, Gα$_{i2}^{-/-}$ mice display an elevated diastolic blood pressure (Pexa, 2012) that can be due to an altered vasotonus. Various (also G$_i$-coupled) vascular GPCRs balance the vasotonus *via* downstream effectors (e.g. COX-1 and COX-2) which are involved in the synthesis of vasoactive agents (e.g. PGI$_2$/prostacyclin). Thus, the aim of this work focuses on the elucidation of the role of endothelial Gα$_{i2}$ in the pathophysiology of the observed stroke phenotype.

Expression analysis at the mRNA and protein level confirmed Gα$_{i2}$ as the predominant Gα$_i$ isoform in Human Umbilical Vein Endothelial Cells (HUVEC) and isolated murine CD146$^+$ lung endothelial cells. Interestingly, endothelial cells from Gα$_{i2}^{-/-}$ mice (with or without a stroke phenotype upon carotid ligation) display up to 2-fold increased mRNA levels of the potent vasoconstrictor Endothelin-1 (ET-1) (Figure 9C). Moreover, expression of COX-1 (producing the vasoconstrictor PGE$_2$) was significantly upregulated (Figure 9A), whereas the mRNA levels for COX-2 (producing the key vasodilatator PGI$_2$) were tendentially reduced (Figure 9B). Of note, the latter finding applied only to stroke-affected Gα$_{i2}^{-/-}$ mice, indicating that COX-2, but not ET-1, may represent a decisive factor in terms of stroke occurrence. In contrast, Gα$_{i3}^{-/-}$ mice, which do not develop a stroke phenotype, express ET-1 and both COX isoforms comparable to wild-type control animals (Figure 9).

To further prove the isoform-specific and anti-apoplectic role of endothelial $G\alpha_{i2}$, a mouse line was generated that lacks $G\alpha_{i2}$ specifically in the endothelium ($G\alpha_{i2}^{fl/fl}$xTie2-cre$^+$; EC-$G\alpha_{i2}$). Remarkably, comparable to $G\alpha_{i2}^{-/-}$ mice, EC-$G\alpha_{i2}$ animals develop also a cerebral stroke phenotype, typically within 2h upon unilateral carotid artery ligation (incidence of ~40%, i.e. 23/58 animals affected). This is not the case for corresponding $G\alpha_{i2}^{fl/fl}$xTie2-cre$^-$ control mice (0/18 animals analyzed). Therefore, an endothelium-specific deficiency of $G\alpha_{i2}$ is sufficient to elicit a cerebral stroke phenotype upon unilateral carotid artery ligation.

Figure 9: qPCR-based expression analysis of COX-1 (A), COX-2 (B), and ET-1 (C) in isolated CD146$^+$ lung endothelial cells from wild-type, $G\alpha_{i2}^{-/-}$ and $G\alpha_{i3}^{-/-}$ animals all subjected to unilateral carotid artery ligation. Numbers of animals analyzed: wild-type (wt), n=12; $G\alpha_{i2}^{-/-}$ (with stroke phenotype), n=4; $G\alpha_{i2}^{-/-}$ (no stroke phenotype), n=6; $G\alpha_{i3}^{-/-}$, n=4. Mean ± s.d. *p<0.05; **p<0.01.

Thus, endothelial-$G\alpha_{i2}$ may play an essential and isoform-specific role in vasotonus regulation by inhibiting vasoconstriction (COX-1/PGE$_2$, ET-1) and promoting vasodilatation (COX-2/PGI$_2$). In particular, mRNA levels for endothelial COX-2 (and potentially also the levels of released PGI$_2$) are decreased in stroke-affected *vs.* non affected animals. This finding is consistent with the observation that inhibition of COX-2 in humans is associated with reduced PGI$_2$ levels and an increased risk of myocardial

infarction (Grosser et al., 2010). In line with that, $G\alpha_{i2}$-deficiency is not only limited to the development of apoplectic stroke, but is also detrimental in conditions of myocardial ischemia (Köhler et al., 2014). Further work is required in both $G\alpha_{i2}$-associated stroke models to better define the underlying molecular pathomechanisms at the receptor-effector level.

The author of this dissertation maintained the $G\alpha_{i2}$- and $G\alpha_{i3}$-deficient mouse strains and was in large part involved in the generation and characterization of the EC-$G\alpha_{i2}$ mouse line. He established and optimized the MACS-based isolation procedure of endothelial cells and performed all molecular biological analyses. In addition, he interpreted and discussed the data and is involved in a first drafting of the manuscript.

4. CHAPTER 3

Platelet Gα_{i2} is an essential mediator of thrombosis and ischemia reperfusion injury in mice[*]

Devanathan V[#], Hagedorn I[#], Köhler D[#], Pexa K, Kraft P, **Singh M**, Rosenberger P, Stoll G, Birnbaumer L, Piekorz RP, Nieswandt B, Beer-Hammer S, Nürnberg B. Manuscript in preparation ([#]equal contribution).

Platelets are crucial for primary hemostasis. However, under pathophysiological conditions, platelets become major players in thrombosis and thereby contribute to ischemic tissue injury in common diseases like cerebral stroke and myocardial infarct. The activation of platelets is to a great extent under the control of all major families of GPCR-associated, heterotrimeric G proteins, including G$_i$. Platelets express like most peripheral organs and cell types the Gα_i family members Gα_{i2} and Gα_{i3}. However, isoform-specific and -redundant roles of Gα_{i2} and Gα_{i3} in normal and pathological platelet function are unclear.

In this study established knockout mouse lines for Gα_{i2} and Gα_{i3} as well as a novel mouse model lacking Gα_{i2} specifically in megakaryocates and platelets have been characterized in regards to platelet function *ex-vivo* and hemostasis *in-vivo*. Moreover, these mouse models were tested in experimental models of thrombosis and ischemia. It is shown that Gα_{i2} represents the major Gα_{i2} isoform expressed in platelets. In contrast to Gα_{i3} deficient and wild-type control mice, G$\alpha_{i2}$$^{-/-}$ animals, display platelet aggregation defects *ex-vivo*, a prolonged tail bleeding time, and a highly impaired thrombus formation and stability in different models of arterial thrombosis. Comparable to G$\alpha_{i2}$$^{-/-}$ animals, mice selectively lacking Gα_{i2} in platelets (PF4-cre) show a similar bleeding defect. Further, these animals were analyzed under conditions of cerebral (tMCAO) and myocardial ischemia. Interestingly, platelet-Gα_{i2}-deficient animals demonstrated both smaller infarcts in the brain with a better neurological outcome as well as a strongly reduced ischemia reperfusion injury in the heart. Taken together, the data in the manuscript indicate that platelet-Gα_{i2} plays an isoform-specific role in controlling hemostasis as well as platelet-associated pathologies.

---

[*]*Enclosure 1*

The author of this dissertation was instrumental in the generation of the mouse line that is conditionally-deficient for $G\alpha_{i2}$ in thrombocytes and moreover maintained animal colonies (breeding setups, genotyping) which were analyzed in this manuscript. In addition, he was involved in the interpretation and discussion of the data and also contributed to the revision of the manuscript.

5.   CHAPTER 4

Role of centrosomal adaptor proteins of the TACC family in the regulation of microtubule dynamics during mitotic cell division[*]

Thakur HC, **Singh M**, Nagel-Steger L, Prumbaum D, Fansa EK, Gremer L, Ezzahoini H, Abts A, Schmitt L, Raunser S, Ahmadian M., Piekorz RP (2013). *Biol Chem*, 394:1411-1423.

The most striking feature of a living cell and entire organism is their ability to reproduce. The simplest type of reproduction is the mitotic division of cells into two daughter cells, which is occurring during the cell cycle and characterized by a series of events that prepare the cells for an actual cell division comprised of karyokinesis and cytokinesis. Mitotic cell division is vital for increasing the number of cells for e.g. during developmental growth and tissue repair while maintaining their genetic heritage. During mitosis, spindle poles, kinetochores, and various microtubule-associated proteins are involved in the regulation of microtubule (MT) dynamics and thereby provide MT stability for proper segregation of chromosomes to both daughter cells. TACC3 (Transforming Acidic Coil-Coiled 3) belongs to a family of evolutionary conserved and cancer-associated centrosomal proteins, which are characterized by a C-terminal coil-coiled (CC) domain required for protein-protein interaction and spindle pole localization.

In this review article, an overview has been given about our current insight into the *in-vitro* (biochemical and structural) and *in-vivo* (cell biological and genetic) characteristics and function of the evolutionary conserved family of TACC proteins. E.g., addressing the structure of highly purified TACC3 protein by electron microscopic analysis revealed an elongated structure and fiber-like appearance. Moreover, the current understanding of the diverse TACC3 interactome has been summarized. TACC3 interacts *via* its C-terminus with its major effector, the MT polymerase chTOG and thereby regulates both positively and negatively MT stability and dynamics dependent on the mitotic phase. Any dysfunction of this protein complex causes malmitosis, faulty cell division, and aneuploidy. As a consequence, cellular transformation is being promoted or cellular senescence or apoptosis results in the case of more severe mitotic defects. Further actual developments summarized in the review include the description of novel TACC3 gene fusion products (e.g. FGFR3-TACC3) generated by intrachromosomal translocation

---

[*] *Enclosure 2*

events and by now identified in various cancer types. These unusual TACC3 gene fusion products display cell transforming activity, however, the underlying molecular mechanisms in terms of an altered TACC3 function remain to be determined.

In the context of this review, the author has contributed the subcellular localization studies using confocal laser scanning microscopy. He was also instrumental for the interpretation and discussion of data presented and for the overall development of the review.

6. CHAPTER 5

The centrosomal adaptor TACC3 and the microtubule polymerase chTOG interact via defined C-terminal subdomains in an Aurora-A kinase independent manner[*]

Thakur HC, **Singh M**, Nagel-Steger L, Kremer J, Prumbaum D, Kalawy FE, Ezzahoini H, Nouri K, Gremer L, Abts A, Schmitt L, Raunser S, Ahmadian MR, Piekorz RP (2014). *J Biol Chem.*, 289:74-88.

Mitotic cell division represents a timely and spatially highly organized and controlled process that is mediated by various protein complexes localized at spindle poles, kinetochores, and microtubules. Centrosomal TACC (Transforming Acidic Coil-Coiled) proteins, which represent mitotic adaptor proteins, play an important role in the regulation of the dynamics and function of the bipolar spindle apparatus. TACC proteins display a C-terminal coiled-coil domain required for protein-protein interaction and spindle pole localization, whereas the role of the N-terminus that contains a central repeat region of unknown function is rather unclear. The major binding partner and effector of TACC3 is the microtubule polymerase chTOG that both promotes and inhibits MT stability and dynamics dependent on the mitotic phase.

This study revealed at a structure-function based level how TACC3 and chTOG interact with each other. The characterization of the TACC3-chTOG protein complex in centrosome-driven spindle assembly at the biophysical (gel filtration), biochemical (pull-down analysis), and cell biological (co-immunoprecipitation and confocal imaging) level is reported. An in-depth analysis of bacterially overexpressed and purified fragments and deletion mutants of TACC3 reveals that the C-terminal TACC domain consists of the two functionally distinct subdomains, CC1 and CC2. CC2 mediates a specific intradomain with the N-terminal repeat region, defining the "inactive" (effector unbound or masked) state of TACC3. Interestingly, specific binding of chTOG to CC1 unmasks the C-terminus of TACC3 resulting in its activated (effector bound) state. It is further demonstrated that the interaction of TACC3 with chTOG is independent from Aurora-A kinase, a major mitotic regulator at centrosomes. However, centrosomal recruitment of the TACC3-chTOG complex depends on Aurora-A kinase mediated phosphorylation of TACC3. In summary, this work identified two functionally diverse modules (CC1, CC2)

---

[*] *Enclosure 3*

within the C-terminal TACC domain of TACC3. These domains modulate and mediate, respectively TACC3-chTOG complex formation that is a prerequisite for normal microtubule dynamics and mitotic spindle assembly during cell division.

The author of this dissertation performed molecular cloning of TACC3-GFP-fusion constructs of TACC3 and its deletion mutants. He further characterized the interaction of these mutants with chTOG by *in-vivo* coimmunoprecipitation assays. Furthermore, he performed subcellular localization studies of the mitotic TACC3-chTOG protein complex using confocal laser scanning microscopy. He has co-designed the concept of the manuscript, interpreted and discussed the data, and also contributed to manuscript writing.

7. CHAPTER 6

The centrosome and mitotic spindle apparatus in cancer and senescence[*]

Schmidt S, Essmann E, Cirstea IC, Kuck F, Thakur HC, **Singh M**, Kletke A, Jänicke RU, Wiek C, Hanenberg H, Ahmadian MR, Schulze-Osthoff K, Nürnberg B and Piekorz RP (2010). *Cell Cycle*, 9:4469-73.

Mitotic cell division is a prerequisite for development, differentiation and organ morphogenesis, as well as proliferative homeostasis and tissue regeneration. The precise segregation of chromosomes during mitosis is ensured by the bipolar spindle apparatus, whose function is mediated by various proteins and protein complexes localized at centrosomes and kinetochores as well as by a plethora of microtubule-associated proteins. Alterations in microtubule dynamics and spindle assembly, centrosomal integrity, and kinetochore-linked mitotic checkpoint signaling, as caused e.g. by spindle poisons like Taxol (Paclitaxel), results typically in malmitosis and aneuploidy. Depending on the nature and severity of the mitotic defect(s) and the downstream stress signaling pathways, cells can undergo apoptosis or a post-mitotic, proliferative arrest.

In this review article (written as a perspective) literature findings about the emerging role of mitotic and centrosomal proteins in cellular senescence and tissue aging are being summarized and discussed. Inhibition or decreased expression of various centrosomal (e.g. Aurora-A, TACC3, NEDD1), kinetochore-localized (e.g. CENP-A), or spindle checkpoint proteins (e.g. Mad2 or BubR1) proteins has been linked to the p53-driven cellular senescence response in cell culture as well as in corresponding novel mouse models. Interestingly, genetically reduced, hypomorphic expression e.g. of the mitotic checkpoint kinase BubR1 resulted in increased aneuploidy without increasing the basal tumorigenesis rate in the animals. However, mice with this genetic insufficiency for BubR1 or animals with a haploinsufficiency for both Bub3 and Rae1 display a progressive progeroid phenotype characterized by a short lifespan and typical pathological signs of accelerated aging. These include an impaired vascular tonus and typical signs of vascular aging, loss of subcutaneous fat, scoliosis, cataracts, impaired wound healing, or infertility. In summary, the literature summarized and discussed in this perspective all together strongly indicates that the mitotic spindle apparatus, and in

---

[*] *Enclosure 4*

particular the mitotic checkpoint, is directly linked to cellular and organismal aging through molecular mechanisms that are currently still not completely understood.

The author of this dissertation has contributed to the compilation of the literature necessary for this review as well as to its preparation and discussion.

8. CHAPTER 7

Senescence-associated lysosomal α-L-fucosidase (SA-α-Fuc): a sensitive and more robust biomarker for cellular senescence beyond SA-β-Gal[*]

Singh M, Piekorz RP (2013). *Cell Cycle*, 12:1996.

This invited News & Views article discusses the description and significance of a novel biomarker for cellular senescence as published by Hildebrandt et al., (Cell Cycle 2013; 12:1922-7). In the recent years cellular senescence emerged as an important (patho)biological phenomenon highly relevant for antitumor defense (likely at the stage of cancer stem cells) and implicated in human tissue aging. In human cells, senescence was first observed as "replicative senescence" or "Hayflick limit" characterized by the fact that normal primary diploid fibroblasts display a finite proliferative capacity in culture before they permanently exit the cell cycle in a senescent state. Cellular senescence can be triggered by various stimuli, including telomere shortening (resulting in replicative senescence), DNA damage, mitotic defects and aneuploidy, reactive oxygen species, or aberrant oncogene activation.

Senescent cells are typically characterized by a flattened morphology and increased cell size, increased metabolic activity, and apoptotic resistance. For the detection of senescent cells both in cell culture and *in-vivo* several molecular and cell biological markers are being employed, however, dependent on the cell type and the type of senescence and senescence stimulus, with varying robustness. The most widely used and established biomarker for the detection of cellular senescence represents the so-called senescence-associated β-galactosidase (SA-β-gal) activity that is associated with an expansion of the lysosomal compartment and an increased granularity. However, the reliability and specificity of SA-β-gal has been questioned. E.g., SA-β-gal is hardly detectable in some types of senescence, whereas false-positive results can be obtained in non-senescent cells dependent on their confluency in cell culture. To overcome this problem, Hildebrandt et al. performed a screen of altered lysosomal activities in senescent cells. The authors identified a novel marker, senescence-associated lysosomal α-L-fucosidase (SA-α-Fuc), as constantly and more robustly unregulated in various types of senescence. Taken together, SA-α-Fuc seems to represent a technically more sensitive marker both for cell culture analyses as well as for the detection of senescent cells during tissue aging.

---

[*] *Enclosure 5*

The author of this dissertation has been instrumental for the compilation of the literature describing established and novel senescence markers as well as for the preparation and discussion of this News & Views article.

9.   CHAPTER 8

Downregulation of miR-15b is associated with increased SIRT4 expression in premature senescence and photoaging of human skin[*]

Kuck F[#], Grether-Beck S[#], **Singh M**[#], Lang A, Graffmann N, Schneider M, Lindecke A, Brenden H, Felsner I, Ezzahoini H, Marini A, Weinhold S, Schmidt S, Stühler K, Köhrer K, Uhrberg M, Krutmann J[#], Piekorz RP[#]. Manuscript in preparation ([#]equal contribution).

The skin represents the first line of defense against environmental noxae and undergoes photoaging upon exposure to UV-A and UV-B radiation. Accordingly, in dermal fibroblasts cellular senescence and photoaging are linked to mitochondrial dysfunction that can be caused by both reactive oxygen species (ROS)-dependent or -independent effector mechanisms. Interestingly, SIRT4 is part of the mitochondrially localized subfamily of sirtuins (SIRT3, SIRT4, and SIRT5) which function as deacetylases or in the case of SIRT4 as ADP-ribosyltransferase. Increased expression of SIRT4 negatively impacts on glutamate metabolism through inhibition of glutamate dehydrogenase and therefore on mitochondrial oxidative capacity. However, the regulation/expression and putative pathological function of mitochondrial sirtuins in cellular senescence and skin aging are unknown.

This study is based on a differential miRNA/mRNA expression profiling of cells undergoing premature senescence upon malmitosis and aneuploidy. Here, decreased miR-15b levels were linked to an increased expression of SIRT4, whereas the mRNA amounts of SIRT3 and SIRT5 were unaltered. Further cellular analyses proved a miR-15b-associated upregulation of SIRT4 expression not only in various cellular model systems of stress-induced senescence, but also in replicative senescence as well as in UV-triggered photoaging of both cultured human dermal fibroblasts and biopsies from photoaged human skin. Enforced expression of miR-15b through transfection of oligonucleotides mimicking miR-15b function reduced the luciferase activity of a SIRT4 3'-untranslated region-based reporter construct, suggesting that SIRT4 is a direct target of miR-15b. At the protein level, upregulation of SIRT4 was accompanied by an increased subcellular colocalization with the mitochondrial marker MTCO2 (mitochondrially encoded cytochrome C oxidase II). Lastly, the age-associated increase in SIRT4 expression

---

[*]*Enclosure 6*

together with decreased miR-15b levels was not skin-specific and also observed in hematopoietic progenitor cells. Taken together, this manuscript identified miR-15b as a negative regulator of SIRT4 expression thereby likely preventing mitochondrial dysfunction that is linked to cell and tissue aging.

The author of this dissertation established the γ-irradiation/human dermal fibroblast senescence model and thereby performed the qPCR-based quantification of SIRT4 and miR-15b expression levels. Moreover, he further analyzed the regulation of SIRT4 expression by employing miR-15b mimics and SIRT4 3'-UTR reporter plasmids in cell transfection studies. In addition, he has co-designed the concept of the manuscript, interpreted and discussed the data, and also contributed to manuscript rewriting.

10. Summary

Heptahelical receptors or GPCRs (G-protein-coupled receptors) are associated with heterotrimeric G-proteins (Gαβγ) and comprise the largest family of transmembrane receptors involved in intracellular signal transduction. Various agonists, including biogenic amines, nucleotides, or peptides bind to and activate their corresponding GPCRs and thereby modulate a plethora of (patho)physiological functions and responses in the body. Heterotrimeric G_i-proteins link GPCRs with adenylyl cyclases and phosphoinositide 3-kinases as major intracellular effectors. Among the family of pertussis toxin-sensitive and highly homologous $G\alpha_i$-proteins, $G\alpha_{i2}$ and $G\alpha_{i3}$ are ubiquitously expressed in peripheral (non-neuronal) cell types with $G\alpha_{i2}$ being typically present at much higher protein levels as $G\alpha_{i3}$. Based on the generation and phenotypic characterization of mouse lines with targeted loss-of-function mutations, isoform-specific as well as redundant biological functions of $G\alpha_{i2}$ and $G\alpha_{i3}$ have been observed. The latter became evident through the constitutive inactivation of both genes in the mouse resulting in embryonic lethality. In contrast, mice lacking either $G\alpha_{i2}$ or $G\alpha_{i3}$ are viable and display organ-associated phenotypes, including an increased susceptibility for heart ischemia ($G\alpha_{i2}^{-/-}$) or an impaired antiautophagic insulin signaling in the liver ($G\alpha_{i3}^{-/-}$).

This dissertation aimed at a further molecular and cell biological phenotyping of $G\alpha_i$-deficient mouse lines to identify novel functions of $G\alpha_{i2}$ and $G\alpha_{i3}$. The results presented in *Part I* suggest an isoform-specific regulatory role of $G\alpha_{i3}$ in sexual-dimorphic, circadian clock gene expression and function in the liver. *Part II* of this thesis describes an antiapoplectic function of endothelial $G\alpha_{i2}$ in vasotonus regulation that is pathophysiologically linked to a cerebral stroke and ischemia phenotype.

Part I

The transcription factors CLOCK and BMAL1 ensure in the liver the circadian expression of the core clock component PER1 and the clock output gene Dbp as well as of transcriptional targets of DBP, in particular members of the cytochrome P450 family. PER1 functions as negative feedback inhibitor of CLOCK/BMAL thereby maintaining the daily period length of approximately 24 h. Interestingly, microarray-based profiling suggested an altered expression of Dbp and cytochrome P450 isoforms in $G\alpha_{i3}^{-/-}$ mice, but not upon $G\alpha_{i2}^{-/-}$ deficiency. To validate and further analyze a possible circadian phenotype, liver tissue was collected and analyzed from $G\alpha_{i3}$-deficient male and female

mice and their respective wild-type controls around the clock, i.e. every 6 h for up to 24 h. Here, the expression level and pattern of the majority of core clock genes (including Per1) and clock output genes was greatly unchanged and not phase-shifted during the normal 12 h light-dark cycle in both male and female knockout mice. Consistent with this finding, the PER1-controlled daily period length of tail fibroblasts isolated from $G\alpha_{i3}^{-/-}$ mice was not different from the period length of wild-type control cells. In contrast, the clock output gene Dbp showed a clearly phase-shifted circadian expression in female, but not male $G\alpha_{i3}^{-/-}$ animals. In line with this, increased levels of the cAMP/PKA-activated transcription factor and Dbp regulator CREB (pSer133-CREB) were detectable in liver nuclear extracts from $G\alpha_{i3}$-deficient female, but not male mice. Consequently, the transcript levels for the DBP target Cyp3a11, a major cytochrome P450 isoform involved in endobiotic and xenobiotic metabolism, were also significantly elevated in livers from $G\alpha_{i3}^{-/-}$ female mice. In summary, the findings in Part I uncover a novel isoform-specific role of $G\alpha_{i3}$ in chronobiology and thereby suggest that the G_{i3}-cAMP/PKA-pCREB signaling axis functions -together with CLOCK/BMAL1- as an important determinant in the sexual-dimorphic, circadian expression and function of DBP.

Part II

Previous findings from the cardiovascular *in-vivo* phenotyping of $G\alpha_i$ knockout mouse lines revealed that lack of $G\alpha_{i2}$, but not $G\alpha_{i3}$ expression results in an increased susceptibility for cerebral stroke and ischemia. This phenotype was not based on anatomical defects in the brain vasculature. Thrombotic insults as possible reason for the stroke phenotype could be also excluded, given that $G\alpha_{i2}^{-/-}$ mice displayed platelet aggregation defects and a strongly impaired thrombus formation and stability. Moreover, a mouse line lacking $G\alpha_{i2}$ specifically in thrombocytes, which was generated and analyzed during this dissertation, was highly protected in from cerebral and myocardial ischemia in corresponding stroke models. Given that the cell-type specific mechanism(s) for the stroke pathology of $G\alpha_{i2}^{-/-}$ mice remained unclear in the foregoing studies, one major aim of this thesis was to investigate, whether an endothelial dysfunction, i.e. an altered vasotonus due to an increased vasoconstriction and/or impaired vasodilatation, represents the basis for the cerebral stroke phenotype of $G\alpha_{i2}^{-/-}$ mice. In this regard, previous findings and literature data indicated, that (i) $G\alpha_{i2}^{-/-}$ animals display an elevated diastolic blood pressure that is linked to an altered vasotonus, and that (ii) various

endothelial G_i-coupled GPCRs balance the vasotonus *via* regulation of the synthesis of vasoactive agents, in particular PGI_2/prostacyclin, PGE_2, and Endothelin-1.

Profiling of purified CD146$^+$ lung endothelial cells from $G\alpha_{i2}^{-/-}$ mice revealed in this work (i) significantly increased transcript levels of the potent vasoconstrictor Endothelin-1, (ii) an increased expression of cyclooxygenase 1 (COX-1), and (iii) a reduction of the mRNA levels for cyclooxygenase 2 (COX-2). In contrast, endothelial cells from $G\alpha_{i3}^{-/-}$ mice, which did not develop a stroke phenotype, expressed ET-1 and both COX isoforms at mRNA levels comparable to wild-type control animals. COX-1 produces the vasoconstrictor PGE_2, whereas COX-2 is associated with the synthesis of the key vasodilatator PGI_2. Interestingly, whereas ET-1 and COX-1 levels were altered both in stroke-unaffected and -affected $G\alpha_{i2}^{-/-}$ mice, COX-2 was reduced only in the latter group, indicating that a weakened COX-2/PGI_2 axis represent a decisive factor for the stroke occurrence in $G\alpha_{i2}^{-/-}$ mice. Consistent with this, pharmacological inhibition of COX-2 is known from the literature to be associated with reduced PGI_2 levels and an increased risk of myocardial infarction.

To prove the isoform-specific and anti-apoplectic role of endothelial $G\alpha_{i2}$ at a genetic level, a conditionally deficient mouse line was generated and analyzed that lacks $G\alpha_{i2}$ specifically in the endothelium. These animals developed an apoplectic phenotype with an incidence of ~40% that was comparable to $G\alpha_{i2}^{-/-}$ mice. Therefore, a cell type-specific deficiency of $G\alpha_{i2}$ in the endothelium is necessary and sufficient to elicit the acute cerebral stroke phenotype observed upon unilateral carotid artery ligation. Overall, the data in Part II indicate that endothelial-$G\alpha_{i2}$ plays an essential and isoform-specific role in vasotonus regulation by inhibiting vasoconstriction (COX-1/PGE_2, ET-1) and/or promoting vasodilatation (COX-2/PGI_2).

11. Zusammenfassung

Heptahelikale Rezeptoren bzw. G-Protein gekoppelte Rezeptoren (GPCR) assoziieren mitheterotrimeren G-Proteinen ($G\alpha\beta\gamma$) und stellen die größte Familie von Transmembran-rezeptoren im Rahmen intrazellulärer Signaltransduktions prozesse dar. Verschiedene Agonisten, wie z.B. biogene Amine, Nukleotide oder Peptide binden an und aktivieren deren GPCR, die dadurch eine Vielzahl (patho)physiologischer Funktionen und Antworten im Körper modulieren. Heterotrimere G_i-Proteine koppeln GPCR mit den beiden intrazellulären Haupteffektoren, Adenylylzyklasen und Phosphoinositid-3-Kinasen. $G\alpha_{i2}$ und $G\alpha_{i3}$ zählen zur Familie der Pertussistoxin-sensitiven und hoch homologen $G\alpha_i$-Proteine, die ubiquitär in allen peripheren (nicht-neuronalen) Zelltypen exprimiert werden. Hierbei wird $G\alpha_{i2}$ gewöhnlich in höheren Mengen vorgefunden als $G\alpha_{i3}$. Durch die Generierung und phänotypische Charakterisierung $G\alpha_i$-defizienter Mauslinien konnten sowohl isoformspezifische als auch redundante biologische Funktionen von $G\alpha_{i2}$ und $G\alpha_{i3}$ beobachtet werden. Für letztere spricht die embryonale Letalität $G\alpha_{i2}$/$G\alpha_{i3}$-doppeldefizienter Tiere. Dagegen sind Mauslinien mit einer Defizienz für $G\alpha_{i2}$ oder $G\alpha_{i3}$ lebensfähig, wobei $G\alpha_i$-isoformspezifische und organassoziierte Phänotypen resultieren. So weisen $G\alpha_{i2}^{-/-}$-Tiere eine deutlich erhöhte Suszeptibilität für Ischämie bei myokardialen Infarkten auf, während $G\alpha_{i3}$-Defizienz die antiautophagische Signaltransduktion von Insulin in der Leber aufhebt.

Die vorliegende Dissertation hatte die weiterführende molekulare und zellbiologische Phänotypisierung $G\alpha_i$-defizienter Mauslinien zur Aufgabe, mit dem Ziel, neue isoform-spezifische Funktionen von $G\alpha_{i2}$ und $G\alpha_{i3}$ zu identifizieren. Die in *Teil I* beschriebenen Befunde lassen eine regulatorische Rolle von $G\alpha_{i3}$ in der sexualdimorphen, zirkadianen Genexpression und Funktion in der Leber vermuten. *Teil II* umfasst Befunde, die auf eine essentielle und zellspezifische Funktion von $G\alpha_{i2}$ in Endothelzellen in der Regulation des Vasotonus deuten. Hierbei nimmt endotheliales $G\alpha_{i2}$ eine antiapoplektische und anti-ischämische Rolle beim zerebralen Schlaganfall ein.

Teil I

Die Transkriptionsfaktoren CLOCK und BMAL1 bewirken in der Leber eine zirkadiane Expression der *coreclock* Komponente PER1 und des *clockoutput* Gens Dbp sowie dessen transkriptionellen Zielgenen. Letztere umfassen vor allem Mitglieder der Cytochrom P450-Familie. PER1 ist als negativer *feedback* Inhibitor von CLOCK/BMAL

an der Sicherstellung der täglichen Periodenlänge von ca. 24 h beteiligt. Interessanterweise ließen initiale Daten aus einer *microarray*-basierten Genexpressionsanalyse vermuten, dass $G\alpha_{i3}$-defiziente Tiere, im Gegensatz zu $G\alpha_{i2}^{-/-}$-Mäusen, eine veränderte Expression von Dbp und Cytochrom P450-Isoformen aufweisen. Um diese Befunde eines möglichen zirkadianen Phänotyps zu validieren, wurde Lebergewebe aus männlichen und weiblichen $G\alpha_{i3}$-defizienten Mäusen und Wildtyp-Kontrolltieren rund um die Uhr, d.h. alle 6 Stunden bis zu 24 Stunden, isoliert und analysiert. Hierbei erwies sich die zirkadiane Expression der allermeisten *coreclock* (inkl. Per1) und *clockoutput* Gene in männlichen wie auch weiblichen $G\alpha_{i3}$*knockout*-Tieren als größtenteils unverändert mit einen normalen Phasenverlauf im 12 h Licht-Dunkel-Zyklus. Entsprechend war die PER1-kontrollierte tägliche Periodenlänge primärer $G\alpha_{i3}^{-/-}$-Fibroblasten vergleichbar mit der Periodenlänge von Wildtyp-Kontrollzellen. Im Gegensatz hierzu zeigte aber Dbp als *clockoutput* Gen eine auffällig phasenverschobene zirkadiane Expression in weiblichen, nicht aber männlichen $G\alpha_{i3}$ *knockout*-Mäusen. Dieser Befund ging einher mit erhöhten Mengen des cAMP/PKA-aktivierten Transkriptionsfaktors und Dbp-Regulators CREB (pSer133-CREB) in nukleären Leberzellextrakten $G\alpha_{i3}$-defizienter weiblicher, nicht aber männlicher Tiere. Des Weiteren waren auch die Transkriptmengen des DBP-Zielgens Cyp3a11, einer wichtigen Cytochrom P450-Isoform im endobiotischen und xenobiotischen Metabolismus, in der Leber $G\alpha_{i3}$-defizienter weiblicher Tiere signifikant erhöht. Zusammenfassend sprechen diese Befunde für eine neue isoformspezifische und chronobiologische Rolle von $G\alpha_{i3}$, wobei der G_{i3}-cAMP/PKA-pCREBSignalweg zusammen mit CLOCK/BMAL1 als wichtiger Regulator der sexualdimorphen Expression und Funktion von Dbp fungiert.

Teil II

Eine vorherige kardiovaskuläre Phänotypisierung $G\alpha_i$-defizienter Mauslinien ergab, dass das Fehlen von $G\alpha_{i2}$, nicht aber von $G\alpha_{i3}$, eine erhöhte Suszeptibilität für zerebrale Schlaganfälle und Ischämie zur Folge hat. Dieser Phänotyp basierte nicht auf anatomischen Defekten im zerebralen Gefäßsystem. Thrombotische Ursachen für den Schlaganfallphänotyp konnten ebenfalls ausgeschlossen werden, da $G\alpha_{i2}^{-/-}$-Tiere thrombozytäre Aggregationsdefekte sowie eine stark eingeschränkte Thrombusbildung und -Stabilität aufwiesen. Des Weiteren konnte gezeigt werden, dass eine im Rahmen dieser Arbeit generierte und analysierte Mauslinie mit einer zelltypspezifischen $G\alpha_{i2}$-

Defizienz in Thrombozyten in Infarktmodellen deutlich geschützter vor zerebraler und myokardialer Ischämie war. Da der zelltypspezifische Mechanismus des Schlaganfallphänotyps von $G\alpha_{i2}^{-/-}$-Tieren unklar blieb, lag ein Hauptziel dieser Arbeit in der Untersuchung einer möglicherweise zugrundeliegenden endothelialen Dysfunktion. Es sollte geklärt werden, ob ein veränderter Vasotonus, d.h. eine erhöhte Vasokonstriktion und/oder eine verminderte Vasodilatation die Basis für die erhöhte Schlaganfallsuszeptibilität bei $G\alpha_{i2}$-Defizienz darstellen könnte. In diesem Zusammenhang stehen vorherige Befunde bzw. Literaturdaten, dass (i) $G\alpha_{i2}^{-/-}$-Tiere einen erhöhten diastolischen Blutdruck aufweisen, der oft mit einem veränderten Vasotonus assoziiert ist, und dass (ii) verschiedene endotheliale, G_i-gekoppelte GPCR an der Balancierung des Vasotonus durch die Regulation der Synthese vasoaktiver Agentien, im Besonderen PGI_2/Prostacyclin, PGE_2 und Endothelin-1, beteiligt sind.

Durcheine eingehende Analyse von $CD146^+$-Endothelzellen, die aus der Lunge $G\alpha_i$-defizienterMäuse isoliert wurden, konnte in dieser Arbeit gezeigt werden, dass Endothelzellen mit einer Defizienz für $G\alpha_{i2}$, nicht aber für $G\alpha_{i3}$, signifikant erhöhte Transkriptmengen für den potenten Vasokonstriktor Endothelin-1 sowie eine veränderte Expression der Cyclooxygenasen COX-1 (erhöht) bzw. COX-2 (erniedrigt) aufweisen. Hierbei sind COX-1 und COX-2 mit der Synthese des Vasokonstriktors PGE_2 bzw. des essentiellen Vasodilatators PGI_2 assoziiert. Während die Expression von ET-1 und COX-1 in Schlaganfall-betroffenen wie auch unbetroffenen $G\alpha_{i2}^{-/-}$-Mäusen gleichermaßen verändert war, konnte eine COX-2 Reduktion nur bei ersteren beobachtet werden. Diese Befunde deuten darauf hin, dass eine insuffiziente $COX2$-PGI_2-Achse eine wichtige Determinante in der Schlaganfallsuszeptibilität $G\alpha_{i2}$-defizienter Tiere darstellt. Hierfür sprechen Literatur-befunde, dass eine pharmakologische Inhibition von COX-2 mit reduzierten PGI_2-Spiegeln und einem erhöhten Risiko für myokardiale Infarkte assoziiert ist.

Um die isoformspezifische und antiapoplektische Rolle von endothelialem $G\alpha_{i2}$ auf genetischer Ebene zu verifizieren, wurde eine Mauslinie mit einer zelltypspezifischen $G\alpha_{i2}$-Defizienz im Endothel generiert und analysiert. Diese Tiere zeigten einen Schlaganfall-phänotyp mit einer mit $G\alpha_{i2}^{-/-}$-Mäusen vergleichbaren Inzidenz von ~40%. Eine endotheliale $G\alpha_{i2}$-Defizienz scheint somit notwendig und ausreichend zu sein, um einen akuten Schlaganfall nach einseitiger Carotidenligatur hervorzurufen. Zusammenfassend lassen die Befunde dieses Teils der Dissertation vermuten, dass

endotheliales $G\alpha_{i2}$ eine essentielle und isoformspezifische Funktion in der Regulation des Vasotonus über eine Inhibition der Vasokonstriktion (COX-1/PGE_2, ET-1) und/oder eine Förderung des Vasodilatation (COX-2/PGI_2) einnimmt.

12. References

Albarran-Juarez, J., Gilsbach, R., Piekorz, R.P., Pexa, K., Beetz, N., Schneider, J., Nürnberg, B., Birnbaumer, L., and Hein, L. (2009). Modulation of alpha2-adrenoceptor functions by heterotrimeric Galphai protein isoforms. J Pharmacol Exp Ther *331*, 35-44.

Balsalobre, A., Marcacci, L., and Schibler, U. (2000). Multiple signaling pathways elicit circadian gene expression in cultured Rat-1 fibroblasts. Curr Biol *10*, 1291-1294.

Banquet, S., Delannoy, E., Agouni, A., Dessy, C., Lacomme, S., Hubert, F., Richard, V., Muller, B., and Leblais, V. (2011). Role of G(i/o)-Src kinase-PI3K/Akt pathway and caveolin-1 in beta(2)-adrenoceptor coupling to endothelial NO synthase in mouse pulmonary artery. Cell Signal *23*, 1136-1143.

Beaulieu, J.M., and Gainetdinov, R.R. (2011). The physiology, signaling, and pharmacology of dopamine receptors. Pharmacol Rev *63*, 182-217.

Betz, H. (1990). Ligand-gated ion channels in the brain: the amino acid receptor superfamily. Neuron *5*, 383-392.

Bian, K., Doursout, M.F., and Murad, F. (2008). Vascular system: role of nitric oxide in cardiovascular diseases. J Clin Hypertens (Greenwich) *10*, 304-310.

Bockaert, J., and Pin, J.P. (1999). Molecular tinkering of G protein-coupled receptors: an evolutionary success. EMBO J *18*, 1723-1729.

Boulanger, C.M., and Vanhoutte, P.M. (1997). G proteins and endothelium-dependent relaxations. J Vasc Res *34*, 175-185.

Breyer, R.M., Bagdassarian, C.K., Myers, S.A., and Breyer, M.D. (2001). Prostanoid receptors: subtypes and signaling. Annu Rev Pharmacol Toxicol *41*, 661-690.

Brown, S.A., Zumbrunn, G., Fleury-Olela, F., Preitner, N., and Schibler, U. (2002). Rhythms of mammalian body temperature can sustain peripheral circadian clocks. Curr Biol *12*, 1574-1583.

Bunger, M.K., Wilsbacher, L.D., Moran, S.M., Clendenin, C., Radcliffe, L.A., Hogenesch, J.B., Simon, M.C., Takahashi, J.S., and Bradfield, C.A. (2000). Mop3 is an essential component of the master circadian pacemaker in mammals. Cell *103*, 1009-1017.

Cabrera-Vera, T.M., Vanhauwe, J., Thomas, T.O., Medkova, M., Preininger, A., Mazzoni, M.R., and Hamm, H.E. (2003). Insights into G protein structure, function, and regulation. Endocr Rev *24*, 765-781.

Calimet, N., Simoes, M., Changeux, J.P., Karplus, M., Taly, A., and Cecchini, M. (2013). A gating mechanism of pentameric ligand-gated ion channels. Proc Natl Acad Sci U S A *110*, E3987-3996.

Campbell, W.B., Gebremedhin, D., Pratt, P.F., and Harder, D.R. (1996). Identification of epoxyeicosatrienoic acids as endothelium-derived hyperpolarizing factors. Circ Res *78*, 415-423.

Caughey, G.E., Cleland, L.G., Penglis, P.S., Gamble, J.R., and James, M.J. (2001). Roles of cyclooxygenase (COX)-1 and COX-2 in prostanoid production by human endothelial cells: selective up-regulation of prostacyclin synthesis by COX-2. J Immunol *167*, 2831-2838.

Changeux, J.P., Devillers-Thiery, A., Galzi, J.L., and Revah, F. (1992). The acetylcholine receptor: a model of an allosteric membrane protein mediating intercellular communication. Ciba Found Symp *164*, 66-89; discussion 87-97.

Chua, B.H., Chua, C.C., Diglio, C.A., and Siu, B.B. (1993). Regulation of endothelin-1 mRNA by angiotensin II in rat heart endothelial cells. Biochim Biophys Acta *1178*, 201-206.

Cismowski, M.J., Takesono, A., Bernard, M.L., Duzic, E., and Lanier, S.M. (2001). Receptor-independent activators of heterotrimeric G-proteins. Life Sci *68*, 2301-2308.

Codina, J., Hildebrandt, J.D., Sekura, R.D., Birnbaumer, M., Bryan, J., Manclark, C.R., Iyengar, R., and Birnbaumer, L. (1984). Ns and Ni, the stimulatory and inhibitory regulatory components of adenylyl cyclases. Purification of the human erythrocyte proteins without the use of activating regulatory ligands. J Biol Chem *259*, 5871-5886.

Cramer, H., Schmenger, K., Heinrich, K., Horstmeyer, A., Boning, H., Breit, A., Piiper, A., Lundstrom, K., Muller-Esterl, W., and Schroeder, C. (2001). Coupling of endothelin receptors to the ERK/MAP kinase pathway. Roles of palmitoylation and G(alpha)q. Eur J Biochem *268*, 5449-5459.

Day, N.S., Ge, T., Codina, J., Birnbaumer, L., Vanhoutte, P.M., and Boulanger, C.M. (1995). G_i proteins and the response to 5-hydroxytryptamine in porcine cultured endothelial cells with impaired release of EDRF. Br J Pharmacol *115*, 822-827.

Defea, K. (2008). Beta-arrestins and heterotrimeric G-proteins: collaborators and competitors in signal transduction. Br J Pharmacol *153 Suppl 1*, S298-309.

DeGeorge, B.R., Jr., Gao, E., Boucher, M., Vinge, L.E., Martini, J.S., Raake, P.W., Chuprun, J.K., Harris, D.M., Kim, G.W., Soltys, S.*, et al.* (2008). Targeted inhibition of cardiomyocyte G_i signaling enhances susceptibility to apoptotic cell death in response to ischemic stress. Circulation *117*, 1378-1387.

Dizayee, S., Kaestner, S., Kuck, F., Hein, P., Klein, C., Piekorz, R.P., Meszaros, J., Matthes, J., Nürnberg, B., and Herzig, S. (2011). Galphai2- and Galphai3-specific regulation of voltage-dependent L-type calcium channels in cardiomyocytes. PLoS One *6*, e24979.

Doi, M., Ishida, A., Miyake, A., Sato, M., Komatsu, R., Yamazaki, F., Kimura, I., Tsuchiya, S., Kori, H., Seo, K.*, et al.* (2011). Circadian regulation of intracellular G-protein signalling mediates intercellular synchrony and rhythmicity in the suprachiasmatic nucleus. Nat Commun *2*, 327.

Downes, G.B., and Gautam, N. (1999). The G protein subunit gene families. Genomics *62*, 544-552.

Edwards, R.A., and Smock, A.Z. (2006). Defective arachidonate release and PGE2 production in Gi alpha2-deficient intestinal and colonic subepithelial myofibroblasts. Inflamm Bowel Dis *12*, 153-165.

Eguchi, S., Hirata, Y., and Marumo, F. (1993). Endothelin subtype B receptors are coupled to adenylate cyclase via inhibitory G protein in cultured bovine endothelial cells. J Cardiovasc Pharmacol *22 Suppl 8*, S161-163.

Fischer, E.H. (1999). Cell signaling by protein tyrosine phosphorylation. Adv Enzyme Regul *39*, 359-369.

Flavahan, N.A., and Vanhoutte, P.M. (1990). Pertussis toxin inhibits endothelium-dependent relaxations evoked by fluoride. Eur J Pharmacol *178*, 121-124.

Foerster, K., Groner, F., Matthes, J., Koch, W.J., Birnbaumer, L., and Herzig, S. (2003). Cardioprotection specific for the G protein G_{i2} in chronic adrenergic signaling through beta 2-adrenoceptors. Proc Natl Acad Sci U S A *100*, 14475-14480.

Fonjallaz, P., Ossipow, V., Wanner, G., and Schibler, U. (1996). The two PAR leucine zipper proteins, TEF and DBP, display similar circadian and tissue-specific expression, but have different target promoter preferences. EMBO J *15*, 351-362.

Forstermann, U., and Munzel, T. (2006). Endothelial nitric oxide synthase in vascular disease: from marvel to menace. Circulation *113*, 1708-1714.

Gachon, F., Olela, F.F., Schaad, O., Descombes, P., and Schibler, U. (2006). The circadian PAR-domain basic leucine zipper transcription factors DBP, TEF, and HLF modulate basal and inducible xenobiotic detoxification. Cell Metab *4*, 25-36.

Gautam, N., Downes, G.B., Yan, K., and Kisselev, O. (1998). The G-protein betagamma complex. Cell Signal *10*, 447-455.

George, J.N. (2000). Platelets. Lancet *355*, 1531-1539.

Giannarelli, C., Zafar, M.U., and Badimon, J.J. (2010). Prostanoid and TP-receptors in atherothrombosis: is there a role for their antagonism? Thromb Haemost *104*, 949-954.

Gilman, A.G. (1995). Nobel Lecture. G proteins and regulation of adenylyl cyclase. Biosci Rep *15*, 65-97.

Gkaliagkousi, E., Corrigall, V., Becker, S., de Winter, P., Shah, A., Zamboulis, C., Ritter, J., and Ferro, A. (2009). Decreased platelet nitric oxide contributes to increased circulating monocyte-platelet aggregates in hypertension. Eur Heart J *30*, 3048-3054.

Gohla, A., Klement, K., Piekorz, R.P., Pexa, K., vom Dahl, S., Spicher, K., Dreval, V., Haussinger, D., Birnbaumer, L., and Nürnberg, B. (2007). An obligatory requirement for the heterotrimeric G protein G_{i3} in the antiautophagic action of insulin in the liver. Proc Natl Acad Sci U S A *104*, 3003-3008.

Gomez, A.M., Ruiz-Hurtado, G., Benitah, J.P., and Dominguez-Rodriguez, A. (2013). Ca(2+) fluxes involvement in gene expression during cardiac hypertrophy. Curr Vasc Pharm *11*, 497-506.

Goulimari, P., Kitzing, T.M., Knieling, H., Brandt, D.T., Offermanns, S., and Grosse, R. (2005). Galpha12/13 is essential for directed cell migration and localized Rho-Dia1 function. J Biol Chem *280*, 42242-42251.

Griffith, T.M., Chaytor, A.T., Taylor, H.J., Giddings, B.D., and Edwards, D.H. (2002). cAMP facilitates EDHF-type relaxations in conduit arteries by enhancing electrotonic conduction via gap junctions. Proc Natl Acad Sci U S A *99*, 6392-6397.

Grosser, T., Yu, Y., and Fitzgerald, G.A. (2010). Emotion recollected in tranquility: lessons learned from the COX-2 saga. Annu Rev Med *61*, 17-33.

Haas, N.B., Cantwell, C.A., Johnson, P.F., and Burch, J.B. (1995). DNA-binding specificity of the PAR basic leucine zipper protein VBP partially overlaps those of the C/EBP and CREB/ATF families and is influenced by domains that flank the core basic region. Mol Cell Biol *15*, 1923-1932.

Hamm, H.E. (1998). The many faces of G protein signaling. J Biol Chem *273*, 669-672.

Hepler, J.R., and Gilman, A.G. (1992). G proteins. Trends Biochem Sci *17*, 383-387.

Hermans, E. (2003). Biochemical and pharmacological control of the multiplicity of coupling at G-protein-coupled receptors. Pharmacol Ther *99*, 25-44.

Hippe, H.J., Ludde, M., Schnoes, K., Novakovic, A., Lutz, S., Katus, H.A., Niroomand, F., Nürnberg, B., Frey, N., and Wieland, T. (2013). Competition for Gbetagamma dimers mediates a specific cross-talk between stimulatory and inhibitory G protein alpha subunits of the adenylyl cyclase in cardiomyocytes. Naunyn-Schmiedeberg's Arch Pharmacol *386*, 459-469.

Hohlfeld, J., Liebau, S., and Forstermann, U. (1990). Pertussis toxin inhibits contractions but not endothelium-dependent relaxations of rabbit pulmonary artery in response to acetylcholine and other agonists. J Pharmacol Exp Ther *252*, 260-264.

Hooks, S.B., Waldo, G.L., Corbitt, J., Bodor, E.T., Krumins, A.M., and Harden, T.K. (2003). RGS6, RGS7, RGS9, and RGS11 stimulate GTPase activity of Gi family G-proteins with differential selectivity and maximal activity. J Biol Chem *278*, 10087-10093.

Hoyer, D. (1990). Serotonin 5-HT3, 5-HT4, and 5-HT-M receptors. Neuropsychopharmacology *3*, 371-383.

Huang, J., Pashkov, V., Kurrasch, D.M., Yu, K., Gold, S.J., and Wilkie, T.M. (2006). Feeding and fasting controls liver expression of a regulator of G protein signaling (Rgs16) in periportal hepatocytes. Comp Hepatol *5*, 8.

Huang, Z., Huang, P.L., Ma, J., Meng, W., Ayata, C., Fishman, M.C., and Moskowitz, M.A. (1996). Enlarged infarcts in endothelial nitric oxide synthase knockout mice are attenuated by nitro-L-arginine. J Cereb Blood Flow Metab *16*, 981-987.

Iadecola, C., Niwa, K., Nogawa, S., Zhao, X., Nagayama, M., Araki, E., Morham, S., and Ross, M.E. (2001a). Reduced susceptibility to ischemic brain injury and N-methyl-D-

aspartate-mediated neurotoxicity in cyclooxygenase-2-deficient mice. Proc Natl Acad Sci U S A *98*, 1294-1299.

Iadecola, C., Sugimoto, K., Niwa, K., Kazama, K., and Ross, M.E. (2001b). Increased susceptibility to ischemic brain injury in cyclooxygenase-1-deficient mice. J Cereb Blood Flow Metab *21*, 1436-1441.

Jackson, S.P. (2011). Arterial thrombosis--insidious, unpredictable and deadly. Nat Med *17*, 1423-1436.

Jiang, M., Spicher, K., Boulay, G., Martin-Requero, A., Dye, C.A., Rudolph, U., and Birnbaumer, L. (2002). Mouse gene knockout and knockin strategies in application to alpha subunits of G_i/G_o family of G proteins. Methods Enzymol *344*, 277-298.

Katada, T. (2012). The inhibitory G protein G(i) identified as pertussis toxin-catalyzed ADP-ribosylation. Biol Pharm Bull *35*, 2103-2111.

Kawasaki, Y., Kohno, T., Zhuang, Z.Y., Brenner, G.J., Wang, H., Van Der Meer, C., Befort, K., Woolf, C.J., and Ji, R.R. (2004). Ionotropic and metabotropic receptors, protein kinase A, protein kinase C, and Src contribute to C-fiber-induced ERK activation and cAMP response element-binding protein phosphorylation in dorsal horn neurons, leading to central sensitization. J Neurosci *24*, 8310-8321.

Ko, C.H., and Takahashi, J.S. (2006). Molecular components of the mammalian circadian clock. Hum Mol Genet *15*, R271-R277.

Köhler, D., Devanathan, V., Bernardo de Oliveira Franz, C., Eldh, T., Novakovic, A., Roth, J.M., Granja, T., Birnbaumer, L., Rosenberger, P., Beer-Hammer, S. Nürnberg, B. (2014). $G\alpha_{i2}$- and $G\alpha_{i3}$-deficient mice display opposite severity of myocardial ischemia reperfusion injury. PLoS One *9*, 10.1371/journal.pone.0098325.

Komaru, T., Tanikawa, T., Sugimura, A., Kumagai, T., Sato, K., Kanatsuka, H., and Shirato, K. (1997). Mechanisms of coronary microvascular dilation induced by the activation of pertussis toxin-sensitive G proteins are vessel-size dependent. Heterogeneous involvement of nitric oxide pathway and ATP-sensitive K+ channels. Circ Res *80*, 1-10.

Kozuska, J.L., and Paulsen, I.M. (2012). The Cys-loop pentameric ligand-gated ion channel receptors: 50 years on. Can J Physiol Pharmacol *90*, 771-782.

Krechowec, S., and Plagge, A. (2008). Physiological dysfunctions associated with mutations of the imprinted Gnas locus. Physiol (Bethesda) *23*, 221-229.

Langosch, D., Becker, C.M., and Betz, H. (1990). The inhibitory glycine receptor: a ligand-gated chloride channel of the central nervous system. Eur J Biochem *194*, 1-8.

Lee, K., Loros, J.J., and Dunlap, J.C. (2000). Interconnected feedback loops in the Neurospora circadian system. Science *289*, 107-110.

Lemmon, M.A., and Schlessinger, J. (2010). Cell signaling by receptor tyrosine kinases. Cell *141*, 1117-1134.

Leung, J.W., Ho, M.C., Lo, A.C., Chung, S.S., and Chung, S.K. (2004). Endothelial cell-specific over-expression of endothelin-1 leads to more severe cerebral damage following transient middle cerebral artery occlusion. J Cardiovasc Pharmacol *44 Suppl 1*, S293-300.

Li, Y., Guo, F., Shen, J., and Rosbash, M. (2014). PDF and cAMP enhance PER stability in Drosophila clock neurons. Proc Natl Acad Sci U S A *111*, E1284-1290.

Lowrey, P.L., and Takahashi, J.S. (2004). Mammalian circadian biology: elucidating genome-wide levels of temporal organization. Annu Rev Genomics Hum Genet *5*, 407-441.

Mamillapalli, R., and Wysolmerski, J. (2010). The calcium-sensing receptor couples to Galpha(s) and regulates PTHrP and ACTH secretion in pituitary cells. J Endocrinol *204*, 287-297.

Mangmool, S., and Kurose, H. (2011). G(i/o) protein-dependent and -independent actions of Pertussis Toxin (PTX). Toxins (Basel) *3*, 884-899.

Martinez-Gonzalez, J., Escudero, I., and Badimon, L. (2004). Simvastatin potenciates PGI(2) release induced by HDL in human VSMC: effect on Cox-2 up-regulation and MAPK signalling pathways activated by HDL. Atherosclerosis *174*, 305-313.

Masu, M., Nakajima, Y., Moriyoshi, K., Ishii, T., Akazawa, C., and Nakanashi, S. (1993). Molecular characterization of NMDA and metabotropic glutamate receptors. Ann N Y Acad Sci *707*, 153-164.

Melien, O. (2007). Heterotrimeric G proteins and disease. Methods Mol Biol *361*, 119-144.

Michel, T., and Vanhoutte, P.M. (2010). Cellular signaling and NO production. Pflugers Arch *459*, 807-816.

Milligan, G., and Kostenis, E. (2006). Heterotrimeric G-proteins: a short history. Br J Pharmacol *147 Suppl 1*, S46-55.

Mirshahi, T., Mittal, V., Zhang, H., Linder, M.E., and Logothetis, D.E. (2002). Distinct sites on G protein beta gamma subunits regulate different effector functions. J Biol Chem *277*, 36345-36350.

Mitsui, S., Yamaguchi, S., Matsuo, T., Ishida, Y., and Okamura, H. (2001). Antagonistic role of E4BP4 and PAR proteins in the circadian oscillatory mechanism. Genes Dev *15*, 995-1006.

Moers, A., Nürnberg, A., Goebbels, S., Wettschureck, N., and Offermanns, S. (2008). Galpha12/Galpha13 deficiency causes localized overmigration of neurons in the developing cerebral and cerebellar cortices. Mol Cell Biol *28*, 1480-1488.

Moncada, S., Palmer, R.M., and Higgs, E.A. (1991). Nitric oxide: physiology, pathophysiology, and pharmacology. Pharmacol Rev *43*, 109-142.

Morlin, B., Hammarstrom, M., Ehren, I., and Sjostrand, N.O. (2002). Does nitric oxide act as a cellular messenger in muscarinic endometrial secretion in the guinea-pig? Acta Physiol Scand *174*, 311-315.

Morris, A.J., and Malbon, C.C. (1999). Physiological regulation of G protein-linked signaling. Physiol Rev *79*, 1373-1430.

Murayama, T., and Ui, M. (1983). Loss of the inhibitory function of the guanine nucleotide regulatory component of adenylate cyclase due to its ADP ribosylation by islet-activating protein, pertussis toxin, in adipocyte membranes. J Biol Chem *258*, 3319-3326.

Neer, E.J. (1994). G proteins: critical control points for transmembrane signals. Protein Sci *3*, 3-14.

Nieswandt, B., Pleines, I., and Bender, M. (2011). Platelet adhesion and activation mechanisms in arterial thrombosis and ischaemic stroke. J Thromb Haemost *9 Suppl 1*, 92-104.

Nofer, J.R., van der Giet, M., Tolle, M., Wolinska, I., von Wnuck Lipinski, K., Baba, H.A., Tietge, U.J., Godecke, A., Ishii, I., Kleuser, B.*, et al.* (2004). HDL induces NO-dependent vasorelaxation via the lysophospholipid receptor S1P3. J Clin Invest *113*, 569-581.

Northup, J.K., Sternweis, P.C., Smigel, M.D., Schleifer, L.S., Ross, E.M., and Gilman, A.G. (1980). Purification of the regulatory component of adenylate cyclase. Proc Natl Acad Sci U S A *77*, 6516-6520.

Nürnberg, B. (2004). The state of GPCR research in 2004. Nat Rev Drug Discov *3*, 575, 577-626.

Nürnberg, B., and Ahnert-Hilger, G. (1996). Potential roles of heterotrimeric G proteins of the endomembrane system. FEBS Lett *389*, 61-65.

Nürnberg, B., Gudermann, T., and Schultz, G. (1995). Receptors and G proteins as primary components of transmembrane signal transduction. Part 2. G proteins: structure and function. J Mol Med (Berl) *73*, 123-132.

O'Neill, J.S., Maywood, E.S., Chesham, J.E., Takahashi, J.S., and Hastings, M.H. (2008). cAMP-dependent signaling as a core component of the mammalian circadian pacemaker. Science *320*, 949-953.

Offermanns, S. (2000). The role of heterotrimeric G proteins in platelet activation. Biol Chem *381*, 389-396.

Offermanns, S. (2003). G-proteins as transducers in transmembrane signalling. Prog Biophys Mol Biol *83*, 101-130.

Offermanns, S. (2006). Activation of platelet function through G protein-coupled receptors. Circ Res *99*, 1293-1304.

Ohlmann, P., Laugwitz, K.L., Nürnberg, B., Spicher, K., Schultz, G., Cazenave, J.P., and Gachet, C. (1995). The human platelet ADP receptor activates G_{i2} proteins. Biochem J *312 (Pt 3)*, 775-779.

Oka, Y., Saraiva, L.R., Kwan, Y.Y., and Korsching, S.I. (2009). The fifth class of Galpha proteins. Proc Natl Acad Sci U S A *106*, 1484-1489.

Oldham, W.M., and Hamm, H.E. (2008). Heterotrimeric G protein activation by G-protein-coupled receptors. Nat Rev Mol Cell Biol *9*, 60-71.

Osei-Owusu, P., Sabharwal, R., Kaltenbronn, K.M., Rhee, M.H., Chapleau, M.W., Dietrich, H.H., and Blumer, K.J. (2012). Regulator of G protein signaling 2 deficiency causes endothelial dysfunction and impaired endothelium-derived hyperpolarizing factor-mediated relaxation by dysregulating Gi/o signaling. J Biol Chem *287*, 12541-12549.

Palmer, R.M., Ashton, D.S., and Moncada, S. (1988). Vascular endothelial cells synthesize nitric oxide from L-arginine. Nature *333*, 664-666.

Passador, L., and Iglewski, W. (1994). ADP-ribosylating toxins. Methods Enzymol *235*, 617-631.

Petrone, A., and Sap, J. (2000). Emerging issues in receptor protein tyrosine phosphatase function: lifting fog or simply shifting? J Cell Sci *113 (Pt 13)*, 2345-2354.

Pexa, K. (2012). Charakterisierung biologischer Funktionen Guaninnukleotid-bindender $G\alpha_i$-Proteine in genetisch modifizierten Mauslinien. Dissertation (Faculty of Mathematics and Natural Science of the Heinrich-Heine University, Düsseldorf, Germany). 2012.

Pieper, G.M. (1998). Review of alterations in endothelial nitric oxide production in diabetes: protective role of arginine on endothelial dysfunction. Hypertension *31*, 1047-1060.

Pineda, V.V., Athos, J.I., Wang, H., Celver, J., Ippolito, D., Boulay, G., Birnbaumer, L., and Storm, D.R. (2004). Removal of G(ialpha1) constraints on adenylyl cyclase in the hippocampus enhances LTP and impairs memory formation. Neuron *41*, 153-163.

Plummer, N.W., Spicher, K., Malphurs, J., Akiyama, H., Abramowitz, J., Nürnberg, B., and Birnbaumer, L. (2012). Development of the mammalian axial skeleton requires signaling through the Galpha(i) subfamily of heterotrimeric G proteins. Proc Natl Acad Sci U S A *109*, 21366-21371.

Pyriochou, A., and Papapetropoulos, A. (2005). Soluble guanylyl cyclase: more secrets revealed. Cell Signal *17*, 407-413.

Reppert, S.M., and Weaver, D.R. (2001). Molecular analysis of mammalian circadian rhythms. Annu Rev Physiol *63*, 647-676.

Reppert, S.M., and Weaver, D.R. (2002). Coordination of circadian timing in mammals. Nature *418*, 935-941.

Richards, J., and Gumz, M.L. (2012). Advances in understanding the peripheral circadian clocks. FASEB J *26*, 3602-3613.

Ripperger, J.A., and Schibler, U. (2006). Rhythmic CLOCK-BMAL1 binding to multiple E-box motifs drives circadian Dbp transcription and chromatin transitions. Nat Genet *38*, 369-374.

Rivera, J., Lozano, M.L., Navarro-Nunez, L., and Vicente, V. (2009). Platelet receptors and signaling in the dynamics of thrombus formation. Haematologica *94*, 700-711.

Rockman, H.A., Koch, W.J., and Lefkowitz, R.J. (2002). Seven-transmembrane-spanning receptors and heart function. Nature *415*, 206-212.

Ross, E.M., and Wilkie, T.M. (2000). GTPase-activating proteins for heterotrimeric G proteins: regulators of G protein signaling (RGS) and RGS-like proteins. Annu Rev Biochem *69*, 795-827.

Rudolph, U., Finegold, M.J., Rich, S.S., Harriman, G.R., Srinivasan, Y., Brabet, P., Boulay, G., Bradley, A., and Birnbaumer, L. (1995). Ulcerative colitis and adenocarcinoma of the colon in G alpha i2-deficient mice. Nat Genet *10*, 143-150.

Sadja, R., Alagem, N., and Reuveny, E. (2002). Graded contribution of the Gbeta gamma binding domains to GIRK channel activation. Proc Natl Acad Sci U S A *99*, 10783-10788.

Sanchez, J., and Holmgren, J. (2008). Cholera toxin structure, gene regulation and pathophysiological and immunological aspects. Cell Mol Life Sci *65*, 1347-1360.

Savi, P., Beauverger, P., Labouret, C., Delfaud, M., Salel, V., Kaghad, M., and Herbert, J.M. (1998). Role of P2Y1 purinoceptor in ADP-induced platelet activation. FEBS Lett *422*, 291-295.

Schneider, R., Linka, R.M., and Reinke, H. (2014). HSP90 affects the stability of BMAL1 and circadian gene expression. J Biol Rhythms *29*, 87-96.

Severin, E.S., and Savvateeva, M.V. (2011). Molecular and physiological mechanisms of membrane receptor systems functioning. Acta Naturae *3*, 20-28.

Shearman, L.P., Sriram, S., Weaver, D.R., Maywood, E.S., Chaves, I., Zheng, B., Kume, K., Lee, C.C., van der Horst, G.T., Hastings, M.H.*, et al.* (2000). Interacting molecular loops in the mammalian circadian clock. Science *288*, 1013-1019.

Shearman, L.P., Zylka, M.J., Weaver, D.R., Kolakowski, L.F., Jr., and Reppert, S.M. (1997). Two period homologs: circadian expression and photic regulation in the suprachiasmatic nuclei. Neuron *19*, 1261-1269.

Shibano, T., Codina, J., Birnbaumer, L., and Vanhoutte, P.M. (1994). Pertussis toxin-sensitive G proteins in regenerated endothelial cells of porcine coronary artery. Am J Physiol *267*, H979-981.

Shimokawa, H., and Morikawa, K. (2005). Hydrogen peroxide is an endothelium-derived hyperpolarizing factor in animals and humans. J Mol Cell Cardiol *39*, 725-732.

Shymanets, A., Prajwal, Bucher, K., Beer-Hammer, S., Harteneck, C., and Nürnberg, B. (2013). p87 and p101 subunits are distinct regulators determining class IB phosphoinositide 3-kinase (PI3K) specificity. J Biol Chem *288*, 31059-31068.

Simon, M.I., Strathmann, M.P., and Gautam, N. (1991). Diversity of G proteins in signal transduction. Science *252*, 802-808.

Smrcka, A.V. (2008). G protein betagamma subunits: central mediators of G protein-coupled receptor signaling. Cell Mol Life Sci *65*, 2191-2214.

Stauss, H.M., Godecke, A., Mrowka, R., Schrader, J., and Persson, P.B. (1999). Enhanced blood pressure variability in eNOS knockout mice. Hypertension *33*, 1359-1363.

Stegner, D., and Nieswandt, B. (2011). Platelet receptor signaling in thrombus formation. J Mol Med (Berl) *89*, 109-121.

Stokkan, K.A., Yamazaki, S., Tei, H., Sakaki, Y., and Menaker, M. (2001). Entrainment of the circadian clock in the liver by feeding. Science *291*, 490-493.

Stratmann, M., Suter, D.M., Molina, N., Naef, F., and Schibler, U. (2012). Circadian Dbp transcription relies on highly dynamic BMAL1-CLOCK interaction with E boxes and requires the proteasome. Mol Cell *48*, 277-287.

Straub, S.G., and Sharp, G.W. (2012). Evolving insights regarding mechanisms for the inhibition of insulin release by norepinephrine and heterotrimeric G proteins. Am J Physiol Cell Physiol *302*, C1687-1698.

Tadevosyan, A., Vaniotis, G., Allen, B.G., Hebert, T.E., and Nattel, S. (2012). G protein-coupled receptor signalling in the cardiac nuclear membrane: evidence and possible roles in physiological and pathophysiological function. J Physiol *590*, 1313-1330.

Taurin, S., Hogarth, K., Sandbo, N., Yau, D.M., and Dulin, N.O. (2007). Gbetagamma-mediated prostacyclin production and cAMP-dependent protein kinase activation by endothelin-1 promotes vascular smooth muscle cell hypertrophy through inhibition of glycogen synthase kinase-3. J Biol Chem *282*, 19518-19525.

Taylor, S.J., and Exton, J.H. (1991). Two alpha subunits of the G_q class of G proteins stimulate phosphoinositide phospholipase C-beta 1 activity. FEBS Lett *286*, 214-216.

ten Dijke, P., and Hill, C.S. (2004). New insights into TGF-beta-Smad signalling. Trends Biochem Sci *29*, 265-273.

Thorin, E., Shreeve, S.M., Thorin-Trescases, N., and Bevan, J.A. (1997). Reversal of endothelin-1 release by stimulation of endothelial alpha2-adrenoceptor contributes to cerebral vasorelaxation. Hypertension *30*, 830-836.

Tischkau, S.A., Mitchell, J.W., Tyan, S.H., Buchanan, G.F., and Gillette, M.U. (2003). Ca2+/cAMP response element-binding protein (CREB)-dependent activation of Per1 is required for light-induced signaling in the suprachiasmatic nucleus circadian clock. J Biol Chem *278*, 718-723.

Tubbs, C., and Thomas, P. (2009). Progestin signaling through an olfactory G protein and membrane progestin receptor-alpha in Atlantic croaker sperm: potential role in induction of sperm hypermotility. Endocrinology *150*, 473-484.

Urano, D., Chen, J.G., Botella, J.R., and Jones, A.M. (2013). Heterotrimeric G protein signalling in the plant kingdom. Open Biol *3*, 120186.

van Hinsbergh, V.W. (2012). Endothelium--role in regulation of coagulation and inflammation. Semin Immunopathol *34*, 93-106.

van Meijeren, C.E., Vleeming, W., Dormans, J.A., van de Kuil, T., Opperhuizen, A., Hendriksen, C.F., and de Wildt, D.J. (2004a). Pertussis toxin relaxes small arteries with no vascular lesions or vascular smooth muscle cell injury. Exp Toxicol Pathol *56*, 139-143.

van Meijeren, C.E., Vleeming, W., van de Kuil, T., Manni, J., Kegler, D., Hendriksen, C.F., and de Wildt, D.J. (2004b). In vivo pertussis toxin treatment reduces contraction of rat resistance arteries but not that of mouse trachea. Eur J Pharmacol *488*, 127-135.

Vanhoutte, P.M. (2006). [Endothelial dysfunction and vascular pathology]. Bull Mem Acad R Med Belg *161*, 529-536; discussion 536-527.

Vanhoutte, P.M. (2009a). COX-1 and vascular disease. Clin Pharmacol Ther *86*, 212-215.

Vanhoutte, P.M. (2009b). Endothelial dysfunction: the first step toward coronary arteriosclerosis. Circ J *73*, 595-601.

Vanhoutte, P.M. (2010). Regeneration of the endothelium in vascular injury. Cardiovasc Drugs Ther *24*, 299-303.

Varga-Szabo, D., Pleines, I., and Nieswandt, B. (2008). Cell adhesion mechanisms in platelets. Arterioscler Thromb Vasc Biol *28*, 403-412.

Vequaud, P., and Thorin, E. (2001). Endothelial G protein beta-subunits trigger nitric oxide-but not endothelium-derived hyperpolarizing factor-dependent dilation in rabbit resistance arteries. Circ Res *89*, 716-722.

Vogt, S., Grosse, R., Schultz, G., and Offermanns, S. (2003). Receptor-dependent RhoA activation in G12/G13-deficient cells: genetic evidence for an involvement of Gq/G11. J Biol Chem *278*, 28743-28749.

Waterson, R.E., Thompson, C.G., Mabe, N.W., Kaur, K., Talbot, J.N., Neubig, R.R., and Rorabaugh, B.R. (2011). Galpha(i2)-mediated protection from ischaemic injury is modulated by endogenous RGS proteins in the mouse heart. Cardiovasc Res *91*, 45-52.

Wei, G., Kibler, K.K., Koehler, R.C., Maruyama, T., Narumiya, S., and Dore, S. (2008). Prostacyclin receptor deletion aggravates hippocampal neuronal loss after bilateral common carotid artery occlusion in mouse. Neuroscience *156*, 1111-1117.

Wettschureck, N., and Offermanns, S. (2005). Mammalian G proteins and their cell type specific functions. Physiol Rev *85*, 1159-1204.

Wiege, K., Ali, S.R., Gewecke, B., Novakovic, A., Konrad, F.M., Pexa, K., Beer-Hammer, S., Reutershan, J., Piekorz, R.P., Schmidt, R.E.*, et al.* (2013). Galphai2 is the essential Galphai protein in immune complex-induced lung disease. J Immunol *190*, 324-333.

Wiege, K., Le, D.D., Syed, S.N., Ali, S.R., Novakovic, A., Beer-Hammer, S., Piekorz, R.P., Schmidt, R.E., Nürnberg, B., and Gessner, J.E. (2012). Defective macrophage migration in Galphai2- but not Galphai3-deficient mice. J Immunol *189*, 980-987.

Wilkie, T.M., and Yokoyama, S. (1994). Evolution of the G protein alpha subunit multigene family. Soc Gen Physiol Ser *49*, 249-270.

Woulfe, D.S. (2010). Akt signaling in platelets and thrombosis. Expert Rev Hematol *3*, 81-91.

Yagita, K., and Okamura, H. (2000). Forskolin induces circadian gene expression of rPer1, rPer2 and dbp in mammalian rat-1 fibroblasts. FEBS Lett *465*, 79-82.

Yamaguchi, S., Mitsui, S., Yan, L., Yagita, K., Miyake, S., and Okamura, H. (2000). Role of DBP in the circadian oscillatory mechanism. Mol Cell Biol *20*, 4773-4781.

Yamajuku, D., Shibata, Y., Kitazawa, M., Katakura, T., Urata, H., Kojima, T., Takayasu, S., Nakata, O., and Hashimoto, S. (2011). Cellular DBP and E4BP4 proteins are critical for determining the period length of the circadian oscillator. FEBS Lett *585*, 2217-2222.

Yamazaki, S., Maruyama, M., Cagampang, F.R., and Inouye, S.T. (1994). Circadian fluctuations of cAMP content in the suprachiasmatic nucleus and the anterior hypothalamus of the rat. Brain Res *651*, 329-331.

Yokokawa, K., Kohno, M., Yasunari, K., Murakawa, K., and Takeda, T. (1991). Endothelin-3 regulates endothelin-1 production in cultured human endothelial cells. Hypertension *18*, 304-315.

Young, A., Powelson, E.B., Whitney, I.E., Raven, M.A., Nusinowitz, S., Jiang, M., Birnbaumer, L., Reese, B.E., and Farber, D.B. (2008). Involvement of OA1, an intracellular GPCR, and G alpha i3, its binding protein, in melanosomal biogenesis and optic pathway formation. Invest Ophthalmol Vis Sci *49*, 3245-3252.

Zhang, E.E., Liu, Y., Dentin, R., Pongsawakul, P.Y., Liu, A.C., Hirota, T., Nusinow, D.A., Sun, X., Landais, S., Kodama, Y.*, et al.* (2010). Cryptochrome mediates circadian regulation of cAMP signaling and hepatic gluconeogenesis. Nat Med *16*, 1152-1156.

Zharikov, S.I., Krotova, K.Y., Belayev, L., and Block, E.R. (2004). Pertussis toxin activates L-arginine uptake in pulmonary endothelial cells through downregulation of PKC-alpha activity. Am J Physiol Lung Cell Mol Physiol *286*, L974-983.

Zuberi, Z., Birnbaumer, L., and Tinker, A. (2008). The role of inhibitory heterotrimeric G proteins in the control of in vivo heart rate dynamics. Am J Physiol Regul Integr Comp Physiol *295*, R1822-1830.

13. Abbreviations

AC	adenylyl cyclase
ADP	adenosine diphosphate
AGS	activators of G-protein signaling
ATP	adenosine triphosphate
β1-AR	beta-1-adrenergic receptor
β2-AR	beta-2-adrenergic receptor
cAMP	cyclic adenosine monophosphate
CD45	cluster of differentiation 45; also called protein tyrosine phosphatase, receptor type, C
cGMP	cyclic guanosine monophosphate
chTOG	colonic and hepatic tumor overexpressed gene protein
COXs	cyclooxygenases
CREB	cAMP response element-binding protein
Cre	*tyrosine recombinase enzyme*, catalyses site directed recombination
Cry	*cryptochrome*
Ct	Cycle threshold
CTX	cholera toxin
Dbp	albumin D-box binding protein
Δ	delta
EC	endothelial cells
EDCF	endothelium-derived contracting factor
EDHF	endothelium-derived hyperpolarizing factor
EDRF	endothelium-derived relaxing factor
eNOS	endothelial expressed Nitric oxide synthase
ERK	*extracellular signal-related kinase*
ET-1	endothelin-1
fl	floxed allele
Gα	alpha subunit of heterotrimeric G-proteins
Gα_i	alpha subunits of heterotrimeric G_i -proteins
Gβ	beta subunit of heterotrimeric G-proteins
G$\beta\gamma$	Gβ and Gγ heterodimer
GDP	guanosine diphosphate
Gγ	gamma subunit of heterotrimeric G-proteins
G_i	heterotrimeric G_i-proteins (G$\alpha\beta\gamma$)
GIRK	G-protein-gated inwardly rectifying potassium channels
GPCR	G-protein-coupled receptor
G-protein	heterotrimeric guanosine nucleotide-binding protein
GTP	guanosine triphosphate
h	hour/hours
HDL	high-density lipoprotein
HLF	hepatic leukemia factor
HUVEC	human umbilical vein endothelial cell
LGIC	ligand-gated ion channels
mg	milligram
miRNA	micro ribonucleic acid
ml	milliliter
M2-AR	muscarinic acetylcholine receptor
NO	nitric oxide
Per	period
PGE_2	prostaglandin E_2
PGI_2	prostacyclin
PI3K	phosphoinositide 3-kinase

PKA	protein kinase A
PTX	pertussis toxin
qPCR	quantitative real-time polymerase chain reaction
RGS	regulators of G-protein signaling
SCN	suprachiasmatic nuclei
SIRT4	Sirtuin 4
Tg	transgenic mice
TACC	transforming acidic coiled-coil

14. Acknowledgments

15. Curriculum Vitae

Madhurendra Singh, M.Sc.

Institute of Biochemistry & Molecular Biology II
Heinrich-Heine University (HHU) Düsseldorf
Universitätsstrasse 01, Building 22.03.03
40225 Düsseldorf, Germany
✉*Madhurendra.Singh@uni-duesseldorf.de*

Nationality: Indian

Education

2010-2014	**Ph.D. in Biochemistry, Molecular Biology, and Cell Biology,** Piekorz Group, *Medical Faculty, Heinrich-Heine University,* Düsseldorf, Germany
2009	**M.Sc. Life Sciences,** *Jawaharlal Nehru University (JNU),* New Delhi, India
2006	**B.Sc. Botany, Chemistry, Zoology,** *Mahatma Gandhi Post Graduate college*, *Gorakhpur University*, Gorakhpur, India
2003	**All India senior school certificate examination,** *Saraswati Shishu Mandir Senior Secondary School*, Gorakhpur, India
2001	**All India secondary school examination,** *Saraswati Shishu Mandir Senior Secondary School*, Gorakhpur, India

Research experience

04/2010-08/2014	PhD student in the supervision of Dr. Roland Piekorz and PD. Dr. Reza Ahmadian in the Institute of Biochemistry and Molecular Biology II, Medical Faculty, Heinrich-Heine-University Düsseldorf, Germany
08/2009-03/2010	Junior research fellow in laboratory of Prof. S. Chakraborty in Molecular Virology Laboratory, School of Life Sciences, Jawaharlal Nehru University (JNU), New Delhi, India
06/2008-06/2009	Master project in the supervision of Dr. S. Chakraborty in Molecular Virology Laboratory, School of Life Sciences, Jawaharlal Nehru University (JNU), New Delhi, India

Publications

[1] Thakur HC, **Singh M**, Nagel-Steger L, Kremer J, Prumbaum D, Kalawy FE, Ezzahoini H, Nouri K, Gremer L, Abts A, Schmitt L, Raunser S, Ahmadian MR, Piekorz RP (2014). The centrosomal adaptor TACC3 and microtubule polymerase chTOG interact via defined C-terminal subdomains in an Aurora-A kinase independent manner. **J. Biol. Chem.** 289, 74-88.

[2] **Singh M**, Piekorz RP (2013). Senescence-associated lysosomal α-L-fucosidase (SA-α-Fuc): a sensitive and more robust biomarker for cellular senescence beyond SA-β-Gal. **Cell Cycle** 12, 1996.

[3] Thakur HC, **Singh M**, Nagel-Steger L, Prumbaum D, Fansa EK, Gremer L, Ezzahoini H, Abts A, Schmitt L, Raunser S, Ahmadian MR, Piekorz RP (2013). Role of centrosomal adaptor proteins of the TACC family in the regulation of microtubule dynamics during mitotic cell division. **Biol. Chem.** 394, 1411-1423.

[4] Schmidt S, Essmann F, Cirstea IC, Kuck F, Thakur HC, **Singh M**, Kletke A, Jänicke RU, Wiek C, Hanenberg H, Ahmadian MR, Schulze-Osthoff K, Nürnberg B, Piekorz RP (2010). The centrosome and mitotic spindle apparatus in cancer and senescence. **Cell Cycle** 9, 4469-4473.

Manuscripts in preparation

[5] Kuck F*, Grether-Beck S*, **Singh M***, Lang A, Graffmann N, Schneider M, Lindecke A, Brenden H, Felsner I, Ezzahoini H, Marini A, Weinhold S, Schmidt S, Stühler K, Köhrer K, Uhrberg M, Krutmann J, Piekorz RP. Downregulation of miR-15b is associated with increased SIRT4 expression in premature senescence and photoaging of human skin. (*equal contribution).

[6] **Singh M**, Pexa K, Kuck F, Stibane D, Lindecke A, Wiek C, Hanenberg H, Köhrer K, von Gall C, Reinke H, Piekorz RP. The G protein Gα_{i3} regulates sexual-dimorphic, circadian expression of the clock controlled gene DBP in murine liver.

[7] Devanathan V*, Hagedorn I*, Köhler D*, Pexa K, Kraft P, **Singh M**, Rosenberger P, Stoll G, Birnbaumer L, Piekorz RP, Nieswandt B, Beer-Hammer S, Nürnberg B. Platelet Gα_{i2} is an essential mediator of thrombosis and ischemia reperfusion injury in mice. (*equal contribution).

Review

Harish C. Thakur[a], Madhurendra Singh, Luitgard Nagel-Steger, Daniel Prumbaum, Eyad Kalawy Fansa, Lothar Gremer, Hakima Ezzahoini, André Abts, Lutz Schmitt, Stefan Raunser, Mohammad R. Ahmadian and Roland P. Piekorz*

Role of centrosomal adaptor proteins of the TACC family in the regulation of microtubule dynamics during mitotic cell division

Abstract: During the mitotic division cycle, cells pass through an extensive microtubule rearrangement process where microtubules forming the mitotic spindle apparatus are dynamically instable. Several centrosomal- and microtubule-associated proteins are involved in the regulation of microtubule dynamics and stability during mitosis. Here, we focus on members of the transforming acidic coiled coil (TACC) family of centrosomal adaptor proteins, in particular TACC3, in which their subcellular localization at the mitotic spindle apparatus is controlled by Aurora-A kinase-mediated phosphorylation. At the effector level, several TACC-binding partners have been identified and characterized in greater detail, in particular, the microtubule polymerase XMAP215/ch-TOG/CKAP5 and clathrin heavy chain (CHC). We summarize the recent progress in the molecular understanding of these TACC3 protein complexes, which are crucial for proper mitotic spindle assembly and dynamics to prevent faulty cell division and aneuploidy. In this regard, the (patho)biological role of TACC3 in development and cancer will be discussed.

Keywords: cancer; centrosome; chTOG/CKAP5; microtubules; mitosis; TACC3.

[a]Present address: Wellcome Trust Centre for Cell Biology, University of Edinburgh, Edinburgh, UK
*Corresponding author: Roland P. Piekorz, Institut für Biochemie und Molekularbiologie II, Medizinische Fakultät der Heinrich-Heine-Universität, D-40225 Düsseldorf, Germany, e-mail: Roland.Piekorz@uni-duesseldorf.de
Harish C. Thakur, Madhurendra Singh, Eyad Kalawy Fansa, Hakima Ezzahoini and Mohammad R. Ahmadian: Institut für Biochemie und Molekularbiologie II, Medizinische Fakultät der Heinrich-Heine-Universität, D-40225 Düsseldorf, Germany
Luitgard Nagel-Steger and Lothar Gremer: Institut für Physikalische Biologie, Heinrich-Heine-Universität, D-40225 Düsseldorf, Germany; and Strukturbiochemie (ICS-6), Forschungszentrum Jülich, Jülich, Germany

Daniel Prumbaum and Stefan Raunser: Max-Planck-Institut für Molekulare Physiologie, Dortmund, Germany
André Abts and Lutz Schmitt: Institut für Biochemie, Heinrich-Heine-Universität, D-40225 Düsseldorf, Germany

Introduction

Mitosis, the shortest phase within the cell cycle, is a fundamental cell division process that is essential for embryonic development and postnatal proliferative tissue homeostasis and function. Normal mitosis ensures an equal distribution of the genetic material duplicated during S-phase into two identical daughter cells (karyokinesis), which become finally separated during cytokinesis. Mitosis is a very complex and tightly controlled process where several biomolecules including numerous proteins and protein complexes are involved as important structural, functional, and regulatory elements. The mitotic spindle apparatus is comprised of centrosomes/spindle poles, spindle microtubules, and microtubule-associated protein complexes (Bornens, 2002, 2012); which are also involved in kinetochore protein interactions at the centromeric region of chromosomes. More than 200 proteins are responsible for spindle pole formation, chromosome alignment and segregation, cytokinesis during the cell division process (Andersen et al., 2003; Hubner et al., 2010; Hutchins et al., 2010; Neumann et al., 2010) (http://www.mitocheck.org/), as well as spindle checkpoint function that monitors correct microtubule-kinetochore attachment, thereby controlling metaphase to anaphase transition (Rieder and Maiato, 2004; Rieder, 2011; Khodjakov and Rieder, 2009; Musacchio, 2011; DeLuca and Musacchio, 2012).

Centrosomes are characteristic features of all metazoans functioning as microtubule organizing centers

(MTOC) at spindle poles (Bornens, 2002, 2012; Azimzadeh and Bornens, 2005). Centrosomes are comprised of a perpendicularly aligned pair of centrioles surrounded by pericentriolar matrix (PCM) components. Microtubules as cytoskeletal elements of the spindle apparatus are hollow cylindrical structures, which are involved in the formation of cilia, flagella, axonemes, and spindle fibers (Nigg and Raff, 2009). In dividing cells, arrays of aster microtubules originate from MTOCs and connect them to the chromosomes at the metaphase plate (Compton, 2000). During the G_2-/M-phase of the cell cycle, cells pass through a huge microtubule arrangement process that functions as an important regulatory switch and consists of microtubule nucleation, elongation, polymerization, and depolymerization (Mitchison and Kirschner, 1984; Desai and Mitchison, 1997). Aster microtubules are, in particular, highly dynamic structures, which are elongated by continuous addition of GTP bound $\alpha\beta$-tubulin heterodimers to the growing plus ends, where their depolymerization is triggered by hydrolysis of bound GTP to GDP and P_i (Mitchison and Kirschner, 1984). Microtubules are dynamically unstable at their plus ends, which is characterized by two different transitions, called catastrophe (transition from polymerization to shrinkage) and rescue (transition from depolymerization to growth) (Figure 1) (Mitchison and Kirschner, 1984; Gardner et al., 2013). Therefore, microtubule length and stability depend on the shift of the equilibrium between these two transition states that is primarily regulated by several microtubule-associated proteins (MAPs).

Among the MAPs, the centrosomal transforming acidic coiled coil (TACC) protein family comprises important components of the mitotic spindle apparatus (Gergely et al., 2000a; Gergely, 2002; Raff, 2002; Peset and Vernos, 2008; Ha et al., 2013a). Vertebrates express three TACC isoforms, TACC1, TACC2, and TACC3 (Still et al., 1999a, 2004; Gomez-Baldo et al., 2010). As discussed below in greater detail, TACCs are regulated by mitotic kinases, in particular, Aurora-A, and function at the mitotic spindle apparatus as adaptor proteins, thereby, interacting, among others, with microtubule polymerases of the evolutionary conserved *Xenopus* microtubule-associated protein 215 kDa (XMAP215)/minispindles (Msps)/colonic and hepatic tumor overexpressed gene (chTOG)/cytoskeleton-associated protein 5 (CKAP5) family. This effector complex plays a key role in the regulation of centrosome-dependent assembly of spindle microtubules as well as their dynamics and stability during mitosis (Conte et al., 2003; Gergely et al., 2003; Peset et al., 2005; Peset and Vernos, 2008).
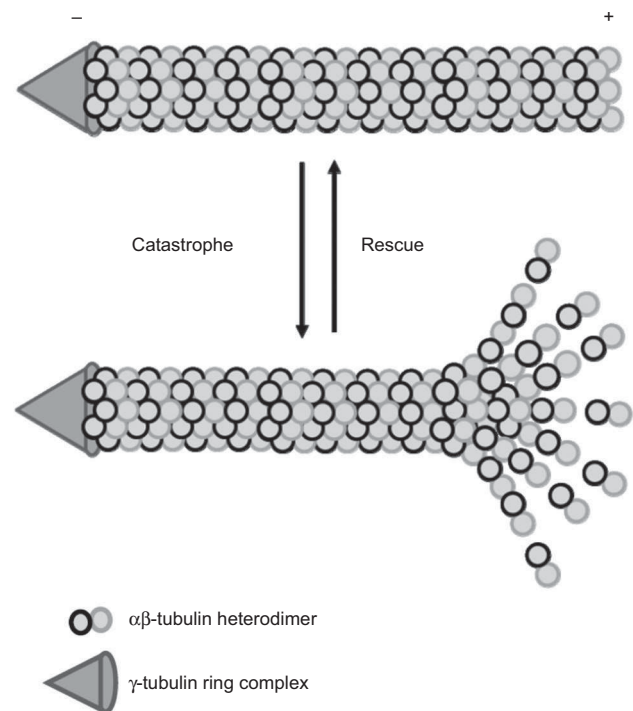
Figure 1 Microtubule dynamics during mitosis.
The γ-tubulin ring complex primes microtubule nucleation and polymerization. Further elongation of microtubules is dependent on the shift in equilibrium between two transition states, catastrophe (polymerization→shrinkage) and rescue (depolymerization→growth). Several MAPs regulate thereby the shift between these two transitions. Microtubule minus (-) and plus ends (+) are indicated.

# Evolution of TACC adaptor proteins – conserved mitotic role and implications for nonmitotic functions

TACC1 was the first human TACC protein family member that was identified and mapped close to the fibroblast *growth factor receptor 1* (*FGFR1*) region at chromosome 8p11 (Still et al., 1999b). Similarly, TACC2 and TACC3 were identified and mapped to be physically linked to the corresponding *FGFR2* and *FGFR3* chromosomal regions 10q26 and 4p16, respectively (Still et al., 1999a, 2004). During evolution, two gene duplication processes gave rise to three distinct *TACC/FGFR* gene pairs (Still et al., 2004). Thus, three TACC isoforms have evolved in all vertebrates analyzed so far, except *Xenopus* sp., where only two isoforms, TACC3/Maskin (*Xenopus laevis*) and TACC2 (*Xenopus tropicalis*), have been reported (Klein et al., 2002; Still et al., 2004; O'Brien et al., 2005; Peset

et al., 2005). In contrast, in organisms other than metazoans, only one single TACC isoform has been identified and characterized, i.e., Spc72 (*Saccaromyces cerevisiae*), Alp7 (*Schizosaccaromyces pombe*), TACC (*Dictyostelium discoideum)*, TAC1 (*Caenohabditis elegans*), and DTACC (*Drosophila melanogaster*) (Chen et al., 1998; Gergely et al., 2000b; Sato et al., 2003, 2004; Srayko et al., 2003; Peset and Vernos, 2008; Samereier et al., 2011). TACC proteins are characterized by their highly conserved C-terminal coiled coil signature domain (TACC domain; Figure 2) (Gergely et al., 2000a; Still et al., 2004; Peset and Vernos, 2008; Gomez-Baldo et al., 2010; Ha et al., 2013b). However, looking at the evolutionary tree of coiled coil structure-containing proteins, the TACC family members form a subfamily, which is different from other typical coiled coil-rich proteins, like keratins, tropomyosins, and kinesins (Still et al., 2004; Gomez-Baldo et al., 2010).

The function of TACC orthologs in centrosomally controlled mitotic spindle assembly and dynamics remained conserved throughout evolution (Gergely, 2002; Still et al., 2004; Peset and Vernos, 2008). Interestingly, in addition to this conserved role, TACC family members of different species have obviously gained additional, mostly nuclear, functions during evolution (Still et al., 2004; Peset and Vernos, 2008), which are far less understood. For example, interaction of the zink finger protein friend of GATA1 (FOG1) or aryl hydrocarbon receptor nuclear translocator (ARNT) with murine TACC3 implicates a function of TACC3 as transcriptional coactivator (Table 1) (Sadek et al., 2000; Garriga-Canut and Orkin, 2004; Partch et al., 2011). In this line, murine TACC3 has been originally

identified in a yeast two-hybrid screen for signal transducer and activator of transcription 5 (Stat5)-binding proteins; however, subsequent in-depth structural and functional interaction analysis in cell culture failed to confirm this interaction (Piekorz et al., 2002). Moreover, binding of the small nuclear ribonucleoproteins small nuclear ribonucleoprotein polypeptide G (SmG) and U6 snRNA-associated Sm-like protein LSm7 (LSM7) to TACC1 suggested a putative role of TACC1 in mRNA processing and homeostasis (Conte et al., 2002, 2003). A complex of TACC3 with tuberous sclerosis 2 (TSC2) has been implicated in the control of cytokinesis and maintenance of the nuclear envelope structure (Gomez-Baldo et al., 2010). Lastly, interactions of the different TACC family members with chromatin modifiers and transcriptional regulators, including glioma-amplified sequence 41 (GAS41), the nuclear receptors thyroid hormone receptor (TR) and retinoid acid receptor (RAR), the SWI/SNF chromatin remodeling complex, the translation initiation factor elF4E, and the histone acetyltransferase pCAF corroborate the putative and diverse functional portfolio that TACC proteins gained during evolution (overview in Table 1) (Still et al., 2004). Nevertheless, *in vivo*, the majority of these nonmitotic (mostly nuclear) functions of TACC proteins need to be critically subjected to an in-depth structure-function analysis *in vivo*, in particular, considering (i) that several TACC-binding partners have been originally identified by employing yeast two-hybrid screening using or fishing out the (rather sticky) TACC domain, and (ii) taking into account that TACC isoforms show rather defined expression profiles *in vivo* (cell type; proliferation status, i.e.,
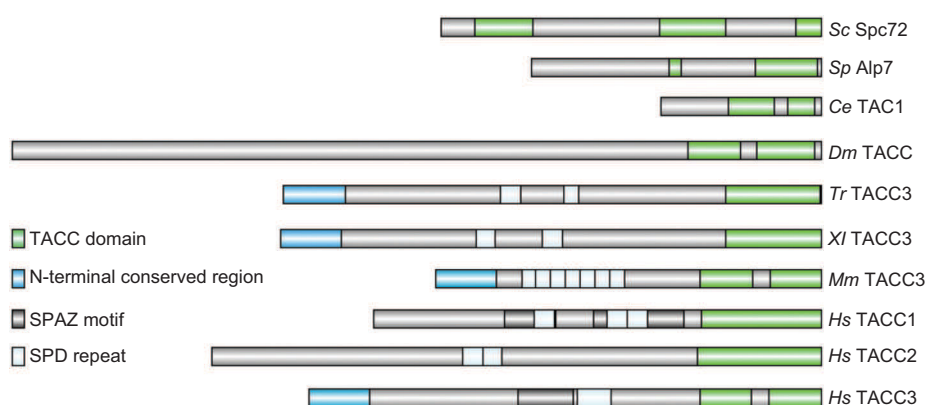
Figure 2 Domain organization of TACC protein family members.
Characteristic domains are indicated, including the highly conserved C-terminal TACC domain that is coiled coil-rich and present in all TACC proteins (green), the conserved first 100 amino acid residues at the N-terminus of TACC3 isoforms of higher eukaryotes (blue), random coil unstructured regions (gray), SPAZ motifs (dark gray), and the SPD-rich repeat region (blue). Species: Sc, *Saccharomyces cereviceae*; Sp, *S. pombe*; Tr, *Takifugu rubripes*; Xl, *X. laevis*; Hs, *H. sapiens*; Ms, *M. musculus*; Dm, *D. melanogaster*; Ce, *C. elegans*. Taken from Thakur (2012) and adapted after Peset and Vernos (2008).

Table 1 Interacting partners of TACC family members in higher eukaryotes.

| TACC family members	Interacting partners	Cellular processes regulated by the respective TACC-protein complex	Reference(s)
DTACC (*D. melanogaster*)	Msps	Microtubule dynamics	(Lee et al., 2001)
	Aurora-A kinase	DTACC-Msps activation	(Barros et al., 2005)
	Centrosomin (Cnn)	Recruitment of TACC/Msps complex and γ-tubulin to centrosomes	(Zhang et al., 2007)
	Mars	Binds protein phosphatase 1 (PP1), may dephosphorylate DTACC	(Tan et al., 2008)
Maskin (*X. laevis*)	XMAP215	Microtubule anchorage at centrosomes	(Kinoshita et al., 2005; Albee et al., 2008)
	Aurora-A kinase	Centrosome-dependent microtubule assembly	(Kinoshita et al., 2005; Albee et al., 2006)
		Control of translation during oocyte maturation	(Pascreau et al., 2005)
	Importin-β	Nuclear localization	(Albee et al., 2006)
	CPEB and eIF-4E	Translational regulation during mitosis	(Stebbins-Boaz et al., 1999)
TACC3 (*M. musculus*)	chTOG/CKAP5	Spindle pole organization/microtubule dynamics	(Data not shown)
	Aurora-A kinase	Cell cycle regulation and spindle pole organization	(Garriga-Canut and Orkin, 2004)
	FOG1	FOGI localization and transcription regulation	(Sadek et al., 2000; Wurdak et al., 2010; Partch et al., 2011)
	ARNT	Proposed function: transcriptional regulation	(Yang et al., 2012)
	DOCK7	Interkinetic nuclear migration and cortical neurogenesis	(Xie et al., 2007)
	Cep120	Interkinetic nuclear migration and neocortex development	(Jeng et al., 2009a)
	Cdh1	Proteasomal degradation of TACC3	(Conte et al., 2003)
TACC1 (*H. sapiens*)	chTOG/CKAP5	Proposed function: mRNA translation and cell division in conjugation with spindle pole organization	(Conte et al., 2003)
	Aurora-A kinase	Proposed role in centrosomal localization and mitotic spindle pole organization	(Delaval et al., 2004)
	Aurora-B kinase	Putative role in cytokinesis	(Conte et al., 2003)
	TRAP & LSM7	Proposed role in mRNA processing	(Conte et al., 2002)
	LSM7 & SmG	Proposed role in mRNA processing	(Lauffart et al., 2002)
	Gas41/YEATS4	Proposed role in transcriptional regulation	(Guyot et al., 2010)
	TR, RAR	Proposed role in transcriptional regulation by nuclear hormone receptors	(Hutchins et al., 2010)
TACC2 (*H. sapiens*)	chTOG/CKAP5	Spindle pole organization/microtubule dynamics	(Lauffart et al., 2003)
	Gas41/YEATS4SWI/SNF	Proposed role in transcriptional regulation and chromatin remodeling	(Dou et al., 2004)
	TTK	Proposed role in mitotic spindle maintenance	(Gergely et al., 2003)
TACC3 (*H. sapiens*)	chTOG/CKAP5	Spindle pole organization	(Conte et al., 2003; Tien et al., 2004; LeRoy et al., 2007)
	Aurora-A kinase	Cell cycle regulation and spindle pole organization	(Mori et al., 2007)
	NDEL1	Centrosomal maturation and separation	(Fu et al., 2010; Lin et al., 2010; Royle, 2012)
	CHC	Centrosomal localization and dynamics of spindle microtubules	(Bargo et al., 2010)
	CDC10	Proposed role: regulation of notch signaling	(Angrisano et al., 2006)
	MBD2	Putative regulation of histone aceryltransferases and transcriptional repression	(Gomez-Baldo et al., 2010)
	TSC2	Proposed role in the maintenance of nuclear envelope structure and control of cell division	(Yang et al., 2012)
	DOCK7	Interkinetic nuclear migration during cortical neurogenesis	

cycling vs. postmitotic), which do not always support the TACC-binding partner interactions observed under *in vitro* conditions.

Insight into structural organization of TACC adaptor proteins

All the TACC protein family members are characterized by their highly conserved C-terminal TACC signature domain comprised of approximately 200 amino acids, whereas the N-terminus is rather variable in both sequence homology and length (Figure 2) (Gergely, 2002; Peset and Vernos, 2008; Ha et al., 2013a). TAC1, the TACC homolog in *C. elegans*, is the smallest member and consists only of the TACC domain without a variable N-terminus (Srayko et al., 2003). Spc72 from *S. cerevisiae* displays three separated coiled coil regions, one each at the N- and C-terminus, and the third in the central part (Chen et al., 1998). Alp7, the TACC homolog in *S. pombe*, shows a smaller N-terminal variable region (Sato et al., 2004). All the other TACC family members contain longer N-terminal variable

regions adjacent to the TACC signature domain (Gergely, 2002; Peset and Vernos, 2008). As is obvious from the TACC3 interactome discussed below (Figure 3), the TACC domain is involved in the interaction with several known binding proteins, in particular, the microtubule polymerase chTOG/CKAP5.

The longer variable N-terminus of DTACC and also, in particular, of the vertebrate TACC3 isoforms contains binding sites for the mitotic serine-threonine kinase Aurora-A that phosphorylates three conserved serine residues (S863 in D-TACC; S33, S620, and S626 in *X. laevis* TACC3/Maskin; S34, S552, and S558 in *Homo sapiens* TACC3; and, putatively, S34, S341 and S347 in *Mus musculus* TACC3) (Giet et al., 2002; Barros et al., 2005; Kinoshita et al., 2005; Peset et al., 2005; LeRoy et al., 2007). As a consequence, Aurora-A phosphorylation of one particular serine (i.e., pS558 in human TACC3 and pS626 in TACC3/Maskin) determines the recruitment and differential subcellular localization of DTACC and TACC3 to centrosomes (pDTACC, pTACC3) compared to the localization along spindle microtubules toward their plus ends (DTACC, TACC3). Furthermore, the longer N-terminus of the TACC family members contains
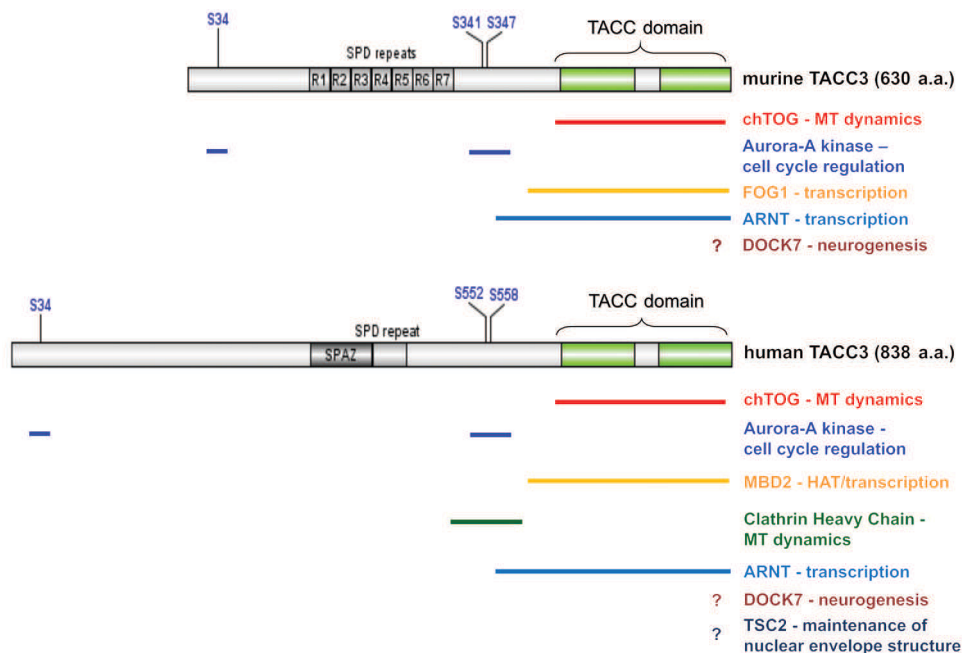
Figure 3 Insight into the TACC3 interactome.
Depicted are proteins known or proposed to interact with different domains of murine (upper part) and human (lower part) TACC3. The majority of the partner proteins depicted bind to the C-terminal coiled coil domain (TACC domain; green) of TACC3. As summarized in Table 1, besides chTOG, interaction of TACC3 with several other proteins, which are involved in different cellular processes, has been described. The binding region(s) between DOCK7 (dedicator of cytokinesis 7) or TSC2 and TACC3 are currently unclear. The three conserved Aurora-A phosphorylation sites present in vertebrate TACC3 isoforms are indicated. MT, microtubules; HAT, histone acetyltransferase. Taken from Thakur (2012).

also a serine-proline (SP)-rich repeat region, named serine, prolin, and aspartate/glutamate (SPD/E)-rich repeats, and the so-called serine-prolin-Azu-1 (SPAZ) motifs (Figure 2) (Peset and Vernos, 2008). In murine TACC3, this region is characterized by the presence of seven perfect repeats of 24 amino acids each (Still et al., 2004). Interestingly, each repeat contains one PXXP motif, which represents a *bona fide* docking site for src homology 3 (SH3) domain-containing proteins (Kay et al., 2000). The role of protein-protein interaction via SH3 domains has been demonstrated in several proteins involved in cellular signal transduction. However, a putative function of the central repeat motifs present in TACC3 isoforms in protein-protein interaction remains to be established. Irrespective of this, the N-termini of several TACC family members mediate the association with several proteins, including LSM7 and SmG (TACC1), eIF-4E and importin-β (Maskin), Gas41 (TACC1 and 2), and TRAP (TACC1), which are all linked to rather diverse cellular processes as summarized in Table 1.

Centrosomes and the PCM are highly enriched with coiled coil-containing proteins (Andersen et al., 2003). Coiled coil motifs or domains are mainly dimeric to heptameric with a parallel or antiparallel orientation of the helices (Mikolajka et al., 2006). To analyze the oligomeric status and structural orientation of the conserved TACC domain, we purified murine TACC3 after bacterial overexpression and subjected it to biophysical characterization. Employing multi-angle light scattering (MALS) and analytical ultracentrifugation-sedimentation velocity (AUC-SV) measurements, we observed that TACC3 displays a polydisperse, dimeric to oligomeric structure and a highly extended shape (Thakur, 2012). Moreover, negative staining and electron microscopy confirmed an elongated fiber-like structure of purified TACC3 with variable lengths (Figure 4). These findings are consistent with overexpression studies in eukaryotic cells where TACC proteins or the coiled coil-rich TACC domain *per se* formed highly ordered polymers with the capability to interact with microtubules (Gergely et al., 2000b).
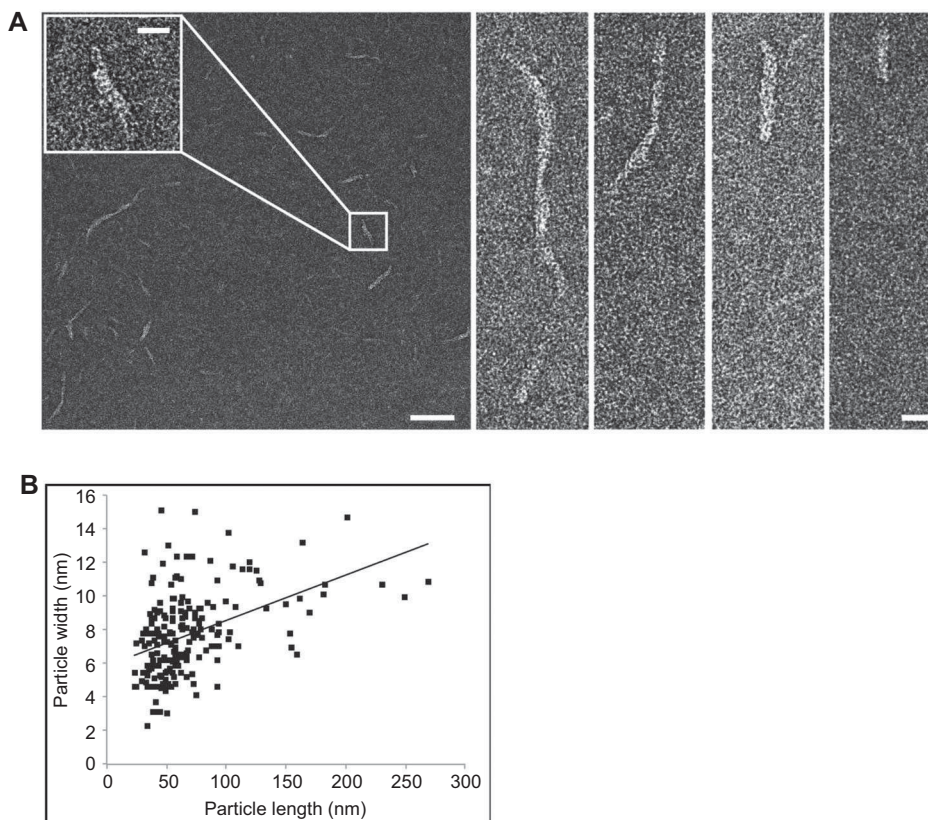
Figure 4 Electron microscopic analysis depicting an elongated structure and fiber-like appearance of highly purified murine TACC3 (A). Bar size in the left panel: 100 nm. Enlarged single TACC3 fibers are shown in the right panels (bar: 10 nm). (B) Quantitative analysis of fiber-like TACC3 molecules reveals average length and width variations of mostly 25–100 nm and 5–10 nm, respectively. For electron microscopic imaging, a Joel JEM-1400 electron microscope equipped with a LaB$_6$ filament was used and operated at an acceleration voltage of 120 kV. Digital micrographs were taken at a corrected magnification of 53.800× and a defocus value of -1.5 μm using a 4k×4k CMOS camera F416 (TVIPS) at low-dose conditions. Taken from Thakur (2012).

TACC3 – interactome analysis and role in mitotic spindle function

Insight into TACC3 function in microtubule dynamics and cell division has been recently elaborated by global interactome studies (Hubner et al., 2010; Hutchins et al., 2010; Neumann et al., 2010). One major effector protein binding to TACC3 via its TACC domain (Figure 3) represents the microtubule polymerase XMAP215/chTOG (Brouhard et al., 2008; Widlund et al., 2011) that colocalizes with TACC3 at the mitotic spindle apparatus (Figure 5A). The interaction of the TACC family members with the respective XMAP215 family member is evolutionary conserved and required for spindle pole organization and, in particular, microtubule dynamics during cell division (Bellanger and Gonczy, 2003; Gergely et al., 2003; Sato et al., 2004; Peset and Vernos, 2008). Deletion mapping of XMAP215 in *X. laevis* suggested that the N-terminal part exhibits microtubule-stabilizing activity that stimulates microtubule growth at the plus ends (Popov et al., 2001; Kinoshita et al., 2002). In particular, the N-terminus of XMAP215/chTOG proteins contains five evolutionary conserved TOG domains, which bind α,β-tubulin heterodimers and, thereby, help to polymerize microtubules (Brouhard

et al., 2008; Al-Bassam and Chang, 2011). Conversely, in oocyte extracts from *X. laevis*, it was demonstrated that the C-terminal part of XMAP215 was able to suppress the growth of microtubules by promoting microtubule catastrophes (Popov et al., 2001). Formation of the TACC3/Maskin-XMAP215/chTOG complex appears to antagonize the microtubule depolymerase activity of the kinesin-like protein XKCM1/MCAK at the plus poles (Kinoshita et al., 2005) and, independent from XKCM1/MCAK function, to stimulate assembly of microtubules at centrosomes (Barr and Gergely, 2008). Taken these findings into account, it seems that TACC3/Maskin functions as an adaptor protein (Hood and Royle, 2011), where binding of the TACC domain to XMAP215/chTOG 'engages' the C-terminal part of XMAP215/chTOG and, thereby, inhibits its microtubule catastrophe-promoting activity. Therefore, during mitotic cell division, the TACC3/Maskin-XMAP215/chTOG protein complex likely causes a shift of the dynamic equilibrium toward the microtubule rescue status (Figure 1). Upon metaphase-anaphase transition and mitotic exit, the TACC3 levels strongly decline by Cdh1-dependent ubiquitination and proteasomal degradation (Jeng et al., 2009a). As a consequence, a gradual increase in depolymerization activity by the 'TACC-free' C-terminal domain of XMAP215/chTOG may then lead to a dynamic equilibrium
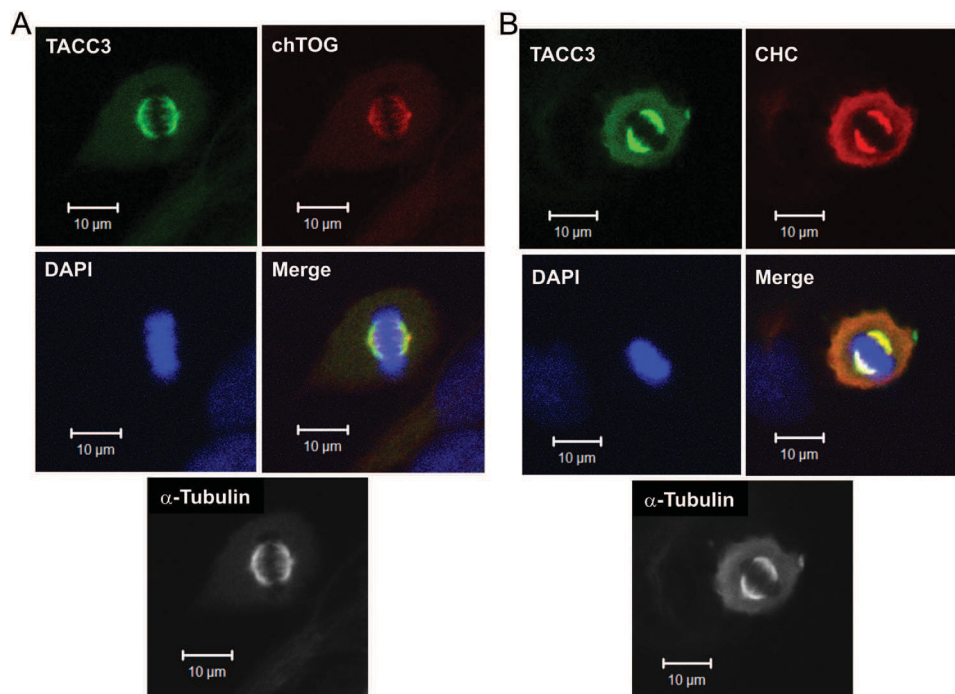
Figure 5 Subcellular colocalization of TACC3 with chTOG and CHC (clathrin heavy chain) in mitotic Hela cells. Images of metaphases were collected under a Zeiss cLSM510-Meta microscope at a 63× magnification.
(A) At centrosomes and the spindle apparatus, TACC3 colocalizes with chTOG and microtubules. (B) CHC colocalizes with TACC3 at centrosomes and a diffused region around the spindle poles. DAPI was used to detect DNA. Taken from Thakur (2012).
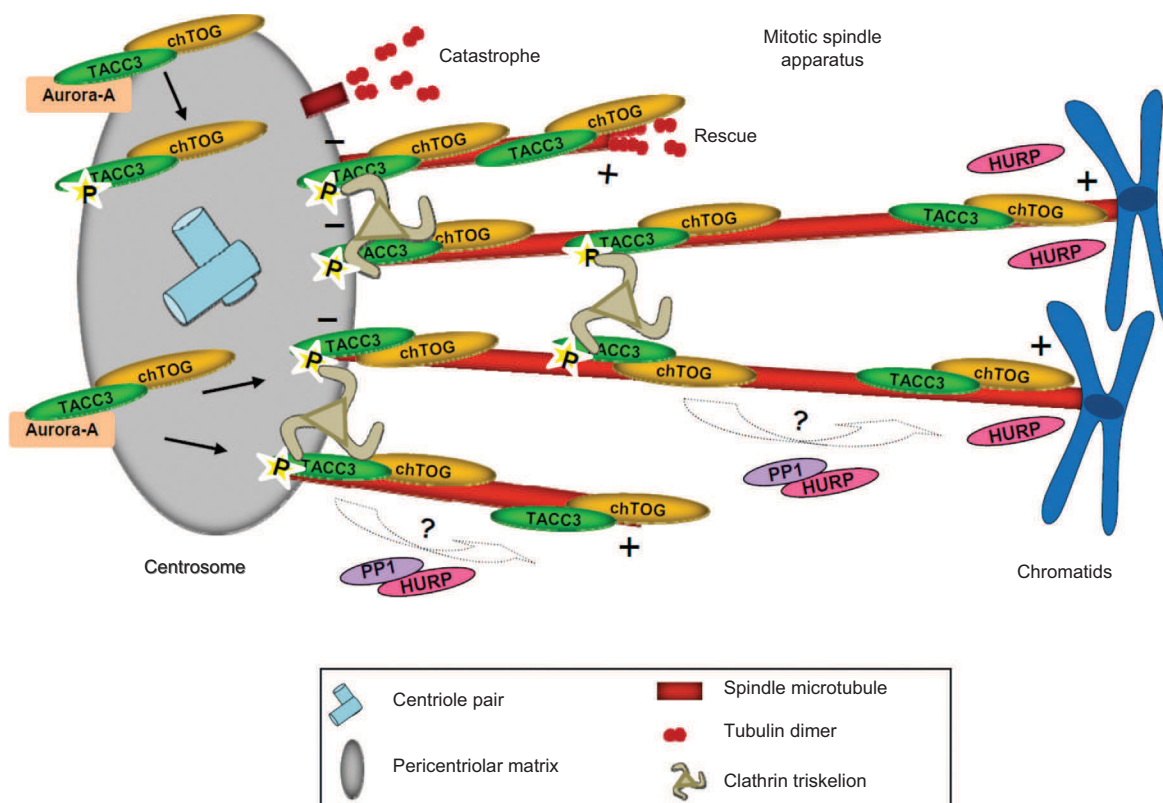
Figure 6 Schematic model summarizing the role of TACC3 in the regulation of microtubule dynamics at the mitotic spindle apparatus. TACC3 in a complex with chTOG localizes at the centrosome and along spindle microtubules in an Aurora-A kinase-regulated manner. The TACC3 (pS558)-chTOG complex interacts with the clathrin triskelion, thereby, mediating microtubule growth kinetics and stability both at the longitudinal level and by providing microtubule cross linking (Booth et al., 2011; Royle, 2012). Interestingly, the RanGTP and Aurora-A regulated and K-fiber-localized HURP may recruit protein phosphatase 1 (PP1) to the mitotic spindle apparatus. It is, therefore, tempting to speculate that TACC3 (pS558) undergoes dephosphorylation by the HURP-controlled PP1 complex prior to localization toward the microtubule plus poles as suggested for DTACC (Tan et al., 2008). Model adapted and taken from Thakur (2012).

shift toward the microtubule catastrophe status. Of note, this proposed mechanism may be evolutionary conserved given the very high sequence identity of the C-termini of mammalian chTOG proteins when, e.g., compared to the C-terminus of XMAP215 from *X. laevis* (Thakur, 2012). Moreover, the 'KKIGSK' sequence and phosphorylation motif present in the C-terminus of XMAP215, which plays a role in (possibly TACC3/Maskin-dependent) centrosomal targeting of XMAP215 (Popov et al., 2001), is also completely conserved in mammalian chTOG proteins. Taken together, although an in-depth structural TACC3-chTOG interaction mapping has not been described yet, a model can be envisioned where TACC3/Maskin regulates spindle microtubule dynamics during mitotic progression through the control of the spatiotemporal localization of XMAP215/chTOG and its microtubule (de)polymerizing activity (Figure 6).

Interestingly, clathrin heavy chain (CHC), which has been recently identified as the interacting partner for the TACC3-chTOG protein complex (Fu et al., 2010; Hubner et al., 2010; Lin et al., 2010; Booth et al., 2011), plays an essential role in the organization of the mitotic spindle where CHC perfectly colocalizes with TACC3 (Figure 5B). Binding of CHC to TACC3/Maskin occurs, in contrast to chTOG, outside of the TACC domain and requires Aurora-A-mediated phosphorylation at serine residues 620 and 626 (Maskin) or 558 (human TACC3; Figure 3) (Fu et al., 2010; Lin et al., 2010). In the following clathrin heavy chain 17 (CHC17), but not the related isoform CHC22, was shown to control spindle pole integrity during early mitosis by stabilizing centrosomal chTOG (Foraker et al., 2012). Moreover, elegant work by Booth et al. demonstrated that the TACC3-chTOG-CHC protein complex is crucial for the stabilization of intermicrotubule bridges and kinetochore fibers, the latter mediating chromosomal movement during mitosis (Booth et al., 2011). Rapid inactivation of the TACC3-chTOG-clathrin axis at defined mitotic stages proved that clathrin, which is recruited to

microtubules by phosphorylated TACC3 (Fu et al., 2011; Royle, 2012), is essential for both spindle assembly and subsequent spindle function (Cheeseman et al., 2013). In summary, TACC3 functions as an adaptor protein and a recruitment factor for both chTOG and clathrin to ensure proper mitotic spindle dynamics and function.

TACC3 – expression pattern and biological role

Mammalian TACC isoforms display differences in the temporal and spatial expression profile as well as in the subcellular localization pattern (Gergely et al., 2000a; Piekorz et al., 2002; Schuendeln et al., 2004). Human *TACC3* was initially identified as gene overexpressed in multiple myeloma (Still et al., 1999a; Eslinger et al., 2010) and various other cancer cell lines and tumor cell types (Ha et al., 2013b). TACC3 is expressed at high levels during embryogenesis and postnatally in proliferating and regenerative cell types, including the hematopoietic system, reproductive organs, and epithelial cells (Hao et al., 2002; Piekorz et al., 2002; Schuendeln et al., 2004). In contrast, TACC2 is found predominantly in postmitotic tissues like the brain and heart (Schuendeln et al., 2004), whereas TACC1 shows a more ubiquitous expression pattern *in vivo* (Lauffart et al., 2006). During cell cycle progression, TACC3 mRNA and protein levels increase dramatically in the late S- and G_2-/M-phase (Piekorz et al., 2002), followed by Cdh1-regulated proteasomal degradation of TACC3 during mitotic exit (Jeng et al., 2009b).

Studies employing mouse knockout models revealed a vital role of TACC3 during embryonic development. Gene deficiency for TACC3 results in embryonic lethality associated with aneuploidy, activation of the mitotic spindle assembly, and postmitotic p53-p21[WAF] checkpoints, apoptosis, impaired proliferation, and overall strong growth retardation (Piekorz et al., 2002; Yao et al., 2007). At this, TACC3 plays, e.g., an essential role in hematopoietic stem cell function or mesenchymal cell expansion that is required for proper formation of the axial skeleton (Yao et al., 2007). Comparable effects, including an induction of growth arrest (by triggering the cellular senescence program) or apoptosis, both dependent on the p53/G_1 checkpoint status, have been observed when TACC3 was depleted by RNA interference in various cell culture models (Schmidt et al., 2010a,b; Schneider et al., 2007, 2008). In contrast, TACC2 is dispensable for normal development, and TACC2 gene deficiency did not cause any detectable mitotic or proliferative defects (Schuendeln et al., 2004). Moreover,

double deficiency for TACC2 and TACC3 did not aggravate the phenotype of TACC3-deficient embryos. As a TACC1 deficiency has not been described yet, possible redundant roles between TACC1 and TACC2 cannot be assessed. Taken together, the reason(s) why mammalians evolved three TACC isoforms with possibly specific roles as well as the degree of functional redundancy between these isoforms remain(s) unclear.

The emerging pathobiological role of TACC proteins in human cancer

TACC genes have been originally discovered in genomic regions that are amplified in breast tumors and multiple myeloma (Still et al., 1999b). Mutations or an altered expression of TACC1 and TACC3 have been subsequently linked to the etiology of breast, ovarian, bladder, non-small-cell lung cancer, prostate, and melanoma tumors (Cully et al., 2005; Lauffart et al., 2005; Jung et al., 2006; Kiemeney et al., 2010; Hodis et al., 2012; Ha et al., 2013a). A role in the androgen-mediated growth of prostate cancer has been suggested for TACC2 (Takayama et al., 2012). Moreover, the *TACC3* gene is amplified in glioma tumors at the genomic level. These tumors show a grade-specific upregulation of TACC3 expression, which is highest in grade IV glioma, a tumor type with poor prognosis (Duncan et al., 2010). Interestingly, intrachromosomal *FGFR1-TACC1* and *FGFR3-TACC3* gene fusions have also been recently detected in subsets of glioblastoma and bladder cancer patients (Singh et al., 2012; Williams et al., 2012; Parker et al., 2011). These fusion proteins display a constitutive FGFR tyrosine kinase activity presumably activating downstream signaling effector pathways, localize to mitotic spindle poles obviously due to the presence of the C-terminally fused TACC domain, are associated with aneuploidy, and display pro-proliferative and oncogenic activities both *in vitro* and *in vivo*. In this regard, TACC3 influences PI3K/Akt and ERK signaling associated with tumorigenic epithelial-mesenchymal transition (EMT) and cell migration/invasion (Ha et al., 2013b).

Moreover, TACC3 linked [e.g., hepatoma up-regulated protein (HURP)] or interacting (e.g., chTOG or TSC2) proteins can be as well altered at the level of structure or expression in different transformed tumor cell types (overview in Ha et al., 2013a), therefore, potentially contributing to tumorigenesis. For example, chTOG and HURP were identified as overexpressed genes in human hepatic carcinomas (Charrasse et al., 1995; Tsou et al., 2003), and mutations of the tumor suppressor protein

TSC2 were initially observed in renal carcinogenesis and hepatic hemangiomatosis (Kobayashi et al., 1999).

Taking these findings into account, it is tempting to speculate that members of the mitotic Aurora-A-TACC3-chTOG axis act as 'driver' factors in tumor development and, hence, represent potential therapeutic targets. Indeed, conditional loss of the TACC3 gene expression leads to apoptosis and tumor regression *in vivo* in the p53^{-/-} mouse sarcolymphoma model (Yao et al., 2011). A role of TACC3 in chemoresistance and the cellular response to antimitotics can also be envisioned, given that RNAi-mediated TACC3 depletion or treatment with the TACC3 inhibitor KSH101 (Wurdak et al., 2010) sensitizes tumor cells to the antiproliferative and apoptotic effects of paclitaxel (Schneider et al., 2008; Schmidt et al., 2010a; Cappell et al., 2012). Consistent with this, TACC depletion renders cells from *D. discoideum* also to be hypersensitive against the microtubule-depolymerizing drug thiabendazole (Samereier et al., 2011).

Conclusion and open questions

The Aurora-A kinase regulated TACC3-chTOG-CHC protein complex plays a pivotal role in centrosomal function and mitotic spindle assembly and dynamics (Figure 6). Despite the current insight into the TACC isoform expression and function (Peset and Vernos, 2008; Zyss and Gergely, 2009; Royle, 2012; Ha et al., 2013b), various molecular and cellular aspects of TACC (patho)biology await further investigation. For instance, there is lack of insight into the three-dimensional structure of the TACC3 domains mediating the interaction with chTOG or clathrin heavy chain. Another issue is the analysis of the role of dephosphorylation as regulatory mechanism to control the mitotic pools of pTACC3 vs. TACC3. An interaction of DTACC with the microtubule-associated protein Mars, which binds directly to protein phosphatase PP1, thereby promoting DTACC dephosphorylation, has been reported (Tan et al., 2008). Interestingly, HURP represents the Mars homolog in higher vertebrates that localizes to kinetochore microtubules (k-fibers) close to chromosomes (Sillje et al., 2006). HURP was described as an oncogenic target of Aurora-A kinase (Yu et al., 2005), thereby, controlling the microtubule-binding capacity of HURP (Wong et al., 2008). Thus, HURP may recruit PP1 or a currently unknown phosphatase to the microtubules and, hence, control spindle dynamics by balancing pTACC3/TACC3 levels (Figure 6). Lastly, structure-function analyses of putative 'driver' TACC1 and TACC3 mutations in human cancers with respect to mitotic loss-of-function or gain-of-function phenotypes is required. The latter apply, in particular, to genomic instability, checkpoint activation, and oncogenic signaling.

References

Al-Bassam, J. and Chang, F. (2011). Regulation of microtubule dynamics by TOG-domain proteins XMAP215/Dis1 and CLASP. Trends Cell Biol. *21*, 604–614.

Andersen, J.S., Wilkinson, C.J., Mayor, T., Mortensen, P., Nigg, E.A., and Mann, M. (2003). Proteomic characterization of the human centrosome by protein correlation profiling. Nature *426*, 570–574.

Azimzadeh, J. and Bornens, M. (2005). The centrosome in evolution. In Centrosomes in Development and Disease (Weinheim, Germany: Wiley-VCH Verlag GmbH & Co. KGaA), pp. 93–122.

Barr, A.R. and Gergely, F. (2008). MCAK-independent functions of ch-Tog/XMAP215 in microtubule plus-end dynamics. Mol. Cell Biol. *28*, 7199–7211.

Barros, T.P., Kinoshita, K., Hyman, A.A., and Raff, J.W. (2005). Aurora A activates D-TACC-Msps complexes exclusively at centrosomes to stabilize centrosomal microtubules. J. Cell Biol. *170*, 1039–1046.

Bellanger, J.M. and Gonczy, P. (2003). TAC-1 and ZYG-9 form a complex that promotes microtubule assembly in *C. elegans* embryos. Curr. Biol. *13*, 1488–1498.

Booth, D.G., Hood, F.E., Prior, I.A., and Royle, S.J. (2011). A TACC3/ch-TOG/clathrin complex stabilises kinetochore fibres by inter-microtubule bridging. EMBO J. *30*, 906–919.

Bornens, M. (2002). Centrosome composition and microtubule anchoring mechanisms. Curr. Opin. Cell Biol. *14*, 25–34.

Bornens, M. (2012). The centrosome in cells and organisms. Science *335*, 422–426.

Brouhard, G.J., Stear, J.H., Noetzel, T.L., Al-Bassam, J., Kinoshita, K., Harrison, S.C., Howard, J., and Hyman, A.A. (2008). XMAP215 is a processive microtubule polymerase. Cell *132*, 79–88.

Cappell, K.M., Sinnott, R., Taus, P., Maxfield, K., Scarbrough, M., and Whitehurst, A.W. (2012). Multiple cancer testis antigens function to support tumor cell mitotic fidelity. Mol. Cell Biol. *32*, 4131–4140.

Charrasse, S., Mazel, M., Taviaux, S., Berta, P., Chow, T., and Larroque, C. (1995). Characterization of the cDNA and pattern of expression of a new gene over-expressed in human hepatomas and colonic tumors. Eur. J. Biochem. *234*, 406–413.

Cheeseman, L.P., Harry, E.F., McAinsh, A.D., Prior, I.A., and Royle, S.J. (2013). Specific removal of TACC3/ch-TOG/clathrin at metaphase deregulates kinetochore fiber tension. J. Cell Sci. *126*, 2102–2113.

Chen, X.P., Yin, H., and Huffaker, T.C. (1998). The yeast spindle pole body component Spc72p interacts with Stu2p and is required for proper microtubule assembly. J. Cell Biol. *141*, 1169–1179.

Compton, D.A. (2000). Spindle assembly in animal cells. Annu. Rev. Biochem. *69*, 95–114.

Conte, N., Charafe-Jauffret, E., Delaval, B., Adelaide, J., Ginestier, C., Geneix, J., Isnardon, D., Jacquemier, J., and Birnbaum, D. (2002). Carcinogenesis and translational controls: TACC1 is down-regulated in human cancers and associates with mRNA regulators. Oncogene *21*, 5619–5630.

Conte, N., Delaval, B., Ginestier, C., Ferrand, A., Isnardon, D., Larroque, C., Prigent, C., Seraphin, B., Jacquemier, J., and Birnbaum, D. (2003). TACC1-chTOG-Aurora A protein complex in breast cancer. Oncogene *22*, 8102–8116.

Cully, M., Shiu, J., Piekorz, R.P., Muller, W.J., Done, S.J., and Mak, T.W. (2005). Transforming acidic coiled coil 1 promotes transformation and mammary tumorigenesis. Cancer Res. *65*, 10363–10370.

DeLuca, J.G. and Musacchio, A. (2012). Structural organization of the kinetochore-microtubule interface. Curr. Opin. Cell Biol. *24*, 48–56.

Desai, A. and Mitchison, T.J. (1997). Microtubule polymerization dynamics. Annu. Rev. Cell Dev. Biol. *13*, 83–117.

Duncan, C.G., Killela, P.J., Payne, C.A., Lampson, B., Chen, W.C., Liu, J., Solomon, D., Waldman, T., Towers, A.J., Gregory, S.G., et al. (2010). Integrated genomic analyses identify ERRFl1 and TACC3 as glioblastoma-targeted genes. Oncotarget *1*, 265–277.

Eslinger, M.R., Lauffart, B., and Still, I.H. (2010). TACC3 (transforming, acidic coiled-coil containing protein 3). Atlas Genet. Cytogenet. Oncol. Haematol. *14*, 527–553

Foraker, A.B., Camus, S.M., Evans, T.M., Majeed, S.R., Chen, C.Y., Taner, S.B., Correa, I.R., Jr., Doxsey, S.J., and Brodsky, F.M. (2012). Clathrin promotes centrosome integrity in early mitosis through stabilization of centrosomal ch-TOG. J. Cell Biol. *198*, 591–605.

Fu, W., Jiang, Q., and Zhang, C. (2011). Novel functions of endocytic player clathrin in mitosis. Cell Res. *21*, 1655–1661.

Fu, W., Tao, W., Zheng, P., Fu, J., Bian, M., Jiang, Q., Clarke, P.R., and Zhang, C. (2010). Clathrin recruits phosphorylated TACC3 to spindle poles for bipolar spindle assembly and chromosome alignment. J. Cell Sci. *123*, 3645–3651.

Gardner, M.K., Zanic, M., and Howard, J. (2013). Microtubule catastrophe and rescue. Curr. Opin. Cell Biol. *25*, 14–22.

Garriga-Canut, M. and Orkin, S.H. (2004). Transforming acidic coiled-coil protein 3 (TACC3) controls friend of GATA-1 (FOG-1) subcellular localization and regulates the association between GATA-1 and FOG-1 during hematopoiesis. J. Biol. Chem. *279*, 23597–23605.

Gergely, F. (2002). Centrosomal TACCtics. Bioessays *24*, 915–925.

Gergely, F., Draviam, V.M., and Raff, J.W. (2003). The ch-TOG/XMAP215 protein is essential for spindle pole organization in human somatic cells. Genes Dev. *17*, 336–341.

Gergely, F., Karlsson, C., Still, I., Cowell, J., Kilmartin, J., and Raff, J.W. (2000a). The TACC domain identifies a family of centrosomal proteins that can interact with microtubules. Proc. Natl. Acad. Sci. USA *97*, 14352–14357.

Gergely, F., Kidd, D., Jeffers, K., Wakefield, J.G., and Raff, J.W. (2000b). D-TACC: a novel centrosomal protein required for normal spindle function in the early *Drosophila* embryo. EMBO J. *19*, 241–252.

Giet, R., McLean, D., Descamps, S., Lee, M.J., Raff, J.W., Prigent, C., and Glover, D.M. (2002). *Drosophila* Aurora A kinase is required to localize D-TACC to centrosomes and to regulate astral microtubules. J. Cell Biol. *156*, 437–451.

Gomez-Baldo, L., Schmidt, S., Maxwell, C.A., Bonifaci, N., Gabaldon, T., Vidalain, P.O., Senapedis, W., Kletke, A., Rosing, M., Barnekow, A., et al. (2010). TACC3-TSC2 maintains nuclear envelope structure and controls cell division. Cell Cycle *9*, 1143–1155.

Ha, G.H., Kim, J.L., and Breuer, E.K. (2013a). Transforming acidic coiled-coil proteins (TACCs) in human cancer. Cancer Lett. DOI: 10.1016/j.canlet.2013.04.022. Epub April 23, 2013.

Ha, G.H., Park, J.S., and Breuer, E.K. (2013b). TACC3 promotes epithelial-mesenchymal transition (EMT) through the activation of PI3K/Akt and ERK signaling pathways. Cancer Lett. *332*, 63–73.

Hao, Z., Stoler, M.H., Sen, B., Shore, A., Westbrook, A., Flickinger, C.J., Herr, J.C., and Coonrod, S.A. (2002). TACC3 expression and localization in the murine egg and ovary. Mol. Reprod. Dev. *63*, 291–299.

Hodis, E., Watson, I.R., Kryukov, G.V., Arold, S.T., Imielinski, M., Theurillat, J.P., Nickerson, E., Auclair, D., Li, L., Place, C., et al. (2012). A landscape of driver mutations in melanoma. Cell *150*, 251–263.

Hood, F.E. and Royle, S.J. (2011). Pulling it together: the mitotic function of TACC3. BioArchitecture *1*, 105–109.

Hubner, N.C., Bird, A.W., Cox, J., Splettstoesser, B., Bandilla, P., Poser, I., Hyman, A., and Mann, M. (2010). Quantitative proteomics combined with BAC TransgeneOmics reveals *in vivo* protein interactions. J. Cell Biol. *189*, 739–754.

Hutchins, J.R., Toyoda, Y., Hegemann, B., Poser, I., Heriche, J.K., Sykora, M.M., Augsburg, M., Hudecz, O., Buschhorn, B.A., Bulkescher, J., et al. (2010). Systematic analysis of human protein complexes identifies chromosome segregation proteins. Science *328*, 593–599.

Jeng, J.-C., Lin, Y.-M., Lin, C.-H., and Shih, H.-M. (2009a). Cdh1 controls the stability of TACC3. Cell Cycle *8*, 3537–3544.

Jeng, J.C., Lin, Y.M., Lin, C.H., and Shih, H.M. (2009b). Cdh1 controls the stability of TACC3. Cell Cycle *8*, 3529–3536.

Jung, C.K., Jung, J.H., Park, G.S., Lee, A., Kang, C.S., and Lee, K.Y. (2006). Expression of transforming acidic coiled-coil containing protein 3 is a novel independent prognostic marker in non-small cell lung cancer. Pathol. Int. *56*, 503–509.

Kay, B.K., Williamson, M.P., and Sudol, M. (2000). The importance of being proline: the interaction of proline-rich motifs in signaling proteins with their cognate domains. FASEB J. *14*, 231–241.

Khodjakov, A. and Rieder, C.L. (2009). The nature of cell-cycle checkpoints: facts and fallacies. J. Biol. *8*, 88.

Kiemeney, L.A., Sulem, P., Besenbacher, S., Vermeulen, S.H., Sigurdsson, A., Thorleifsson, G., Gudbjartsson, D.F., Stacey, S.N., Gudmundsson, J., Zanon, C., et al. (2010). A sequence variant at 4p16.3 confers susceptibility to urinary bladder cancer. Nat. Genet. *42*, 415–419.

Kinoshita, K., Habermann, B., and Hyman, A.A. (2002). XMAP215: a key component of the dynamic microtubule cytoskeleton. Trends Cell Biol. *12*, 267–273.

Kinoshita, K., Noetzel, T.L., Pelletier, L., Mechtler, K., Drechsel, D.N., Schwager, A., Lee, M., Raff, J.W., and Hyman, A.A. (2005). Aurora A phosphorylation of TACC3/maskin is required for centrosome-dependent microtubule assembly in mitosis. J. Cell Biol. *170*, 1047–1055.

Klein, S.L., Strausberg, R.L., Wagner, L., Pontius, J., Clifton, S.W., and Richardson, P. (2002). Genetic and genomic tools for *Xenopus* research: the NIH *Xenopus* initiative. Dev. Dyn. *225*, 384–391.

Kobayashi, T., Minowa, O., Kuno, J., Mitani, H., Hino, O., and Noda, T. (1999). Renal carcinogenesis, hepatic hemangiomatosis, and embryonic lethality caused by a germ-line Tsc2 mutation in mice. Cancer Res. *59*, 1206–1211.

Lauffart, B., Dimatteo, A., Vaughan, M.M., Cincotta, M.A., Black, J.D., and Still, I.H. (2006). Temporal and spatial expression of TACC1 in the mouse and human. Dev. Dyn. *235*, 1638–1647.

Lauffart, B., Vaughan, M., Eddy, R., Chervinsky, D., DiCioccio, R., Black, J., and Still, I. (2005). Aberrations of TACC1 and TACC3 are associated with ovarian cancer. BMC Women's Health *5*, 8.

LeRoy, P.J., Hunter, J.J., Hoar, K.M., Burke, K.E., Shinde, V., Ruan, J., Bowman, D., Galvin, K., and Ecsedy, J.A. (2007). Localization of human TACC3 to mitotic spindles is mediated by phospho-rylation on Ser558 by Aurora A: a novel pharmacodynamic method for measuring Aurora A activity. Cancer Res. *67*, 5362–5370.

Lin, C.H., Hu, C.K., and Shih, H.M. (2010). Clathrin heavy chain mediates TACC3 targeting to mitotic spindles to ensure spindle stability. J. Cell Biol. *189*, 1097–1105.

Mikolajka, A., Yan, X., Popowicz, G.M., Smialowski, P., Nigg, E.A., and Holak, T.A. (2006). Structure of the N-terminal domain of the FOP (FGFR1OP) protein and implications for its dimerization and centrosomal localization. J. Mol. Biol. *359*, 863–875.

Mitchison, T. and Kirschner, M. (1984). Dynamic instability of microtubule growth. Nature *312*, 237–242.

Musacchio, A. (2011). Spindle assembly checkpoint: the third decade. Philos. Trans. R. Soc. Lond. B Biol. Sci. *366*, 3595–3604.

Neumann, B., Walter, T., Heriche, J.K., Bulkescher, J., Erfle, H., Conrad, C., Rogers, P., Poser, I., Held, M., Liebel, U., et al. (2010). Phenotypic profiling of the human genome by time-lapse microscopy reveals cell division genes. Nature *464*, 721–727.

Nigg, E.A. and Raff, J.W. (2009). Centrioles, centrosomes, and cilia in health and disease. Cell *139*, 663–678.

O'Brien, L.L., Albee, A.J., Liu, L., Tao, W., Dobrzyn, P., Lizarraga, S.B., and Wiese, C. (2005). The *Xenopus* TACC homologue, maskin, functions in mitotic spindle assembly. Mol. Biol. Cell *16*, 2836–2847.

Parker, B.C., Annala, M.J., Cogdell, D.E., Granberg, K.J., Sun, Y., Ji, P., Li, X., Gumin, J., Zheng, H., Hu, L., et al. (2011). Coactivators necessary for transcriptional output of the hypoxia inducible factor, HIF, are directly recruited by ARNT PAS-B. Proc. Natl. Acad. Sci. USA *108*, 7739–7744.

Peset, I., Seiler, J., Sardon, T., Bejarano, L.A., Rybina, S., and Vernos, I. (2005). Function and regulation of Maskin, a TACC family protein, in microtubule growth during mitosis. J. Cell Biol. *170*, 1057–1066.

Peset, I. and Vernos, I. (2008). The TACC proteins: TACC-ling microtubule dynamics and centrosome function. Trends Cell Biol. *18*, 379–388.

Piekorz, R.P., Hoffmeyer, A., Duntsch, C.D., McKay, C., Nakajima, H., Sexl, V., Snyder, L., Rehg, J., and Ihle, J.N. (2002). The centrosomal protein TACC3 is essential for hematopoietic stem cell function and genetically interfaces with p53-regulated apoptosis. EMBO J. *21*, 653–664.

Popov, A.V., Pozniakovsky, A., Arnal, I., Antony, C., Ashford, A.J., Kinoshita, K., Tournebize, R., Hyman, A.A., and Karsenti, E. (2001). XMAP215 regulates microtubule dynamics through two distinct domains. EMBO J. *20*, 397–410.

Raff, J.W. (2002). Centrosomes and cancer: lessons from a TACC. Trends Cell Biol. *12*, 222–225.

Rieder, C.L. (2011). Mitosis in vertebrates: the G2/M and M/A transitions and their associated checkpoints. Chromosome Res. *19*, 291–306.

Rieder, C.L. and Maiato, H. (2004). Stuck in division or passing through: what happens when cells cannot satisfy the spindle assembly checkpoint. Dev. Cell *7*, 637–51.

Royle, S.J. (2012). The role of clathrin in mitotic spindle organisation. J. Cell Sci. *125*, 19–28.

Sadek, C.M., Jalaguier, S., Feeney, E.P., Aitola, M., Damdimopoulos, A.E., Pelto-Huikko, M., and Gustafsson, J.A. (2000). Isolation and characterization of AINT: a novel ARNT interacting protein expressed during murine embryonic development. Mech. Dev. *97*, 13–26.

Samereier, M., Baumann, O., Meyer, I., and Graf, R. (2011). Analysis of *Dictyostelium* TACC reveals differential interactions with CP224 and unusual dynamics of *Dictyostelium* microtubules. Cell. Mol. Life Sci. *68*, 275–287.

Sato, M., Koonrugsa, N., Toda, T., Vardy, L., Tournier, S., and Millar, J.B. (2003). Deletion of Mia1/Alp7 activates Mad2-dependent spindle assembly checkpoint in fission yeast. Nat. Cell Biol. *5*, 764–766; author reply 766.

Sato, M., Vardy, L., Angel Garcia, M., Koonrugsa, N., and Toda, T. (2004). Interdependency of fission yeast Alp14/TOG and coiled coil protein Alp7 in microtubule localization and bipolar spindle formation. Mol. Biol. Cell *15*, 1609–1622.

Schmidt, S., Essmann, F., Cirstea, I.C., Kuck, F., Thakur, H.C., Singh, M., Kletke, A., Jänicke, R.U., Wiek, C., Hanenberg, H., et al. (2010a). The centrosome and mitotic spindle apparatus in cancer and senescence. Cell Cycle *9*, 4469–4473.

Schmidt, S., Schneider, L., Essmann, F., Cirstea, I.C., Kuck, F., Kletke, A., Jänicke, R.U., Wiek, C., Hanenberg, H., Ahmadian, et al. (2010b). The centrosomal protein TACC3 controls paclitaxel sensitivity by modulating a premature senescence program. Oncogene *29*, 6184–6192.

Schneider, L., Essmann, F., Kletke, A., Rio, P., Hanenberg, H., Schulze-Osthoff, K., Nürnberg, B., and Piekorz, R.P. (2008). TACC3 depletion sensitizes to paclitaxel-induced cell death

and overrides p21WAF-mediated cell cycle arrest. Oncogene *27*, 116–125.

Schneider, L., Essmann, F., Kletke, A., Rio, P., Hanenberg, H., Wetzel, W., Schulze-Osthoff, K., Nürnberg, B., and Piekorz, R.P. (2007). The transforming acidic coiled coil 3 protein is essential for spindle-dependent chromosome alignment and mitotic survival. J. Biol. Chem. *282*, 29273–29283.

Schuendeln, M.M., Piekorz, R.P., Wichmann, C., Lee, Y., McKinnon, P.J., Boyd, K., Takahashi, Y., and Ihle, J.N. (2004). The centrosomal, putative tumor suppressor protein TACC2 is dispensable for normal development, and deficiency does not lead to cancer. Mol. Cell. Biol. *24*, 6403–6409.

Sillje, H.H., Nagel, S., Korner, R., and Nigg, E.A. (2006). HURP is a Ran-importin beta-regulated protein that stabilizes kinetochore microtubules in the vicinity of chromosomes. Curr. Biol. *16*, 731–742.

Singh, D., Chan, J.M., Zoppoli, P., Niola, F., Sullivan, R., Castano, A., Liu, E.M., Reichel, J., Porrati, P., Pellegatta, S., et al. (2012). Transforming fusions of FGFR and TACC genes in human glioblastoma. Science *337*, 1231–1235.

Srayko, M., Quintin, S., Schwager, A., and Hyman, A.A. (2003). *Caenorhabditis elegans* TAC-1 and ZYG-9 form a complex that is essential for long astral and spindle microtubules. Curr. Biol. *13*, 1506–1511.

Still, I., Vettaikkorumakankauv, A., DiMatteo, A., and Liang, P. (2004). Structure-function evolution of the transforming acidic coiled coil genes revealed by analysis of phylogenetically diverse organisms. BMC Evol. Biol. *4*, 16.

Still, I.H., Hamilton, M., Vince, P., Wolfman, A., and Cowell, J.K. (1999a). Cloning of TACC1, an embryonically expressed, potentially transforming coiled coil containing gene, from the 8p11 breast cancer amplicon. Oncogene *18*, 4032–4038.

Still, I.H., Vince, P., and Cowell, J.K. (1999b). The third member of the transforming acidic coiled coil-containing gene family, TACC3, maps in 4p16, close to translocation breakpoints in multiple myeloma, and is upregulated in various cancer cell lines. Genomics *58*, 165–170.

Takayama, K., Horie-Inoue, K., Suzuki, T., Urano, T., Ikeda, K., Fujimura, T., Takahashi, S., Homma, Y., Ouchi, Y., and Inoue, S. (2012). TACC2 is an androgen-responsive cell cycle regulator promoting androgen-mediated and castration-resistant growth of prostate cancer. Mol. Endocrinol. *26*, 748–761.

Tan, S., Lyulcheva, E., Dean, J., and Bennett, D. (2008). Mars promotes dTACC dephosphorylation on mitotic spindles to ensure spindle stability. J. Cell Biol. *182*, 27–33.

Thakur, H.C. (2012). Biochemical and biophysical characterization of the centrosomal protein TACC3. Dissertation (Faculty of Mathematics and Natural Sciences of the Heinrich Heine University, Düsseldorf, Germany), November 2012.

Tsou, A.P., Yang, C.W., Huang, C.Y., Yu, R.C., Lee, Y.C., Chang, C.W., Chen, B.R., Chung, Y.F., Fann, M.J., Chi, C.W., et al. (2003). Identification of a novel cell cycle regulated gene, HURP, overexpressed in human hepatocellular carcinoma. Oncogene *22*, 298–307.

Widlund, P.O., Stear, J.H., Pozniakovsky, A., Zanic, M., Reber, S., Brouhard, G.J., Hyman, A.A., and Howard, J. (2011). XMAP215 polymerase activity is built by combining multiple tubulin-binding TOG domains and a basic lattice-binding region. Proc. Natl. Acad. Sci. USA *108*, 2741–2746.

Williams, S.V., Hurst, C.D., and Knowles, M.A. (2012). Oncogenic FGFR3 gene fusions in bladder cancer. Hum. Mol. Genet. *22*, 795–803.

Wong, J., Lerrigo, R., Jang, C.Y., and Fang, G. (2008). Aurora A regulates the activity of HURP by controlling the accessibility of its microtubule-binding domain. Mol. Biol. Cell *19*, 2083–2091.

Wurdak, H., Zhu, S., Min, K.H., Aimone, L., Lairson, L.L., Watson, J., Chopiuk, G., Demas, J., Charette, B., Halder, R., et al. (2010). A small molecule accelerates neuronal differentiation in the adult rat. Proc. Natl. Acad. Sci. USA *107*, 16542–16547.

Yao, R., Natsume, Y., and Noda, T. (2007). TACC3 is required for the proper mitosis of sclerotome mesenchymal cells during formation of the axial skeleton. Cancer Sci. *98*, 555–562.

Yao, R., Natsume, Y., Saiki, Y., Shioya, H., Takeuchi, K., Yamori, T., Toki, H., Aoki, I., Saga, T., and Noda, T. (2011). Disruption of Tacc3 function leads to *in vivo* tumor regression. Oncogene *31*, 135–148.

Yu, C.T., Hsu, J.M., Lee, Y.C., Tsou, A.P., Chou, C.K., and Huang, C.Y. (2005). Phosphorylation and stabilization of HURP by Aurora-A: implication of HURP as a transforming target of Aurora-A. Mol. Cell Biol. *25*, 5789–5800.

Zyss, D. and Gergely, F. (2009). Centrosome function in cancer: guilty or innocent? Trends Cell Biol. *19*, 334–346.

Harish C. Thakur, Madhurendra Singh,
Luitgard Nagel-Steger, Jana Kremer, Daniel
Prumbaum, Eyad Kalawy Fansa, Hakima
Ezzahoini, Kazem Nouri, Lothar Gremer,
André Abts, Lutz Schmitt, Stefan Raunser,
Mohammad R. Ahmadian and Roland P.
Piekorz

Access the most updated version of this article at doi: 10.1074/jbc.M113.532333

Find articles, minireviews, Reflections and Classics on similar topics on the JBC Affinity Sites.

Alerts:

- When this article is cited
- When a correction for this article is posted

Click here to choose from all of JBC's e-mail alerts

Supplemental material:
http://www.jbc.org/content/suppl/2013/11/22/M113.532333.DC1.html

This article cites 81 references, 39 of which can be accessed free at
http://www.jbc.org/content/289/1/74.full.html#ref-list-1

The Centrosomal Adaptor TACC3 and the Microtubule Polymerase chTOG Interact via Defined C-terminal Subdomains in an Aurora-A Kinase-independent Manner*⒮

Harish C. Thakur[‡1], **Madhurendra Singh**[‡], **Luitgard Nagel-Steger**[§¶], **Jana Kremer**[‡], **Daniel Prumbaum**[‖], **Eyad Kalawy Fansa**[‡2], **Hakima Ezzahoini**[‡], **Kazem Nouri**[‡], **Lothar Gremer**[§¶], **André Abts**[**], **Lutz Schmitt**[**], **Stefan Raunser**[‖], **Mohammad R. Ahmadian**[‡2], and **Roland P. Piekorz**[‡3]

From the ‡Institut für Biochemie und Molekularbiologie II, Medizinische Fakultät der Heinrich-Heine-Universität, D-40225 Düsseldorf, Germany, §Institut für Physikalische Biologie, Heinrich-Heine-Universität, 40225 Düsseldorf, Germany, ¶ICS-6, Strukturbiochemie, Forschungszentrum, 52425 Jülich, Germany, **Institut für Biochemie, Heinrich-Heine-Universität, 40225 Düsseldorf, Germany, and ‖Max-Planck-Institut für Molekulare Physiologie, 44227 Dortmund, Germany

Background: The TACC3-chTOG protein complex is essential for mitotic spindle assembly.
Results: TACC3-chTOG binding is directed and mediated by specific intradomain and interdomain interactions that are not affected by Aurora-A kinase.
Conclusion: Formation of the TACC3-chTOG complex is Aurora-A-independent, in contrast to its recruitment to the spindle apparatus.
Significance: Novel insight into regulation and domain specificity of TACC3-chTOG interaction is provided.

The cancer-associated, centrosomal adaptor protein TACC3 (transforming acidic coiled-coil 3) and its direct effector, the microtubule polymerase chTOG (colonic and hepatic tumor overexpressed gene), play a crucial function in centrosome-driven mitotic spindle assembly. It is unclear how TACC3 interacts with chTOG. Here, we show that the C-terminal TACC domain of TACC3 and a C-terminal fragment adjacent to the TOG domains of chTOG mediate the interaction between these two proteins. Interestingly, the TACC domain consists of two functionally distinct subdomains, CC1 (amino acids (aa) 414–530) and CC2 (aa 530–630). Whereas CC1 is responsible for the interaction with chTOG, CC2 performs an intradomain interaction with the central repeat region of TACC3, thereby masking the TACC domain before effector binding. Contrary to previous findings, our data clearly demonstrate that Aurora-A kinase does not regulate TACC3-chTOG complex formation, indicating that Aurora-A solely functions as a recruitment factor for the TACC3-chTOG complex to centrosomes and proximal mitotic spindles. We identified with CC1 and CC2, two functionally diverse modules within the TACC domain of TACC3 that modulate and mediate, respectively, TACC3 interaction with chTOG required for spindle assembly and microtubule dynamics during mitotic cell division.

The centrosome represents the main microtubule (MT)[4] organizing center in all metazoans and is thereby responsible for equal partitioning of chromosomes to daughter cells during the mitotic phase of the cell cycle (1–5). Numerical and structural abnormalities of centrosomes are associated with aneuploidy, chromosomal instability and transformation, developmental defects, apoptotic cell death, and cell cycle arrest through induction of premature senescence (6–12). Cancer cells *e.g.* counteract extra centrosomes and, therefore, the danger of multipolar divisions and excess aneuploidy/cell death through centrosome clustering (13–15). This process became an attractive pharmacological tumor target (16, 17).

During the cell cycle centrosomes undergo a division and maturation process called the centrosome cycle (4, 18, 19). Mitotic centrosomes are structurally made up of one pair of centrioles surrounded by the pericentriolar matrix (20). More than two hundred proteins are involved in centrosome assembly, organization, and function (19, 21–23). These proteins have structural, functional/enzymatic, and regulatory/signaling roles in MT nucleation and spindle dynamics, mitotic progression, and cytokinesis (24). Recent work by the Mitocheck consortium (25, 26) provided a global confirmation of known and identification of novel cell division genes and their protein

---

⒮ This article contains supplemental Table S1 and Figs. S1–S11.
[1] Present address: Wellcome Trust Centre for Cell Biology, The University of Edinburgh, Edinburgh EH9 3JR, Scotland, United Kingdom.
[2] Supported by Bundesministerium für Bildung und Forschung (NGFNplus program Grant 01GS08100).
[3] To whom correspondence should be addressed: Institut für Biochemie und Molekularbiologie II, Universitätsklinikum der Heinrich-Heine-Universität, D-40225 Düsseldorf, Germany. Tel.: 49-211-81-12739; Fax: 49-211-81-12726; E-mail: Roland.Piekorz@uni-duesseldorf.de.

[4] The abbreviations used are: MT, microtubule; aa, amino acid; SEC, size exclusion chromatography; aSEC, analytical SEC; CBB, Coomassie Brilliant Blue; CC, coiled-coil; chTOG, colonic and hepatic tumor overexpressed gene; ITC, isothermal titration calorimetry; 7R, serine-proline-glutamate-rich repeat region; TACC, transforming acidic coiled-coil; XMAP215, *Xenopus* microtubule associated protein 215 kDa; ARNT, aryl hydrocarbon receptor nuclear translocator.

complexes that require biochemical and functional elucidation in greater detail.

Members of the centrosomal TACC (transforming acidic coiled-coil) family of proteins are important structural components of the mitotic spindle apparatus (27–29). TACCs are conserved in all metazoans and play a vital role as adaptor proteins in the regulation of centrosomal integrity and spindle MT stability and dynamics (27, 28, 30–34). Vertebrates express three TACC isoforms, TACC1, TACC2, and TACC3, of which the latter is typically found at high levels in proliferative and regenerative cell types and tissues (35–37). During the cell cycle TACC3 expression increases strongly in the G_2/M phase (38) followed by Cdh1-dependent degradation of TACC3 during mitotic exit (39). TACC3 deficiency leads to growth retardation and embryonic lethality (38, 40), in line with the anti-proliferative impact of shRNA mediated gene silencing of TACC3 (41, 42).

A crucial regulator of TACC3 is the mitotic kinase Aurora-A that phosphorylates TACC3 (pTACC3) and thereby determines its differential centrosomal/proximal spindle (pTACC3) *versus* distal spindle MT (TACC3) localization during (pro)-metaphase (43–46). Interestingly, recent findings expand the function of TACC3 and the Aurora-A-TACC3 axis to the regulation of kinetochore-microtubule connections (47) and central spindle assembly at later stages of mitosis (48), respectively. Other known TACC3 binding partners with regulatory/effector functions include the endocytic and vesicle trafficking protein clathrin (*i.e.* clathrin heavy chain) (49, 50) that binds to the clathrin interaction domain of pTACC3 to ensure intermicrotubule bridging and mitotic spindle organization (51, 52). Moreover, the evolutionary conserved interaction between TACCs and MT polymerases of the XMAP215 family is crucial for spindle pole stabilization and growth of centrosomal MTs (43, 46, 53). Family members, which comprise XMAP215 in *Xenopus laevis,* Msps in *Drosophila melanogaster, and* chTOG/CKAP5 (cytoskeleton associated protein 5) in *Homo sapiens*, are identified by the presence of several "TOG" domains involved in MT binding.

TACC proteins are structurally characterized by a rather variable N-terminal region of which the approximately first 100 residues are uniquely conserved among vertebrate TACC3 isoforms. Further features include a central serine-proline-glutamate-rich repeat region (28, 33) that in the case of murine TACC3 is characterized by seven perfect repeats of 24 amino acids each (thereafter referred to as "7R") (33, 38) as well as a highly conserved, coiled-coil-containing C terminus (thereafter referred to as "CC" or "TACC domain"). This signature domain is composed of ~200 amino acids (aa) (27, 33, 55), required for centrosomal localization, and known to be involved in protein-protein interaction (28). Here, TACC proteins interact from yeast to human through their TACC domain with the C terminus of XMAP215 family members (28, 46, 56, 57), thereby targeting them to spindle poles. In contrast, the functional role of the N-terminal part of TACC3 outside of the TACC domain is rather undefined besides being a substrate for Aurora-A-mediated phosphorylation that is required for centrosomal and proximal spindle localization of TACC3 (28).

From the analysis of *X. laevis* TACC3, it has been proposed that the N-terminal part masks the TACC domain and thereby inhibits its function (58, 59). Aurora-A mediated phosphorylation of TACC3 was implicated to "unmask" and thereby expose the TACC domain to intermolecular interaction with XMAP215 (46, 59). However, the molecular basis/details of the masking/unmasking mechanism of the TACC domain and its interaction with the C terminus of XMAP215 remained enigmatic. Here, we subjected recombinant murine TACC3 and the C-terminal part of the murine XMAP215 homologue chTOG to a deletion and biochemical interaction analysis. We identify within the TACC domain two functionally distinct subdomains, CC1 (aa 414–530) and CC2 (aa 530–630), which are involved in interdomain and intradomain protein interaction, respectively. We demonstrate that TACC3 forms a stable intramolecular complex through the interaction of 7R with CC2 (TACC domain "masked"). Interestingly, the C terminus of chTOG (aa 1806–2032) right hand to the putative MT-interacting TOG6 domain (52) binds selectively to the CC1 module and thereby disrupts the intramolecular CC2–7R complex, thereby giving rise to the effector-bound state of the TACC domain (TACC domain "unmasked"). Neither intradomain interaction of TACC3 nor its binding to chTOG was affected by Aurora-A kinase. Thus, consecutive intra- and intermolecular protein interactions direct and determine TACC3-chTOG protein complex formation before its Aurora-A-regulated centrosomal and proximal spindle recruitment required for MT growth and mitotic spindle assembly.

EXPERIMENTAL PROCEDURES

In Silico Analysis of TACC3—Protein sequences of TACC family members were retrieved from the NCBI database and used for further analysis. For sequence alignment and evolutionary analysis of conserved domains, the ClustalW multiple sequence alignment algorithm was used (60), and alignment was analyzed with JALVIEW. Further analysis of the coiled-coil boundary in the TACC domain of murine TACC3 was performed using the COILS server in 14, 21, and 28 residue scan mode (61). Algorithms and tools from the EXPASY proteomic server were employed for sequence-based protein characterization.

Cloning of Expression Constructs—Coding sequences for murine TACC3 and its variants were amplified using sequence-specific primer and cloned into the pGEX-4T1-NTEV expression vector. The following constructs were created: full-length TACC3 (aa 1–630); TACC3-ΔN (Δ1–118); TACC3-ΔR (Δ141–308), lacking the serine-proline-glutamate-rich repeat region; TACC3-ΔNΔR (Δ1–118 and Δ141–308); 7R (aa 119–324) comprising the serine-proline-glutamate-rich repeat region; CC (TACC domain; aa 414–630); CC1 (aa 414–530); CC2 (aa 530–630) (62). Moreover, pGEX-4T1-NTEV-based expression constructs for C-terminal fragments of human chTOG were created: chTOG-Cterm (aa 1574–2032), chTOG-A (aa 1544–1805), and chTOG-B (aa 1806–2032). To generate TACC3 deletion mutants fused at the C terminus to GFP, the following constructs were cloned in a pEGFP-N1 (Clontech)-based vector: full-length TACC3; TACC-ΔCC1 and TACC-ΔCC2 lacking the CC1 or CC2 subdomains, respec-

Molecular Basis of TACC3-chTOG Complex Formation

tively; TACC-ΔCC lacking the entire TACC domain. All constructs were validated by DNA sequencing.

Overexpression and Purification—GST fusion proteins were overexpressed in *Escherichia coli* BL21 Rosetta strain (Novagen). Protein extraction was carried out by incubating cells at 4 °C with DNase I (10 μg/ml) followed by cell lysis in a microfluidizer (model M110S, Microfluidics Corp.) at a pressure of 10.000 p.s.i. Bacterial lysates were centrifuged to collect soluble fractions, and GST-tagged proteins were isolated from the supernatant via GST affinity purification. Upon cleavage of the GST tag with tobacco etch virus protease (4 units/mg, 4 °C, overnight) or thrombin (2 units/mg, 4 °C, overnight) proteins were subjected to gel filtration using a standard buffer containing 30 mM Tris-HCl, pH 7.5, 200 mM NaCl, 3 mM DTT, and 2 mM EDTA. The GST tag from the TACC3-ΔN and TACC3-ΔNΔR deletion mutants could not be cleaved by tobacco etch virus protease for unknown reasons (data not shown), thus employing thrombin for both GST tag removal and cleavage at the internal site (supplemental Fig. S4). The final purity was analyzed on SDS-PAGE, proteins were concentrated using centrifugal ultrafiltration devices (Amicon Ultra; Millipore), and protein concentration was determined by the Bradford assay. For mass spectrometric analysis of thrombin-cleaved TACC3, the protein was desalted by passing through NAP-25 columns (GE Healthcare) and analyzed by MALDI-TOF at the central BMFZ facility of the Heinrich-Heine-University Düsseldorf.

Immunoblotting—Proteins were separated using SDS-PAGE gels and transferred to nitrocellulose membranes (Hybond C, GE Healthcare). Blots were probed overnight with primary antibodies: αTACC3 (N18) and αTACC3 (C18), both generated in rabbits (38), are specific for the N and C terminus of murine TACC3, respectively; αGST (Abcam); αchTOG (Abcam, QED Bioscience/Acris, and Novus Biologicals); αGFP (Roche Applied Science). After three washing steps membranes were incubated with horseradish peroxidase-coupled secondary antibodies for 1 h. Signals were visualized by the ECL detection system (GE Healthcare), and images were collected using the INTAS chemostar imager.

Analytical Gel Filtration/Size Exclusion Chromatography (SEC)—Gel filtration was performed using a Superose 6 10/300 GL column connected to an ÄKTA™ purifier (GE Healthcare) and UV900 detector. For molecular weight determination, the column was calibrated with standard proteins of known molecular mass: thyroglobulin (669 kDa), ferritin (440 kDa), aldolase (158 kDa), ovalbumin (43 kDa), carbonic anhydrase (29 kDa), ribonuclease A (13.7 kDa), and aprotinin (6.5 kDa). Protein samples (50–200 μg) were injected onto the preequilibrated column, and elution fractions of 0.5 ml were collected. Elution profiles were recorded using UNICORN4.11 software, and peak fractions were analyzed by SDS-PAGE followed by Coomassie Brilliant Blue (CBB) staining and immunoblotting.

GST Pulldown Assay—GST, GST-fused TACC3 variants, and fragments of the C terminus of chTOG (chTOG-Cterm) were expressed in *E. coli* and purified using standard protocols. To obtain prey proteins, the GST tag was cleaved off with tobacco etch virus protease and cleared by reverse GSH affinity purification. GSH-Sepharose beads (GE Healthcare) in a 100-μl volume were washed 3 times with standard buffer. GST and GST-fused proteins (10–20 μM) were added and incubated in a final volume of 200 μl at 4 °C for 1 h. Blocking with 5% BSA (2 h at 4 °C) was performed followed by three washing steps with standard buffer (30 mM Tris-HCl, pH 7.5, 200 mM NaCl, 3 mM DTT, 2 mM EDTA). Finally, samples were incubated at an equimolar ratio with prey proteins at 4 °C for 2 h. After five washing steps, 100 μl of 2× Laemmli buffer was added, and samples were heat-denatured (5 min at 95 °C) and analyzed by SDS-PAGE followed by CBB staining and immunoblotting.

Isothermal Titration Calorimetry (ITC)—Purified TACC3 variants and chTOG-Cterm were first subjected to gel filtration (Superose 6 XK16/60) using ITC buffer (30 mM Tris-HCl, pH 7.5, 200 mM NaCl, 1 mM Tris(2-carboxyethyl)phosphine, 2 mM EDTA). For the 7R fragment, buffer was exchanged by overnight dialysis against ITC buffer using Slide-A-Lyzer dialysis cassettes (Thermo Scientific). All ITC measurements were carried out at 20 °C using a VP-ITC microcalorimeter (Microcal) (63, 64). Proteins were loaded into the sample cell and titrated with their putative interaction partners (10–15-fold higher protein concentration in the syringe compared with the concentration in the cell; titration volume 8, 10, or 15 μl; spacing of 150–180 s; reference power of 13 μcal s^{-1}, stirring at 310 rpm). The final data analysis was carried out using Origin software (Microcal Software). The experimental data were evaluated using Origin 7.0 software (Microcal Software) to determine the binding parameters, including association constant (K_a), number of binding sites (N), and enthalpy (ΔH). Control measurements were performed by titrating buffer to the protein and vice versa.

Immunoprecipitation—Purified TACC3 proteins before and after thrombin cleavage (~10–15 μg) were mixed with 2 μl of rabbit antisera (αTACC3 N18 or αTACC3 C18) (38) and incubated overnight at 4 °C. Thereafter, 25 μl of protein A/G-agarose (Santa Cruz Biotechnology) preabsorbed with BSA was added, and the volume was adjusted to 100 μl with IP buffer (30 mM Tris-HCl, 200 mM NaCl, 2 mM EDTA). After an incubation period of 1 h the beads were washed with IP buffer, and protein complexes were eluted with 2× Laemmli loading buffer and analyzed by SDS-PAGE and immunoblotting using primary antibodies (N18, C18) and horseradish peroxidase-conjugated secondary antibodies. Moreover, total cell lysates from HEK293 cells, which were transfected with expression vectors for TACC3 or TACC3 deletion mutants fused C-terminally to GFP, were prepared essentially as described (32) and thereafter subjected to immunoprecipitation using αGFP antibodies (Roche Applied Science). chTOG was detected in the co-immunoprecipitates using an αchTOG antibody from QED Bioscience/Acris.

Protein Kinase Assay—Purified human Aurora-A kinase (Signal Chem) was employed according to the manufacturer's instructions. In brief, kinase assays were performed in a volume of 25 μl by mixing 5 μl (0.1 μg/μl) of Aurora-A kinase (diluted in kinase assay buffer: 5 mM MOPS, pH 7.2, 2.5 mM β-glycerol phosphate, 5 mM MgCl$_2$, 1 mM EGTA, 0.4 mM EDTA, 50 ng/μl BSA) with 1 μg of purified TACC3 protein (before and after thrombin cleavage) or 1 μg of the TACC3-chTOG complex as a substrate. The final volume was adjusted to 20 μl with double distilled H$_2$O, and reactions were started by adding 5 μl of 10

mM ATP (dissolved in 25 mM MOPS, pH 7.2, 12.5 mM β-glycerol phosphate, 25 mM MgCl$_2$, 5 mM EGTA, 0.4 mM EDTA). Reactions were incubated at 30 °C for 15 min and stopped by the addition of 10 μl of 2× Laemmli loading buffer. Samples were separated by SDS-PAGE, and phosphorylated proteins were subsequently detected by Pro-Q Diamond (Molecular Probes, Invitrogen) and CBB staining.

Eukaryotic Cell Culture—HEK293 and HeLa cells were cultured in Dulbecco's modified Eagle's medium supplemented with 10% fetal calf serum (Invitrogen), 2 mM L-glutamine, 100 units/ml penicillin, and 100 μg/ml streptomycin. GFP-fused TACC3 expression vectors were transfected into HEK293 cells using the TurboFect transfection reagent (ThermoScientific). The Aurora-A kinase inhibitor MLN8237 (Selleckchem) was applied in cell culture at a concentration of 0.5 μM for 2 h (65).

Confocal Laser Scanning Microscopy—Cells were seeded at densities of 8×10^3 cells/cm^2 on coverslips and fixed with ice-cold methanol/acetone (1:1) for 20 min at -20 °C upon MLN8237 treatment. Subsequently, cells were incubated in IF buffer (4% bovine serum albumin, 0.05% saponin in PBS) for 1 h and stained in IF buffer with the following primary antibodies at the indicated dilutions: anti-α-tubulin (DM1a,1:500, Sigma, or YOL1/34, Acris Antibodies, Hiddenhausen, Germany); αTACC3 (H300 or D2, Santa Cruz Biotechnology); anti-γ-tubulin (GTU-88, 1:100, Sigma); αchTOG (1:500, Acris); αpT288 Aurora-A (1:500; Cell Signaling). DNA was detected using 4,6-diamidino-2-phenylindole (DAPI, 1 mg/ml; Sigma). Analyses were performed with a LSM510-Meta confocal microscope (Zeiss) equipped with 40/1.3 or 63/1.4 immersion objectives and excitation wavelengths of 364, 488, 543, and 633 nm.

RESULTS

The TACC Domain of TACC3 Consists of Two Distinct Coiled-coil Subdomains—To examine the primary structure of murine TACC3 and thereby define functional modules in TACC3, sequence alignments of vertebrate TACC family members were performed. Consistent with previous findings (28, 33, 55), the N termini of TACC3 isoforms are characterized by a variable length and different amino acid composition as compared with other vertebrate TACC family members. Interestingly, the first 100 amino acids of TACC3 isoforms display a sequence identity of up to 75% (data not shown) followed by the central repeat region that in the case of murine TACC3 comprises seven conserved serine-proline-glutamate-rich repeats (7R) each consisting of 24 amino acids. Interestingly, coiled-coil prediction analysis indicated the presence of one breaking region that divides the C-terminal TACC domain of mammalian TACC3 proteins into two coiled-coil-containing subdomains, CC1 and CC2 (supplemental Fig. S1). Here, CC2 clearly revealed a higher amino acid sequence identity than the CC1 subdomain (supplemental Fig. S2). Overall, the domain organization of vertebrate TACC3 proteins emphasizes their isoform-specific functional roles as compared with TACC1 and TACC2. That is exemplified by the embryonic lethality caused by TACC3 deficiency, which is not observed for TACC2 deficiency (37, 38, 40), as well as by the selective interaction of the aryl hydrocarbon receptor nuclear translocator (ARNT) with TACC3 but not with TACC1 and TACC2 (66).

Moreover, we identified a unique and functional thrombin cleavage site (^{410}LEPR/GL^{415}) close to the TACC domain of murine TACC3 (Fig. 1A) that is absent in all other TACC3 proteins and TACC isoforms. This cleavage site resembles a *bona fide* recognition site for thrombin (^{410}LVPR/GS^{415}). Although the thrombin site present in murine TACC3 might not have any physiological relevance, it was used as a tool in this study to analyze the intra- and intermolecular interaction of murine TACC3.

Purification of Deletion Mutants and Fragments of TACC3 and chTOG—Based on the *in silico* analysis we cloned murine TACC3 and its variants (supplemental Fig. S3) as well as C-terminal fragments of chTOG (supplemental Fig. S5A) into the prokaryotic expression vector pGEX-4T1-NTEV. Proteins fused N-terminally to glutathione S-transferase (GST) were purified, cleaved using tobacco etch virus protease to remove the GST tag, and finally separated by gel filtration and/or reverse glutathione affinity chromatography (supplemental Figs. S4 and S5, B and C). Thrombin cleavage of TACC3 resulted in two fragments, a larger N-terminal part (TACC3-N7R, aa 1–413) and a smaller C-terminal fragment (CC, aa 414–630) containing the TACC domain (Fig. 1A and supplemental Fig. S4A). The identity and size of the CC fragment (25.2 kDa) was corroborated by mass spectrometry using MALDI-TOF. The adaptability of the thrombin site was also confirmed for the deletion mutants TACC3-ΔR, TACC3-ΔN, and TACC3-ΔNΔR (supplemental Fig. S3 and S4).

Intradomain Association Leads to an Intramolecular Masked State of TACC3—We next subjected TACC3 to analytical size exclusion chromatography (aSEC) using a Superose 6 10/300 column. Interestingly, TACC3 eluted before and after thrombin cleavage in peak fractions with apparent molecular masses of ~1200 and ~630 kDa, respectively (Fig. 1B), the latter being unexpectedly the only peak detected after thrombin cleavage. Subsequent peak fraction analysis by SDS-PAGE and CBB staining as well as immunoblotting demonstrated the co-elution of both fragments, TACC3-N7R and CC (Fig. 1C). These findings strongly suggested the formation of a tight complex between the N- and C-terminal parts of TACC3. We confirmed this intramolecular interaction by co-immunoprecipitation of TACC3 before and after thrombin cleavage using antibodies specific for the N or C termini of murine TACC3 (38). As indicated in Fig. 1D, TACC3-N7R and CC was co-immunoprecipitated in both directions. Of note, thrombin cleavage of TACC3 did not result in changes in its secondary structure as indicated from circular dichroism measurements (supplemental Fig. S11A).

The Intramolecular Interaction of TACC3 Is Mediated between the 7R and CC2 Domains—To identify the domains involved in intradomain TACC3 interaction, we deleted the conserved N-terminal region (Δ1–118; TACC-ΔN) and the central 7R region (Δ141–308; TACC3-ΔR) (supplemental Fig. S3). The respective purified TACC3 variants were analyzed before and after thrombin cleavage by aSEC. The absence of the first 118 amino acids did not have any detectable effect on the elution pattern of TACC3-ΔN that was comparable to full-length TACC3 (Fig. 2B). Also, upon thrombin cleavage, both protein fragments (named TACC3–7R and TACC3-CC in Fig.
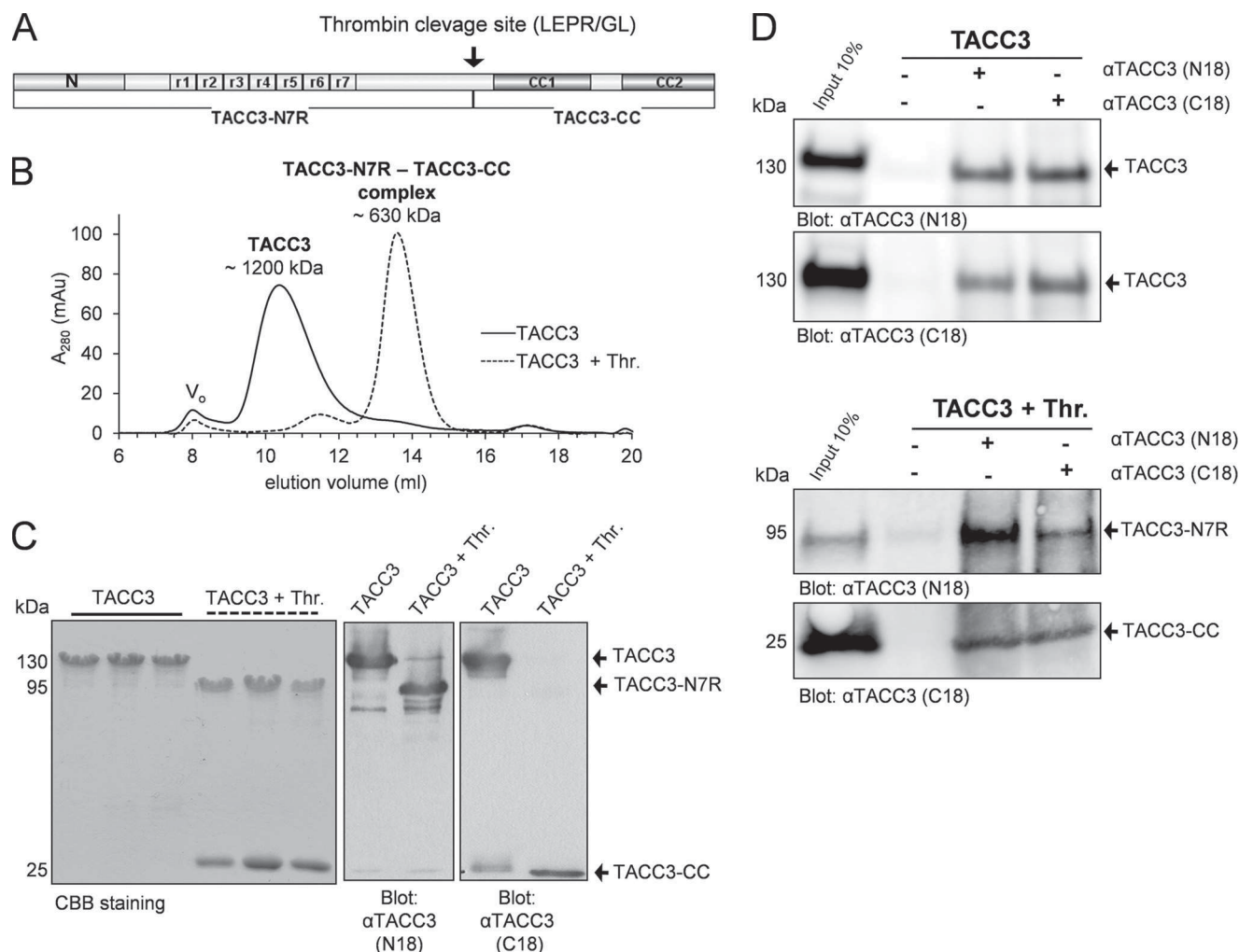
FIGURE 1. **Thrombin cleavage of murine TACC3 generates two N- and C-terminal fragments staying in one intramolecular complex.** *A*, a novel and unique thrombin site divides TACC3 into two separate parts, TACC3-N7R and TACC3-CC. *N* specifies the conserved ~100 amino acid residues at the N terminus. *CC1* and *CC2* indicate two distinct coiled-coil subdomains in the C terminus. *r1* to *r7* denotes the central region in TACC3 consisting of seven serine-proline-glutamate-rich repeats (*7R*). *B*, determination of the apparent molecular mass of TACC3 by aSEC (Superpose 6, 10/300). Elution profiles of TACC3 before (*solid line*) and after thrombin cleavage (*dashed line*) are indicated. V_o, void volume. *mAu*, milliabsorbance units. *C*, peak elution fractions were analyzed by SDS-PAGE followed by CBB staining (*left panel*) and immunoblotting (*central* and *right panels* employing N18 and C18 antibodies directed against the N- or C-terminal end of TACC3, respectively) (38). *D*, co-immunoprecipitation analysis of TACC3 before (*upper panel*) and after thrombin cleavage (*lower panel*) was performed either without antibody input (beads control, *lane 2*) or by using N18 and C18 antibodies (*lanes 3* and *4*). *Thr.*, thrombin.

2) still co-eluted in one peak, suggesting that the conserved N-terminal region is not essentially involved in the intramolecular interaction of TACC3. In contrast, deletion of the 7R region abolished intradomain binding and resulted after thrombin cleavage in the separation of the fragments (named TACC3-N and TACC3-CC in Fig. 3) in two distinct peaks with apparent molecular masses of 160 and 630 kDa, respectively). Their identity was reconfirmed by immunoblot analysis (Fig. 3*C*). Thus, the central serine-proline-glutamate-rich repeat region (7R) is required for the intramolecular interaction with the C-terminal CC domain.

We further validated this finding by subjecting the isolated domains, *i.e.* GST-7R (bait) and CC (prey) (supplemental Fig. S3) to pulldown-based interaction analysis. GST alone was used as the control. Although CC showed an unspecific binding to the beads, we could still detect a clearly stronger binding of CC when GST-7R was used as bait and analyzed by immunoblotting (Fig. 3*D*). Last, to determine the region within the TACC

domain that binds to the central repeat region, we purified 7R and the CC subdomains CC1 and CC2 (supplemental Fig. S3 and S4*E*) and analyzed their interaction by employing ITC. As indicated in Fig. 3*E*, significant calorimetric changes as well as changes in the temperature as a function of the molar ratio of the interacting proteins were observed when 7R was titrated onto CC2. In contrast, binding of 7R to CC1 could not be detected (Fig. 3*E*, *lower panel*). We conclude that the central repeat region, *i.e.* 7R, binds selectively to CC2 and thereby mediates intramolecular TACC3 binding potentially masking the C terminus of TACC3 before intermolecular protein interaction.

TACC3 Interacts with chTOG via Its CC1 Domain—We next characterized the interdomain binding between TACC3 and its major effector, the MT polymerase chTOG. We employed the C terminus of chTOG as bait (GST-chTOG-Cterm; supplemental Fig. S5) in pulldown assays demonstrating a strong interaction between chTOG-Cterm and the CC domain of
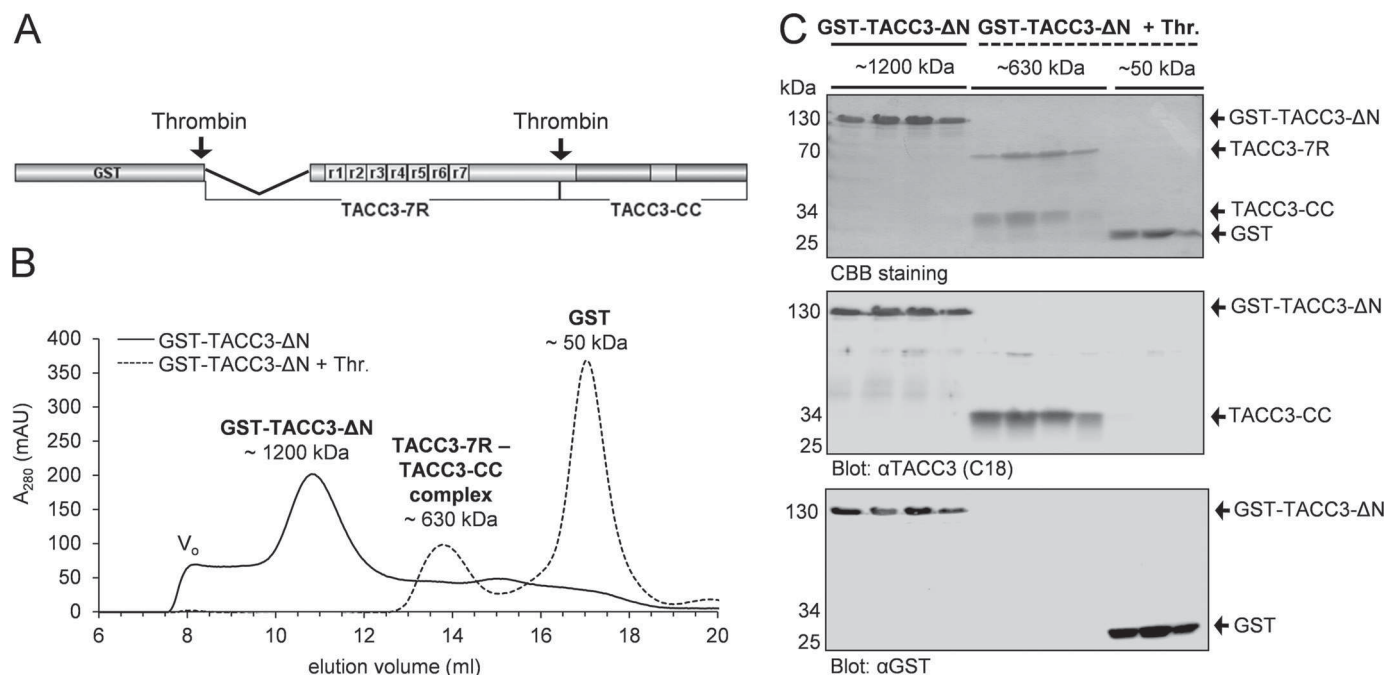
FIGURE 2. **The N-terminal 118 amino acids are not involved in intramolecular complex formation of murine TACC3.** *A*, primary structure of TACC3-ΔN lacking the N-terminal part of 118 aa. *B*, aSEC (Superpose 6, 10/300) elution profiles of GST-TACC3-ΔN before (*solid line*) and after (*dashed line*) thrombin cleavage. *V_o*, void volume. *mAu*, milliabsorbance units. *C*, peak elution fractions were analyzed by SDS-PAGE followed by CBB staining (*upper panel*) and immunoblotting using anti-TACC3 C18 (*middle panel*) or anti-GST antibodies (*lower panel*). GST was used as a control.

TACC3 (Fig. 4*A*). Interestingly, when analyzing the relative contribution of the two coiled-coil-containing subdomains of the TACC domain (*i.e.* CC1 and CC2; supplemental Fig. S3) to chTOG-Cterm binding in aSEC experiments, we observed a prominent peak shift of CC1 mixed with chTOG-Cterm that did not occur in the case of CC2 (Fig. 4, *B* and *C*). This selective CC1-chTOG-Cterm interaction was still observable in the presence of equimolar amounts of CC2, *i.e.* when mixing and analyzing all three fragments together (Fig. 4*D*). Of note, CC1 and CC2 did not interact with each other (supplemental Fig. S7). Subsequent ITC-based binding measurements revealed a strong association between CC1 and chTOG-Cterm with a K_d of 0.7 μM and a binding stoichiometry ($n = 0.83$) of nearly 1:1 (Fig. 4*E*). Consistent with the aSEC data, we did not detect any interaction between CC2 and chTOG-Cterm in ITC experiments (Fig. 4*E*). Importantly, we confirmed these findings also *in vivo* by expressing deletion mutants of TACC3 lacking either the TACC domain (CC) or one of its subdomains (*i.e.* CC1 or CC2) in HEK293 cells as C-terminally tagged GFP fusion proteins. Transfected cells were subjected to co-immunoprecipitation analysis using GFP-specific antibodies. As indicated in Fig. 5, deletion of CC1, but not of the CC2 subdomain, abrogated interaction with endogenous chTOG, strongly indicating that also under *in vivo* conditions the CC1 domain specifically determines binding of TACC3 to chTOG.

chTOG Binds to TACC3 via a C-terminal Region after the MT-interacting TOG Domains—Having localized CC1 as part in the TACC domain that binds to the C terminus of chTOG, we now narrowed down the TACC3 interacting part within the C terminus of chTOG. For this, we purified and analyzed two subdomains, chTOG-A (aa 1544–1805), which contains the putative, MT-interacting TOG6 domain (52), and chTOG-B

(aa 1806–2032) within the C terminus of chTOG (supplemental Fig. S5). As indicated in the pulldown-based interaction analysis in Fig. 6, chTOG-B, but not chTOG-A, efficiently bound to TACC3 or its isolated CC1 domain. Consistent with this, employing aSEC and subsequent peak fraction analysis on SDS-PAGE, we observed a clear complex formation for chTOG-B-CC1 but no interaction and peak shift when chTOG-A and CC1 were mixed together (supplemental Fig. 10, *A* and *B*). Thus, chTOG binds specifically via a C-terminal fragment adjacent to the putative MT-binding TOG6 domain to the CC1 domain of TACC3.

Interaction of chTOG with TACC3 Abrogates Intradomain Masking of TACC3—Based on the findings above, we next addressed the relation between the intradomain TACC3 interaction (mediated through 7R and CC2) and intermolecular CC1-chTOG-Cterm binding thereby analyzing the "directionality" of formation of these protein complexes. As indicated in Fig. 7*A*, GST-fused chTOG-Cterm was able to pull down full-length TACC3 or its C terminus (CC) produced upon thrombin cleavage of TACC3. However, in the latter case, the N-terminal part of TACC3 (TACC3-N7R) could not be detected in GST-chTOG-Cterm pulldown complexes by immunoblotting (Fig. 7*A*, *last lane*) strongly indicating that chTOG-Cterm binding uncouples the intramolecular TACC3 interaction. These findings were further validated by subjecting the TACC3-chTOG-Cterm protein complex before and after thrombin cleavage to aSEC. Fig. 7*B* shows that both TACC3 alone and TACC3 bound to chTOG-Cterm eluted on aSEC comparably at a peak fraction equivalent to an apparent molecular mass of ~1200 kDa. In contrast, when TACC3 was prebound to chTOG-Cterm and then subjected to thrombin cleavage, a shift of the TACC3 complex (TACC3-N7R-CC; apparent mass of ~630 kDa) toward an

Molecular Basis of TACC3-chTOG Complex Formation
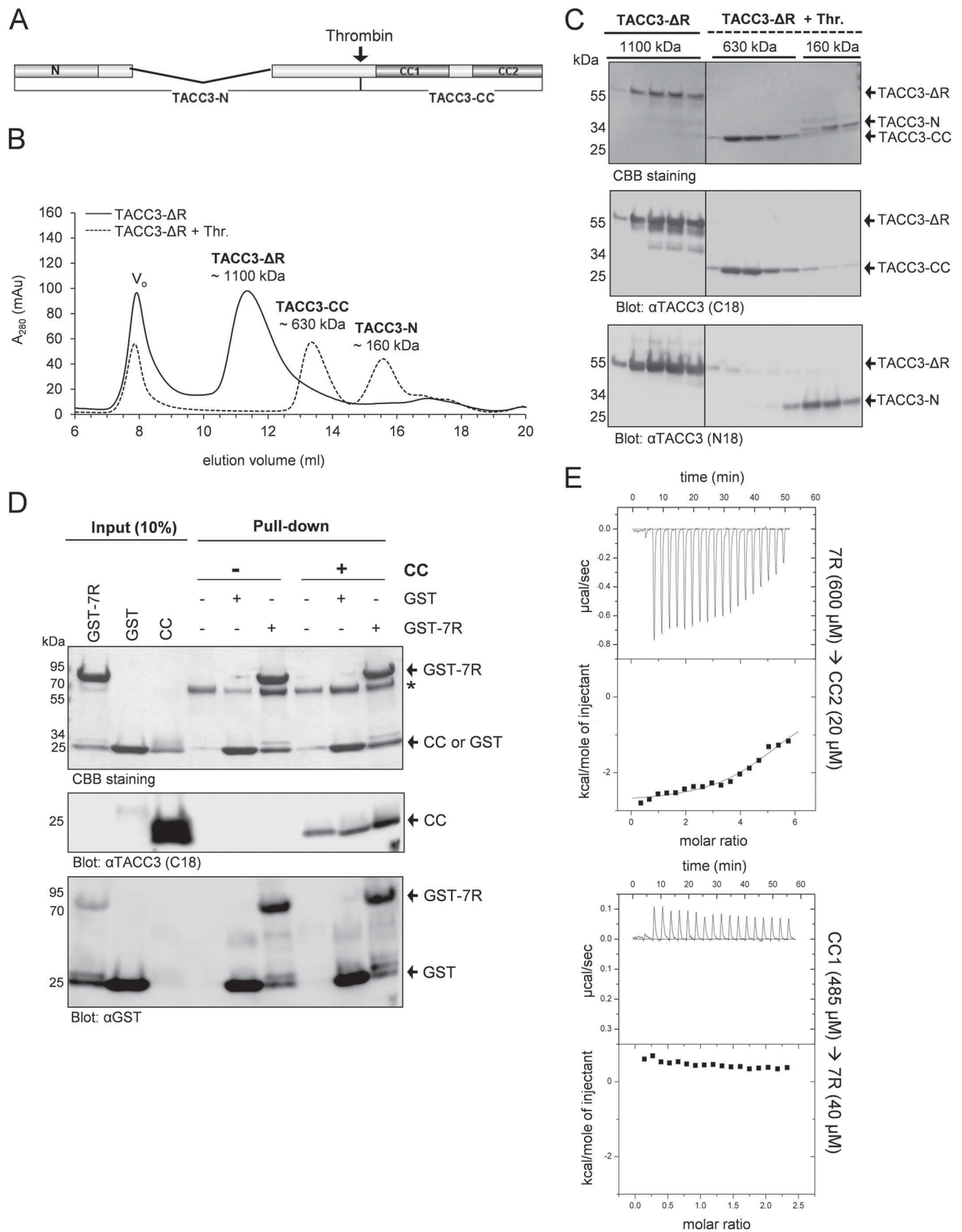
earlier elution volume corresponding to an apparent mass of ~800 kDa was detected (Fig. 7*C*). SDS-PAGE analysis confirmed that this peak shift was due to the interaction of chTOG-Cterm with the TACC domain, once more indicating that the intramolecular interaction between 7R and CC2 is relieved upon chTOG-Cterm binding to CC1. We conclude that 7R-CC2 and CC1-chTOG-Cterm are consecutive and mutually exclusive interactions representing the two distinct masked and unmasked states of the C-terminal TACC domain of TACC3.

Aurora-A Kinase Does Not Interfere with TACC3-chTOG Complex Formation—Aurora-A kinase phosphorylates and targets TACC3 to centrosomes and proximal mitotic spindles as a prerequisite for TACC3-chTOG protein complex-dependent centrosomal MT assembly and dynamics (43–46). Sequence alignment and phosphorylation prediction revealed that murine TACC3 displays three putative Aurora-A phosphorylation sites (Ser-34, -341, and -347) that are localized in the N-terminal part outside of the CC domain (Fig. 1*A*) and are conserved in human TACC3 (Ser-34, -552, and -558) as well as *X. laevis* TACC3 (Ser-33, -620, and -626) (28). Our *in vitro* data presented above already indicated that Aurora-A-mediated phosphorylation of TACC3 is not required to expose the TACC domain for intermolecular protein interaction. However, the time point when Aurora-A phosphorylates TACC3, *i.e.* before or after chTOG binding, remained unclear. We, therefore, subjected (i) TACC3 before and after thrombin cleavage, (ii) TACC3-ΔR lacking the central repeat region required for intramolecular masking, and (iii) TACC3 prebound to chTOG-Cterm to *in vitro* kinase assays. As shown in Fig. 8, under all these conditions the N terminus of TACC3 outside of the TACC domain was efficiently phosphorylated by Aurora-A kinase. Thus, Aurora-A phosphorylates TACC3 independent from the masked or unmasked status of the TACC domain and does thereby not discriminate between the unbound or chTOG-bound state.

These *in vitro* findings were also tested *in vivo* by employing the Aurora-A kinase inhibitor MLN8237 in cell culture under conditions where Aurora-A kinase activity (as monitored by autophosphorylation at Thr-288) was abrogated (supplemental Fig. S8*A*). As indicated in supplemental Fig. 8, *B–D*, MLN8237-mediated inhibition of Aurora-A kinase impaired spindle formation and colocalization of TACC3 and chTOG to microtubules and spindle poles. However, centrosomal colocalization of TACC3 and chTOG was still detectable despite the occurrence of fragmented centrosomes. Consistent with this, employing co-immunoprecipitation analysis, interaction of TACC3 with chTOG was still detectable in MLN8237-treated cells (supplemental Fig. S9). Taken together, these findings emphasize that Aurora-A functions solely as a recruitment factor of the TACC3-chTOG complex to centrosomes and proxi-

mal spindle microtubules (43–46) without affecting its formation and protein interaction.

DISCUSSION

This study provides novel molecular insight into the basis of spindle MT stability and dynamics during mitosis by determining the interaction between the centrosomal adaptor protein TACC3 and the MT polymerase chTOG. The main findings of our work are as follows. 1) The C-terminal TACC domain of TACC3 consists of two functionally distinct modules, CC1 and CC2. 2) CC2 performs an intradomain interaction with the central repeat region (7R), a complex that masks intermolecular interaction of TACC3. 3) chTOG directly binds CC1 via a C-terminal fragment adjacent to N-terminal MT binding TOG domains. 4) Aurora-A kinase, a major regulator of TACC3, does not interfere with TACC3-chTOG complex formation either *in vitro* or *in vivo*. 5) Thus, Aurora-A solely acts as a centrosomal/proximal spindle recruitment factor for the TACC3-chTOG complex consistent with previous findings (43–46).

Our data argue against the possibility that the evolutionary conserved interaction between TACC3 and chTOG family members, as observed by several groups (31, 53, 58, 59, 67), requires the complete TACC domain. By analyzing the TACC3-chTOG protein complex, we define CC1 as an chTOG interacting domain. Moreover, we show that the deletion mutant TACC3-ΔCC1, in contrast to TACC3-ΔCC2, fails to co-immunoprecipitate/interact with chTOG *in vivo* (Fig. 5). Our findings are consistent with recent work of Hood *et al.* (52) that has analyzed the interaction of human TACC3 and chTOG isoforms using a deletion mapping approach. The authors narrowed down the corresponding human CC1 domain to a short region of 12 amino acids (aa 673–684) that appears to be sufficient for chTOG binding and chTOG localization on spindle MTs *in vivo* (52). Interestingly, centrosomal localization of chTOG was apparently reduced but still detectable, further indicating that chTOG may be recruited to centrosomes via both TACC3-dependent and -independent mechanisms.

As indicated in our model (Fig. 9), the mutually exclusive intradomain 7R-CC2 and interdomain CC1-chTOG interactions, respectively, provide novel functional insight into the subdomain selectivity and directionality of TACC3-chTOG complex formation. Our findings obtained by ITC analysis (Figs. 3*E* and 4*E*) are of particular relevance by providing clear insights into differential binding affinities for a strong chTOG-Cterm-CC1 interaction *versus* a weak 7R-CC2 interaction. Accordingly, we propose that chTOG binding to CC1 results in a conformational change of the CC2 subdomain, which is in turn released from its intramolecular complex with 7R and hence unmasks both CC2 and the central repeat region of

FIGURE 3. **Deletion of the central repeat (7R) domain prevents intramolecular TACC3 complex formation.** *A*, primary structure of TACC3-ΔR lacking the 7R domain. *B*, elution profile of TACC3-ΔR on analytical gel filtration (Superpose 6, 10/300) before (*solid line*) and after (*dashed line*) thrombin cleavage. *V_o*, void volume. *C*, peak elution fractions were analyzed on SDS-PAGE (4–15% gradient gel) followed by CBB staining (*upper panel*) and immunoblotting using the indicated antibodies (*middle* and *lower panels*). *Thr.*, thrombin. *D*, the interaction between the isolated repeat region (*7R*) and the TACC domain (*CC*) was analyzed by pulldown assays and immunoblotting using N18 and C18 antibodies against TACC3. The *asterisk* indicates bovine albumin used to reduce unspecific binding to GSH-Sepharose beads. *E*, analysis of the interaction between 7R and subdomains of the TACC domain (CC1, CC2) employing ITC. Heat changes after association of the indicated protein fragments indicate that 7R selectively interacts with CC2 (*upper panel*) but not CC1 (*lower panel*). See supplemental Fig. S6 for experimental ITC controls.
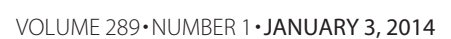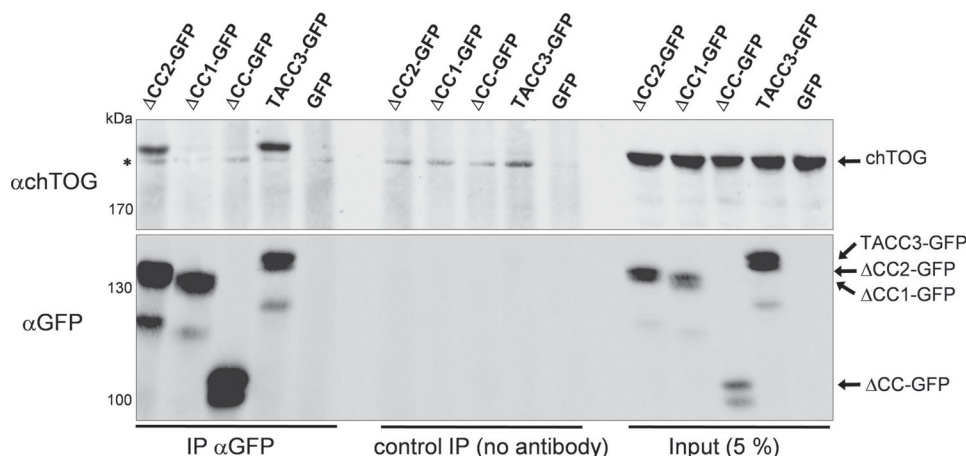
FIGURE 5. **The CC1 subdomain is required for binding of TACC3 to chTOG *in vivo*.** HEK293 cells were transfected with expression constructs for TACC3 or the indicated C-terminal deletion mutants all C-terminally fused to GFP. After 48 h, total cell lysates were prepared and subjected to co-immunoprecipitation analysis using a GFP-specific antibody followed by SDS-PAGE analysis and detection of chTOG in the immunoprecipitates. *mAu*, milliabsorbance units; *IP*, immunoprecipitation. The *asterisk* indicates an unspecific band.
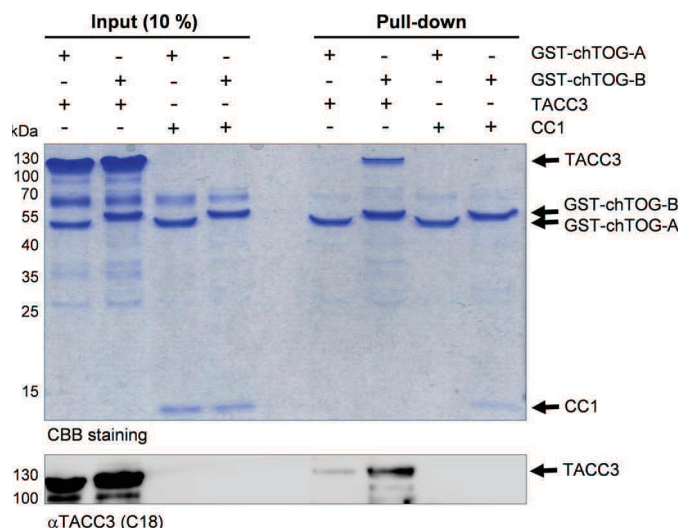

FIGURE 6. **The C terminus of chTOG following the six TOG domains binds to the CC1 subdomain of TACC3.** The interaction between the C terminus of chTOG (divided into the subfragments chTOG-A and chTOG-B; supplemental Fig. S5) with full-length TACC3 or its CC1 subdomain was analyzed by pull-down assays and subsequently detected by CBB staining and immunoblotting using antibodies against the C-terminal end of TACC3 (C18). chTOG-B, but not the TOG6 domain containing fragment chTOG-A (supplemental Fig. S5), displays a selective interaction with TACC3.

TACC3. As a consequence, not only CC2, but also 7R may become available for further interactions with other downstream binding partners. However, in the latter case, no protein is currently known that binds to the central repeat domain of TACC3 despite the presence of *bona fide* PXXP binding motifs known to interact with SH3 domain-containing proteins in intracellular signaling processes. This is different for the TACC domain that has been identified by yeast two hybrid-based

screening as well as pulldown and immunoprecipitation assays as major binding partner for various, functionally rather diverse proteins. These include factors involved in cortical neurogenesis (Cep192, DOCK7) (68, 69), hematopoietic development (FOG-1) (70), hypoxia response and gene expression (ARNT) (66), transcriptional regulation (MBD2) (71), and regulation of mTOR signaling (TSC2) (55). Interestingly, FOG-1 and ARNT have been proposed to bind to a region containing the last 20 residues of the CC2 subdomain (66, 72). Consistently, CC2 may be involved not only in intradomain but also in intermolecular protein interactions, whereas CC1 may only undergo intermolecular effector binding.

Aurora-A-mediated phosphorylation of TACC3 seems not to interfere with TACC3 intradomain and TACC3-chTOG interdomain interactions under *in vitro* conditions (Fig. 8). Accordingly, *in vivo*, TACC3-chTOG interaction and centrosomal colocalization was still detectable in HeLa cells that have been subjected to treatment with the Aurora-A kinase inhibitor MLN8237 (supplemental Figs. S8 and S9). These findings also contradict the previous model proposing that Aurora-A-mediated phosphorylation of *X. laevis* TACC3 triggers unmasking of the TACC domain and thereby exposes it for intermolecular interaction (*i.e.* XMAP215 binding) and centrosomal targeting (46, 59). In fact, Aurora-A-mediated phosphorylation of TACC3 seems to be solely required for targeting of the TACC3-chTOG complex to centrosomes and spindle MTs (28, 44). In the latter case, pTACC-chTOG interacts with another key effector in mitotic spindle assembly, the clathrin heavy chain, thereby cross-linking and stabilizing MT bundles (31, 51, 52).

Based on this study a sequential function of TACC3-chTOG effector complexes in the course of mitosis can be proposed.

FIGURE 4. **The CC1 subdomain of TACC3 mediates chTOG binding.** *A*, interaction between the C terminus of chTOG (chTOG-Cterm; aa 1574–2032; supplemental Fig. S6) and the CC domain of TACC3 was analyzed by pulldown assays and immunoblotting using antibodies against the C-terminal end of TACC3 (C18) and GST. *B* and *C*, binding of purified TACC subdomains (*CC1* or *CC2*) to chTOG-Cterm was analyzed by aSEC (superpose 6, 10/300) followed by SDS-PAGE and CBB staining of the respective peak fractions. *D*, chTOG-Cterm interacts in a competition experiment selectively with CC1 when mixed with both CC1 and CC2 fragments. Samples were analyzed by aSEC followed by SDS-PAGE and CBB staining of the respective peak fractions. The *dotted box* indicates elution fractions from the analysis of the CC1+CC2+chTOG-Cterm mixture employing anti-chTOG and anti-TACC3 (C18 recognizing CC2, but not CC1) antibodies. *E*, analysis of binding of chTOG-Cterm to CC1 (*left panel*) and CC2 (*right panel*) using ITC confirms selective protein complex formation between chTOG-Cterm and CC1. See supplemental Fig. S6 for experimental ITC controls.
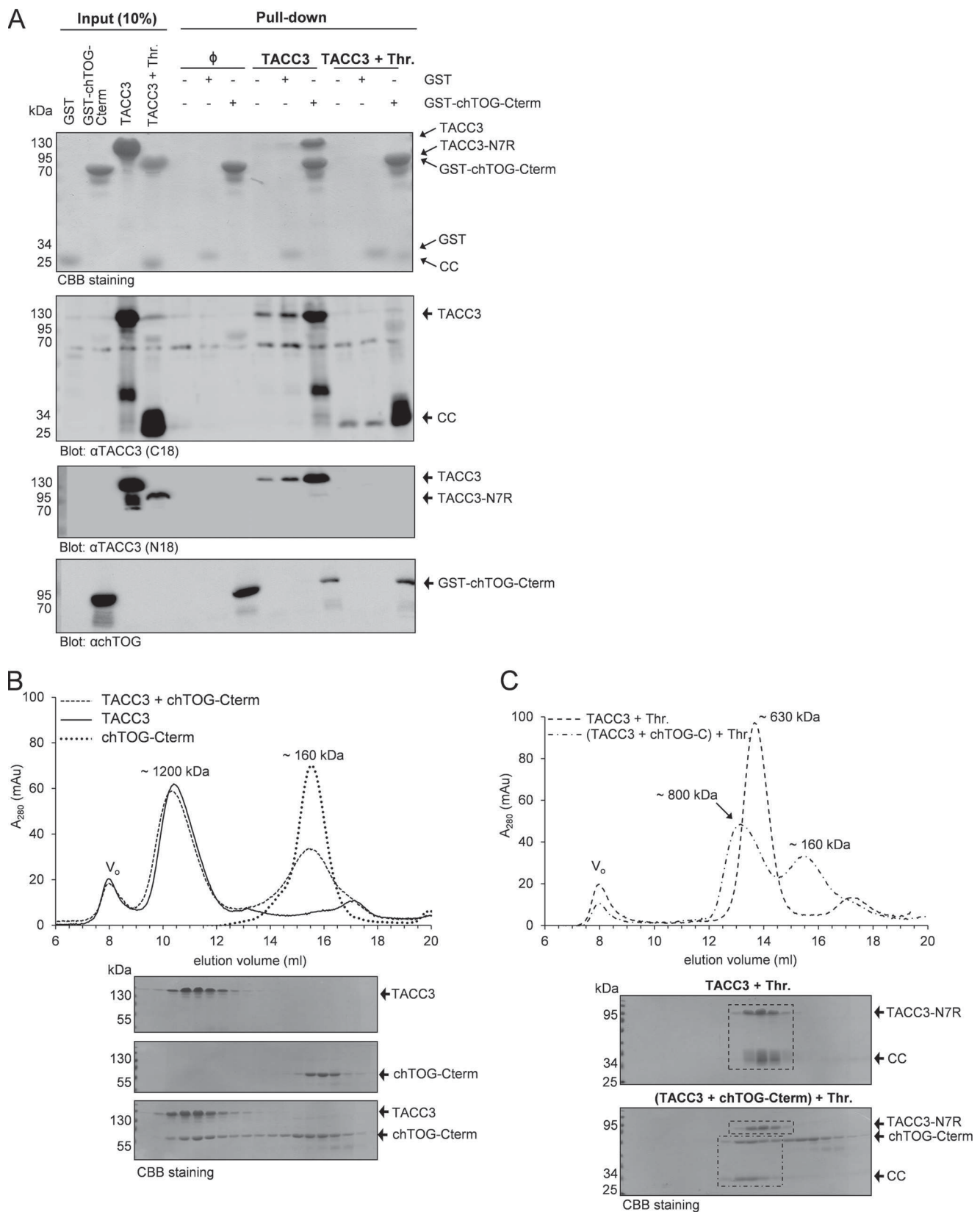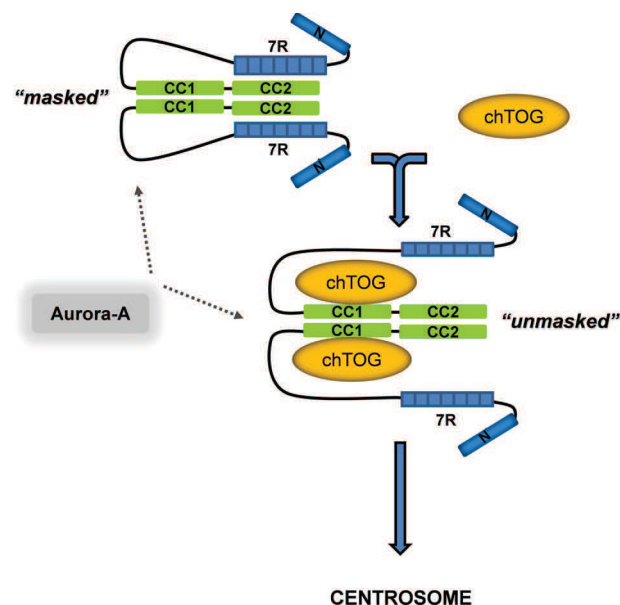
FIGURE 7. **Binding of chTOG-Cterm to TACC3 disrupts the intradomain interaction of TACC3.** *A,* the interaction between chTOG-Cterm and thrombin-cleaved TACC3 was analyzed by pulldown assays and immunoblotting using the indicated antibodies. Intramolecular interaction of TACC3-N7R with CC is thereby abrogated upon chTOG-Cterm binding, as chTOG-Cterm pulls down CC but not TACC3-N7R (*last lane*). *Thr.,* thrombin. *B* and *C,* aSEC-based analysis of the TACC3 - chTOG-Cterm complex was performed employing uncleaved TACC3 (*B*) or thrombin-cleaved TACC3 either alone or prebound to chTOG-Cterm (*C*). Peak fractions were analyzed by SDS-PAGE and CBB staining. The *dashed lines* within the CBB-stained SDS-PAGE gels highlight the peak shift of the chTOG-Cterm-CC complex (but not of TACC3-N7R) after thrombin cleavage. *mAu*, milliabsorbance units.
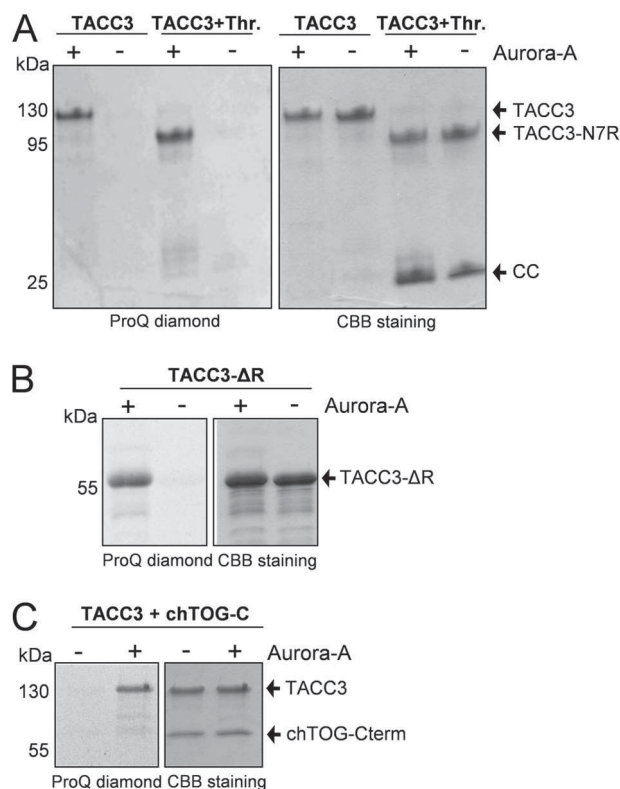
FIGURE 8. **Aurora-A kinase phosphorylates murine TACC3 *in vitro* independent from its intra- or intermolecular binding status.** Kinase assays were performed in the presence and absence of purified Aurora-A kinase employing uncleaved and thrombin-cleaved TACC3 (*A*), TACC3-ΔR (*B*), and the TACC3-chTOG-Cterm complex (*C*). Phosphorylated protein fragments were visualized by ProQ diamond staining. *Thr.*, thrombin.

FIGURE 9. **Integrative model for the domain specificity and directionality of TACC3-chTOG complex formation.** We propose that the intradomain (7R-CC2; TACC3 masked) and intermolecular (CC1-chTOG; TACC3 unmasked) binding states of TACC3 are mutually exclusive, thereby defining a directionality of TACC3 regulated adaptor function toward chTOG binding and function. TACC3 can be phosphorylated by Aurora-A kinase in both binding states, indicating that Aurora-A acts as a centrosomal recruitment factor but is not involved in exposing the TACC domain for intermolecular interaction with chTOG or TACC3-chTOG complex formation. Moreover, based on biophysical characterization of murine TACC3 (supplemental Fig. 11, *B* and *C*, and supplemental Table S1; Ref. 34) we conclude that TACC3 displays an dimeric to oligomeric state. *Thr.*, thrombin.

TACC3 interacts with the C terminus of chTOG thereby targeting it in an Aurora-A-dependent manner to spindle poles. On the other hand, the evolutionary conserved N terminus of chTOG likely comprises MT-stabilizing activity as demonstrated for XMAP215. In particular, XMAP215/chTOG proteins contain a variable number of TOG domains that bind to $\alpha\beta$-tubulin heterodimers, load them as MT polymerase (73) to the plus ends of MTs, and thereby inhibit "MT catastrophes." In contrast, the C-terminal part of XMAP215 (and likely also chTOG) suppresses MT growth by promoting MT catastrophes (74). Therefore, the engagement of chTOG-Cterm by the CC1 subdomain of TACC3 during G$_2$/M transition and metaphase might be a vital step in shifting the equilibrium toward MT polymerization. Upon mitotic exit, Cdh1 and ubiquitin-dependent degradation of TACC3 (39) then "disengages" the MT catastrophe promoting activity of the C terminus of XMAP215/chTOG. As a consequence, a shift of the equilibrium occurs toward MT "shrinkage" and disassembly of the spindle apparatus. Thus, TACC3 family members may function as "engagement factors" for the C terminus of XMAP215/chTOG to ensure a dynamic balance between MT rescue and catastrophe during the course of mitosis.

Besides a better molecular understanding regarding the mechanism and directionality of TACC3-chTOG interaction, we furthermore obtained novel insight into the unusual biophysical properties of TACC3. Analysis by aSEC (*e.g.* Fig. 1) clearly demonstrated that TACC3 displays a higher oligomeric mass and/or an elongated rod-like structure, obviously due to the presence of the coiled-coil containing TACC domain that elutes inherently at an apparent molecular mass of ~630 kDa (Fig. 3*B*). Moreover, endogenous TACC3 or FLAG-tagged TACC3 from transfected eukaryotic cells behaves on aSEC comparable to purified TACC3 (data not shown). These findings are in accordance with the observation that TACC isoforms overexpressed in HeLa cells form in a TACC domain-dependent manner punctuate-like structures resembling cytoplasmic polymers (data not shown) (27). Employing further analytical methods including multiangle light scattering and analytical ultracentrifugation allowed us to conclude that TACC3 is characterized by a oligomeric (*i.e.* dimeric to hexameric) structure and a highly extended shape (supplemental Fig. 11, *B* and *C*, and supplemental Table S1). These findings are consistent with data from electron microscopic analysis where TACC3 depicts an elongated, fiber-like appearance (34). Another abnormality of murine TACC3 represents its migration in SDS-PAGE gels at 120–130 kDa (Fig. 1*C*) as compared with its theoretical molecular mass of 70.5 kDa. Interestingly, this unusual "gel shifting" is not based on the presence of the coiled-coil containing TACC domain (data not shown) but is rather caused by the central repeat region (supplemental Fig. S4, *B versus A*). As proof, deletion of the 7R domain restored normal gel migration of TACC3 (Fig. 3*C* and supplemental Fig. S4*B*). Of note, abnormal SDS-PAGE migration of acidic proteins can be caused by an altered binding of surfactants (like SDS) (75), a possibility that remains to be clarified for TACC3 and in particular the 7R domain.

Molecular Basis of TACC3-chTOG Complex Formation

Biological and pathobiological roles of TACC3 are underlined by several observations. TACC3 deficiency leads to severe growth retardation and embryonic lethality (38, 40). This is in line with the anti-proliferative and cell cycle arrest/senescence-inducing impact of shRNA-mediated gene silencing of TACC3 (41, 42). Moreover, it could be shown that TACC3 depletion sensitizes cells to the apoptotic and senescence-inducing effects of mitotic spindle poisons. Accordingly, inducible gene disruption of TACC3 *in vivo* in the p53$^{-/-}$ sarcolymphoma model is highly effective in causing apoptotic tumor regression (76). Interestingly, besides quantitative deregulation of gene expression of TACC isoforms in several tumor types, TACC1 and TACC3 point mutants have been identified in melanoma and ovarian cancer patients (77, 78). Moreover, oncogenic fusions between TACC and fibroblast growth factor receptor genes have been recently described in glioblastoma multiforme and bladder cancer patients (79, 80). The impact of these structural and tumor-associated alterations on Aurora-A-mediated regulation and function of TACCs is currently unknown and requires a more in-depth molecular understanding of TACC-effector interactions. Irrespective, it is tempting to speculate that these TACC mutants translate through loss-of-function or gain-of-function mechanisms into chromosomal instability and aneuploidy and thereby support cellular transformation (81, 82). Taken all these points into account, TACC3 represents an attractive antitumor target that may be at least indirectly drug-treatable at the level of its interactome. This assumption is supported by the recent identification of small drugs that act as inhibitors of protein-protein interaction and thereby impair the half-life and stability of TACC3 (KSH101), disrupt the TACC3-ARNT complex (KG-548), or inhibit the function of the TACC3-chTOG complex (spindlactone) (54, 66, 83, 84).

REFERENCES

1. Bornens, M. (2012) The centrosome in cells and organisms. *Science* **335**, 422–426
2. Compton, D. A. (2000) Spindle assembly in animal cells. *Annu. Rev. Biochem.* **69**, 95–114
3. Delgehyr, N., Sillibourne, J., and Bornens, M. (2005) Microtubule nucleation and anchoring at the centrosome are independent processes linked by ninein function. *J. Cell Sci.* **118**, 1565–1575
4. Mattison, C., and Winey, M. (2006) *The Centrosome Cycle/Cell Cycle Regulation* (Kaldis, P., ed.) pp. 925–925, Springer, Berlin
5. Nigg, E. A. (2004) *Centrosomes in Development and Disease,* Wiley-VCH Verlag, Weinheim
6. Anderhub, S. J., Krämer, A., and Maier, B. (2012) Centrosome amplification in tumorigenesis. *Cancer Lett.* **322**, 8–17
7. Basto, R., Brunk, K., Vinadogrova, T., Peel, N., Franz, A., Khodjakov, A., and Raff, J. W. (2008) Centrosome amplification can initiate tumorigenesis in flies. *Cell* **133**, 1032–1042
8. Bettencourt-Dias, M., Hildebrandt, F., Pellman, D., Woods, G., and Godinho, S. A. (2011) Centrosomes and cilia in human disease. *Trends Genet.* **27**, 307–315
9. Chan, J. Y. (2011) A clinical overview of centrosome amplification in human cancers. *Int. J. Biol. Sci.* **7**, 1122–1144
10. Mardin, B. R., and Schiebel, E. (2012) Breaking the ties that bind. new advances in centrosome biology. *J. Cell Biol.* **197**, 11–18
11. Schmidt, S., Essmann, F., Cirstea, I. C., Kuck, F., Thakur, H. C., Singh, M., Kletke, A., Jänicke, R. U., Wiek, C., Hanenberg, H., Ahmadian, M. R., Schulze-Osthoff, K., Nürnberg, B., and Piekorz, R. P. (2010) The centrosome and mitotic spindle apparatus in cancer and senescence. *Cell Cycle* **9**, 4469–4473
12. Zyss, D., and Gergely, F. (2009) Centrosome function in cancer. Guilty or innocent? *Trends Cell Biol.* **19**, 334–346
13. Fielding, A. B., Lim, S., Montgomery, K., Dobreva, I., and Dedhar, S. (2011) A critical role of integrin-linked kinase, ch-TOG, and TACC3 in centrosome clustering in cancer cells. *Oncogene* **30**, 521–534
14. Kwon, M., Godinho, S. A., Chandhok, N. S., Ganem, N. J., Azioune, A., Thery, M., and Pellman, D. (2008) Mechanisms to suppress multipolar divisions in cancer cells with extra centrosomes. *Genes Dev.* **22**, 2189–2203
15. Marthiens, V., Piel, M., and Basto, R. (2012) Never tear us apart. The importance of centrosome clustering. *J. Cell Sci.* **125**, 3281–3292
16. Krämer, A., Maier, B., and Bartek, J. (2011) Centrosome clustering and chromosomal (in)stability. A matter of life and death. *Mol. Oncol.* **5**, 324–335
17. Raab, M. S., Breitkreutz, I., Anderhub, S., Rønnest, M. H., Leber, B., Larsen, T. O., Weiz, L., Konotop, G., Hayden, P. J., Podar, K., Fruehauf, J., Nissen, F., Mier, W., Haberkorn, U., Ho, A. D., Goldschmidt, H., Anderson, K. C., Clausen, M. H., and Krämer, A. (2012) GF-15, a novel inhibitor of centrosomal clustering, suppresses tumor cell growth *in vitro* and *in vivo*. *Cancer Res.* **72**, 5374–5385
18. Meraldi, P., and Nigg, E. A. (2002) The centrosome cycle. *FEBS Lett.* **521**, 9–13
19. Nigg, E. A., and Stearns, T. (2011) The centrosome cycle. Centriole biogenesis, duplication, and inherent asymmetries. *Nat. Cell Biol.* **13**, 1154–1160
20. Cunha-Ferreira, I., Bento, I., and Bettencourt-Dias, M. (2009) From zero to many. Control of centriole number in development and disease. *Traffic* **10**, 482–498
21. Andersen, J. S., Wilkinson, C. J., Mayor, T., Mortensen, P., Nigg, E. A., and Mann, M. (2003) Proteomic characterization of the human centrosome by protein correlation profiling. *Nature* **426**, 570–574
22. Jakobsen, L., Vanselow, K., Skogs, M., Toyoda, Y., Lundberg, E., Poser, I., Falkenby, L. G., Bennetzen, M., Westendorf, J., Nigg, E. A., Uhlen, M., Hyman, A. A., and Andersen, J. S. (2011) Novel asymmetrically localizing components of human centrosomes identified by complementary proteomics methods. *EMBO J.* **30**, 1520–1535
23. Müller, H., Schmidt, D., Steinbrink, S., Mirgorodskaya, E., Lehmann, V., Habermann, K., Dreher, F., Gustavsson, N., Kessler, T., Lehrach, H., Herwig, R., Gobom, J., Ploubidou, A., Boutros, M., and Lange, B. M. (2010) Proteomic and functional analysis of the mitotic *Drosophila* centrosome. *EMBO J.* **29**, 3344–3357
24. Doxsey, S., McCollum, D., and Theurkauf, W. (2005) Centrosomes in cellular regulation. *Annu. Rev. Cell Dev. Biol.* **21**, 411–434
25. Hutchins, J. R., Toyoda, Y., Hegemann, B., Poser, I., Hériché, J. K., Sykora, M. M., Augsburg, M., Hudecz, O., Buschhorn, B. A., Bulkescher, J., Conrad, C., Comartin, D., Schleiffer, A., Sarov, M., Pozniakovsky, A., Slabicki, M. M., Schloissnig, S., Steinmacher, I., Leuschner, M., Ssykor, A., Lawo, S., Pelletier, L., Stark, H., Nasmyth, K., Ellenberg, J., Durbin, R., Buchholz, F., Mechtler, K., Hyman, A. A., and Peters, J. M. (2010) Systematic analysis of human protein complexes identifies chromosome segregation proteins. *Science* **328**, 593–599
26. Neumann, B., Walter, T., Hériché, J. K., Bulkescher, J., Erfle, H., Conrad, C., Rogers, P., Poser, I., Held, M., Liebel, U., Cetin, C., Sieckmann, F., Pau, G., Kabbe, R., Wünsche, A., Satagopam, V., Schmitz, M. H., Chapuis, C., Gerlich, D. W., Schneider, R., Eils, R., Huber, W., Peters, J. M., Hyman, A. A., Durbin, R., Pepperkok, R., and Ellenberg, J. (2010) Phenotypic profiling of the human genome by time-lapse microscopy reveals cell division genes. *Nature* **464**, 721–727
27. Gergely, F., Karlsson, C., Still, I., Cowell, J., Kilmartin, J., and Raff, J. W. (2000) The TACC domain identifies a family of centrosomal proteins that

can interact with microtubules. *Proc. Natl. Acad. Sci. U.S.A.* **97,** 14352–14357

28. Peset, I., and Vernos, I. (2008) The TACC proteins. TACC-ling microtubule dynamics and centrosome function. *Trends Cell Biol.* **18,** 379–388

29. Raff, J. W. (2002) Centrosomes and cancer. Lessons from a TACC. *Trends Cell Biol.* **12,** 222–225

30. Gergely, F. (2002) Centrosomal TACCtics. *Bioessays* **24,** 915–925

31. Hood, F. E., and Royle, S. J. (2011) Pulling it together. The mitotic function of TACC3. *Bioarchitecture* **1,** 105–109

32. Schneider, L., Essmann, F., Kletke, A., Rio, P., Hanenberg, H., Wetzel, W., Schulze-Osthoff, K., Nürnberg, B., and Piekorz, R. P. (2007) The transforming acidic coiled coil 3 protein is essential for spindle-dependent chromosome alignment and mitotic survival. *J. Biol. Chem.* **282,** 29273–29283

33. Still, I. H., Vettaikkorumakankauv, A. K., DiMatteo, A., and Liang, P. (2004) Structure-function evolution of the transforming acidic coiled coil genes revealed by analysis of phylogenetically diverse organisms. *BMC Evol. Biol.* **4,** 16

34. Thakur, H. C., Singh, M., Nagel-Steger, L., Prumbaum, D., Fansa, E. K., Gremer, L., Ezzahoini, H., Abts, A., Schmitt, L., Raunser, S., Ahmadian, M. R., and Piekorz, R. P. (2013) Role of centrosomal adaptor proteins of the TACC family in the regulation of microtubule dynamics during mitotic cell division. *Biol. Chem.* **394,** 1411–1423

35. Hao, Z., Stoler, M. H., Sen, B., Shore, A., Westbrook, A., Flickinger, C. J., Herr, J. C., and Coonrod, S. A. (2002) TACC3 expression and localization in the murine egg and ovary. *Mol. Reprod. Dev.* **63,** 291–299

36. Sadek, C. M., Pelto-Huikko, M., Tujague, M., Steffensen, K. R., Wennerholm, M., and Gustafsson, J. A. (2003) TACC3 expression is tightly regulated during early differentiation. *Gene Expr. Patterns* **3,** 203–211

37. Schuendeln, M. M., Piekorz, R. P., Wichmann, C., Lee, Y., McKinnon, P. J., Boyd, K., Takahashi, Y., and Ihle, J. N. (2004) The centrosomal, putative tumor suppressor protein TACC2 is dispensable for normal development, and deficiency does not lead to cancer. *Mol. Cell. Biol.* **24,** 6403–6409

38. Piekorz, R. P., Hoffmeyer, A., Duntsch, C. D., McKay, C., Nakajima, H., Sexl, V., Snyder, L., Rehg, J., and Ihle, J. N. (2002) The centrosomal protein TACC3 is essential for hematopoietic stem cell function and genetically interfaces with p53-regulated apoptosis. *EMBO J.* **21,** 653–664

39. Jeng, J. C., Lin, Y. M., Lin, C. H., and Shih, H. M. (2009) Cdh1 controls the stability of TACC3. *Cell Cycle* **8,** 3529–3536

40. Yao, R., Natsume, Y., and Noda, T. (2007) TACC3 is required for the proper mitosis of sclerotome mesenchymal cells during formation of the axial skeleton. *Cancer Sci.* **98,** 555–562

41. Schmidt, S., Schneider, L., Essmann, F., Cirstea, I. C., Kuck, F., Kletke, A., Jänicke, R. U., Wiek, C., Hanenberg, H., Ahmadian, M. R., Schulze-Osthoff, K., Nürnberg, B., and Piekorz, R. P. (2010) The centrosomal protein TACC3 controls paclitaxel sensitivity by modulating a premature senescence program. *Oncogene* **29,** 6184–6192

42. Schneider, L., Essmann, F., Kletke, A., Rio, P., Hanenberg, H., Schulze-Osthoff, K., Nürnberg, B., and Piekorz, R. P. (2008) TACC3 depletion sensitizes to paclitaxel-induced cell death and overrides p21WAF-mediated cell cycle arrest. *Oncogene* **27,** 116–125

43. Barros, T. P., Kinoshita, K., Hyman, A. A., and Raff, J. W. (2005) Aurora A activates D-TACC-Msps complexes exclusively at centrosomes to stabilize centrosomal microtubules. *J. Cell Biol.* **170,** 1039–1046

44. Kinoshita, K., Noetzel, T. L., Pelletier, L., Mechtler, K., Drechsel, D. N., Schwager, A., Lee, M., Raff, J. W., and Hyman, A. A. (2005) Aurora A phosphorylation of TACC3/maskin is required for centrosome-dependent microtubule assembly in mitosis. *J. Cell Biol.* **170,** 1047–1055

45. LeRoy, P. J., Hunter, J. J., Hoar, K. M., Burke, K. E., Shinde, V., Ruan, J., Bowman, D., Galvin, K., and Ecsedy, J. A. (2007) Localization of human TACC3 to mitotic spindles is mediated by phosphorylation on Ser-558 by Aurora A. A novel pharmacodynamic method for measuring Aurora A activity. *Cancer Res.* **67,** 5362–5370

46. Peset, I., Seiler, J., Sardon, T., Bejarano, L. A., Rybina, S., and Vernos, I. (2005) Function and regulation of Maskin, a TACC family protein, in microtubule growth during mitosis. *J. Cell Biol.* **170,** 1057–1066

47. Fu, W., Chen, H., Wang, G., Luo, J., Deng, Z., Xin, G., Xu, N., Guo, X., Lei, J., Jiang, Q., and Zhang, C. (2013) Self-assembly and sorting of acentro-somal microtubules by TACC3 facilitate kinetochore capture during the mitotic spindle assembly. *Proc. Natl. Acad. Sci. U.S.A.* **110,** 15295–15300

48. Lioutas, A., and Vernos, I. (2013) Aurora A kinase and its substrate TACC3 are required for central spindle assembly. *EMBO Rep.* **14,** 829–836

49. Fu, W., Jiang, Q., and Zhang, C. (2011) Novel functions of endocytic player clathrin in mitosis. *Cell Res.* **21,** 1655–1661

50. Royle, S. J. (2012) The role of clathrin in mitotic spindle organisation. *J. Cell Sci.* **125,** 19–28

51. Booth, D. G., Hood, F. E., Prior, I. A., and Royle, S. J. (2011) A TACC3/ch-TOG/clathrin complex stabilises kinetochore fibres by inter-microtubule bridging. *EMBO J.* **30,** 906–919

52. Hood, F. E., Williams, S. J., Burgess, S. G., Richards, M. W., Roth, D., Straube, A., Pfuhl, M., Bayliss, R., and Royle, S. J. (2013) Coordination of adjacent domains mediates TACC3-ch-TOG-clathrin assembly and mitotic spindle binding. *J. Cell Biol.* **202,** 463–478

53. Gergely, F., Draviam, V. M., and Raff, J. W. (2003) The ch-TOG/XMAP215 protein is essential for spindle pole organization in human somatic cells. *Genes Dev.* **17,** 336–341

54. Yao, R., Kondoh, Y., Natsume, Y., Yamanaka, H., Inoue, M., Toki, H., Takagi, R., Shimizu, T., Yamori, T., Osada, H., and Noda, T. (2013) A small compound targeting TACC3 revealed its different spatiotemporal contributions for spindle assembly in cancer cells. *Oncogene* DOI:10.1038/onc.2013.382

55. Gómez-Baldó, L., Schmidt, S., Maxwell, C. A., Bonifaci, N., Gabaldón, T., Vidalain, P. O., Senapedis, W., Kletke, A., Rosing, M., Barnekow, A., Rottapel, R., Capellá, G., Vidal, M., Astrinidis, A., Piekorz, R. P., and Pujana, M. A. (2010) TACC3-TSC2 maintains nuclear envelope structure and controls cell division. *Cell Cycle* **9,** 1143–1155

56. Lauffart, B., Howell, S. J., Tasch, J. E., Cowell, J. K., and Still, I. H. (2002) Interaction of the transforming acidic coiled-coil 1 (TACC1) protein with ch-TOG and GAS41/NuBI1 suggests multiple TACC1-containing protein complexes in human cells. *Biochem. J.* **363,** 195–200

57. Sato, M., Vardy, L., Angel Garcia, M., Koonrugsa, N., and Toda, T. (2004) Interdependency of fission yeast Alp14/TOG and coiled coil protein Alp7 in microtubule localization and bipolar spindle formation. *Mol. Biol. Cell* **15,** 1609–1622

58. Albee, A. J., Tao, W., and Wiese, C. (2006) Phosphorylation of maskin by Aurora-A is regulated by RanGTP and importin β. *J. Biol. Chem.* **281,** 38293–38301

59. Albee, A. J., and Wiese, C. (2008) Xenopus TACC3/maskin is not required for microtubule stability but is required for anchoring microtubules at the centrosome. *Mol. Biol. Cell* **19,** 3347–3356

60. Thompson, J. D., Higgins, D. G., and Gibson, T. J. (1994) ClustalW. Improving the sensitivity of progressive multiple sequence alignment through sequence weighting, position-specific gap penalties and weight matrix choice. *Nucleic Acids Res.* **22,** 4673–4680

61. Lupas, A., Van Dyke, M., and Stock, J. (1991) Predicting coiled coils from protein sequences. *Science* **252,** 1162–1164

62. Thakur, H. C. (2012) *Biochemical and biophysical characterization of the centrosomal protein TACC3.* Doctoral dissertation, Faculty of Mathematics and Natural Sciences of the Heinrich Heine University, Düsseldorf, Germany

63. Eberth, A., Lundmark, R., Gremer, L., Dvorsky, R., Koessmeier, K. T., McMahon, H. T., and Ahmadian, M. R. (2009) A BAR domain-mediated autoinhibitory mechanism for RhoGAPs of the GRAF family. *Biochem. J.* **417,** 371–377

64. Risse, S. L., Vaz, B., Burton, M. F., Aspenström, P., Piekorz, R. P., Brunsveld, L., and Ahmadian, M. R. (2013) SH3-mediated targeting of Wrch1/RhoU by multiple adaptor proteins. *Biol. Chem.* **394,** 421–432

65. Sardon, T., Pache, R. A., Stein, A., Molina, H., Vernos, I., and Aloy, P. (2010) Uncovering new substrates for Aurora A kinase. *EMBO Rep.* **11,** 977–984

66. Partch, C. L., and Gardner, K. H. (2011) Coactivators necessary for transcriptional output of the hypoxia inducible factor, HIF, are directly recruited by ARNT PAS-B. *Proc. Natl. Acad. Sci. U.S.A.* **108,** 7739–7744

67. Cassimeris, L., and Morabito, J. (2004) TOGp, the human homolog of XMAP215/Dis1, is required for centrosome integrity, spindle pole orga-

nization, and bipolar spindle assembly. *Mol. Biol. Cell* **15,** 1580 –1590

68. Xie, Z., Moy, L. Y., Sanada, K., Zhou, Y., Buchman, J. J., and Tsai, L.-H. (2007) Cep120 and TACCs control interkinetic nuclear migration and the neural progenitor pool. *Neuron* **56,** 79 –93

69. Yang, Y. T., Wang, C. L., and Van Aelst, L. (2012) DOCK7 interacts with TACC3 to regulate interkinetic nuclear migration and cortical neurogenesis. *Nat. Neurosci.* **15,** 1201–1210

70. Garriga-Canut, M., and Orkin, S. H. (2004) Transforming acidic coiled-coil protein 3 (TACC3) controls friend of GATA-1 (FOG-1) subcellular localization and regulates the association between GATA-1 and FOG-1 during hematopoiesis. *J. Biol. Chem.* **279,** 23597–23605

71. Angrisano, T., Lembo, F., Pero, R., Natale, F., Fusco, A., Avvedimento, V. E., Bruni, C. B., and Chiariotti, L. (2006) TACC3 mediates the association of MBD2 with histone acetyltransferases and relieves transcriptional repression of methylated promoters. *Nucleic Acids Res.* **34,** 364 –372

72. Simpson, R. J., Yi Lee, S. H., Bartle, N., Sum, E. Y., Visvader, J. E., Matthews, J. M., Mackay, J. P., and Crossley, M. (2004) A classic zinc finger from friend of GATA mediates an interaction with the coiled-coil of transforming acidic coiled-coil 3. *J. Biol. Chem.* **279,** 39789 –39797

73. Brouhard, G. J., Stear, J. H., Noetzel, T. L., Al-Bassam, J., Kinoshita, K., Harrison, S. C., Howard, J., and Hyman, A. A. (2008) XMAP215 is a processive microtubule polymerase. *Cell* **132,** 79 – 88

74. Popov, A. V., Pozniakovsky, A., Arnal, I., Antony, C., Ashford, A. J., Kinoshita, K., Tournebize, R., Hyman, A. A., and Karsenti, E. (2001) XMAP215 regulates microtubule dynamics through two distinct domains. *EMBO J.* **20,** 397– 410

75. Shi, Y., Mowery, R. A., Ashley, J., Hentz, M., Ramirez, A. J., Bilgicer, B., Slunt-Brown, H., Borchelt, D. R., and Shaw, B. F. (2012) Abnormal SDS-PAGE migration of cytosolic proteins can identify domains and mechanisms that control surfactant binding. *Protein Sci.* **21,** 1197–1209

76. Yao, R., Natsume, Y., Saiki, Y., Shioya, H., Takeuchi, K., Yamori, T., Toki, H., Aoki, I., Saga, T., and Noda, T. (2012) Disruption of Tacc3 function leads to *in vivo* tumor regression. *Oncogene* **31,** 135–148

77. Hodis, E., Watson, I. R., Kryukov, G. V., Arold, S. T., Imielinski, M., Theurillat, J. P., Nickerson, E., Auclair, D., Li, L., Place, C., Dicara, D., Ramos, A. H., Lawrence, M. S., Cibulskis, K., Sivachenko, A., Voet, D., Saksena, G., Stransky, N., Onofrio, R. C., Winckler, W., Ardlie, K., Wagle, N., Wargo, J., Chong, K., Morton, D. L., Stemke-Hale, K., Chen, G., Noble, M., Meyerson, M., Ladbury, J. E., Davies, M. A., Gershenwald, J. E., Wagner, S. N., Hoon, D. S., Schadendorf, D., Lander, E. S., Gabriel, S. B., Getz, G., Garraway, L. A., and Chin, L. (2012) A landscape of driver mutations in melanoma. *Cell* **150,** 251–263

78. Lauffart, B., Vaughan, M. M., Eddy, R., Chervinsky, D., DiCioccio, R. A., Black, J. D., and Still, I. H. (2005) Aberrations of TACC1 and TACC3 are associated with ovarian cancer. *BMC Women's Health* **5,** 8

79. Singh, D., Chan, J. M., Zoppoli, P., Niola, F., Sullivan, R., Castano, A., Liu, E. M., Reichel, J., Porrati, P., Pellegatta, S., Qiu, K., Gao, Z., Ceccarelli, M., Riccardi, R., Brat, D. J., Guha, A., Aldape, K., Golfinos, J. G., Zagzag, D., Mikkelsen, T., Finocchiaro, G., Lasorella, A., Rabadan, R., and Iavarone, A. (2012) Transforming fusions of FGFR and TACC genes in human glioblastoma. *Science* **337,** 1231–1235

80. Williams, S. V., Hurst, C. D., and Knowles, M. A. (2013) Oncogenic FGFR3 gene fusions in bladder cancer. *Hum. Mol. Genet.* **22,** 795– 803

81. Vitre, B. D., and Cleveland, D. W. (2012) Centrosomes, chromosome instability (CIN) and aneuploidy. *Curr. Opin. Cell Biol.* **24,** 809 – 815

82. Holland, A. J., and Cleveland, D. W. (2012) Losing balance. The origin and impact of aneuploidy in cancer. *EMBO Rep.* **13,** 501–514

83. Guo, Y., Partch, C. L., Key, J., Card, P. B., Pashkov, V., Patel, A., Bruick, R. K., Wurdak, H., and Gardner, K. H. (2013) Regulating the ARNT/TACC3 axis. Multiple approaches to manipulating protein/protein interactions with small molecules. *ACS Chem. Biol.* **8,** 626 – 635

84. Wurdak, H., Zhu, S., Min, K. H., Aimone, L., Lairson, L. L., Watson, J., Chopiuk, G., Demas, J., Charette, B., Halder, R., Weerapana, E., Cravatt, B. F., Cline, H. T., Peters, E. C., Zhang, J., Walker, J. R., Wu, C., Chang, J., Tuntland, T., Cho, C. Y., and Schultz, P. G. (2010) A small molecule accelerates neuronal differentiation in the adult rat. *Proc. Natl. Acad. Sci. U.S.A.* **107,** 16542–16547

SUPPLEMENTARY EXPERIMENTAL PROCEDURES

Multiangle Light Scattering (MALS) – Light scattering measurement of purified TACC3 (before and after thrombin cleavage) was performed on a MALS instrument (miniDAWN™ TREOS) under asymmetric Flow-Field-Flow-Fractionation conditions (Eclipse™ AF4, Wyatt Technology). Protein separation by size was achieved within a very thin flow against a perpendicular force field. For exact protein mass calculation, UV absorptions at 280 nm (Agilent Infinity 1260) and refractive index signals (OptilabRex, Wyatt Technology) were collected. In particular, AF4 membranes were equilibrated with standard buffer followed by injection of 50µl of protein sample (3.86 mg/ml). Movement of the protein sample on the AF4 membrane was monitored and degree of scattered light and UV absorption (A_{280nm}) were measured. Raw data were analyzed and processed using ASTRA software (Wyatt Technology) to calculate molecular mass averages and polydispersity indexes of analyzed protein samples.

CD (circular dichroism) spectroscopy – CD spectroscopic measurements were performed on a J715 spectropolarimeter (JASCO) in 50 mM sodium phosphate buffer (1.09% Na_2HPO_4 and 0.13% NaH_2PO_4, pH 7.5; 150 mM NaCl; 1 mM EDTA). Protein samples were subjected to buffer exchange through gel filtration. The CD spectrum was measured in the wavelength range of 190 nm to 260 nm with a data pitch of 0.2 nm with ten accumulations per reading. The spectrum was recorded and converted into molar ellipticity using the following formula: Molar ellipticity [ө] in deg.cm^2/dmol = [Δε (in mdeg) × mean residue weight]/[pathlength (in mm) × concentration (mg/ml)]. Final data processing was carried out with help of the K2D3 CD spectra analysis program by selecting 41 data points from 200 nm to 240 nm at a data pitch interval of 1 nm.

Analytical ultracentrifugation sedimentation velocity centrifugation (AUC-SV) – AUC-SV was performed using an Optima XL-A analytical ultracentrifuge (Beckman Coulter) with a 4-hole titanium rotor (AnTi-60; Beckman). For SV experiments, cells with a standard aluminum two-channel centerpiece and quartz windows were used. Samples were prepared by gel filtration using standard buffer and concentrated up to 20 µM. The rotor temperature was equilibrated at 10°C in the vacuum chamber. After loading the sample (400 µl) as well as reference buffer (420 µl), radial scans at 280 nm with 20 µm radial resolution were recorded at 3 to 5 min intervals during sedimentation at 37.000 rpm. Partial specific volume of the protein, solvent density, and solvent viscosity were calculated from standard tables using the UltraScan II program (Version 14.3). The collected radial scans were analyzed using the continuous distribution [c(s)) analysis module in the SEDFIT program (Version 12.1) as well as two-dimensional spectral analysis combined with genetic algorithm (GA) and final Monte Carlo statistics as implemented in UltraScan II. SEDFIT data evaluation was performed as follows: Sedimentation coefficient increments of 0.1 S were used in the appropriate range for each sample. The frictional coefficient was allowed to float during the fitting. The weight average sedimentation coefficient was obtained by integrating the range of sedimentation coefficients in which peaks were present. The c(s) distribution was converted to a c($s_{20, w}$) distribution using the SEDFIT program. Additional data were evaluated with the UltraScan II software, which in contrast to c(s) in SEDFIT provides each detected species with an individual shape factor, i.e. frictional ratio. After a primary data

evaluation by 2DSA the time invariant noise was subtracted. These noise corrected data were fitted according to a model of non-interacting species with a parsimoniuosly regulated genetic algorithm to find the sum of solutions of the Lamm equation with the lowest number of individual species that describes the measured data best.

SUPPLEMENTARY TABLES AND FIGURE LEGENDS

TABLE S1. Statistics from analytical ultracentrifugation sedimentation velocity experiments to determine biophysical parameters including the molecular weight of purified murine TACC3 before and after thrombin cleavage. The data revealed the presence of one major species for TACC3 (species 1) and two major species (species 1 and 2) for thrombin cleaved TACC3. The full length protein showed a nearly dimeric molecular mass (1.56 times of the monomeric mass of 70 kDa), sediment faster $[S_{10,w}(S)=3.12]$, and displayed a highly extended shape ($f/f_0=2.55$). Upon thrombin cleavage of TACC3, two major species appeared: species 1 (62.3%) displayed a molecular mass of 52.55 kDa and a relatively high sedimentation rate $[S_{10,w}(S)=2.20]$ as well as a highly extended shape; species 2 (29.3 %) had a molecular mass of 61.92 kDa, a relatively slow sedimentation rate $[S_{10,w}(S)=1.28]$, and a very extended and open conformation ($f/f_0=4.26$). Values in small brackets indicate the results from two independent experiments.

FIGURE S1. *In silico* prediction of coiled-coil subdomains reveals "break regions" within the CC domain of higher vertebrate TACC3 isoforms. The very C-terminal region of TACC family members consisting of 250 residues was subjected to coiled-coil structure prediction using the COILS2 software in scanning modes of 14, 21, and 28 residues (green, blue, and red lines, respectively). *A*, comparison of the TACC domain of TACC3 isoforms from *Takifugu rubripes* (*Tr*-TACC3), *Xenopus laevis* (*Xl*-TACC3/Maskin), *Bos taurus* (*Bt*-TACC3), and *Oryctolagus cuniculus* (*Oc*-TACC3). *B*, comparison of the TACC domain of murine (*Mm*) and human (*Hs*) TACC proteins. Red arrows indicate "break regions" which are typical for TACC3 isoforms and separate the TACC domain into two coiled-coil-containing parts, CC1 and CC2.

FIGURE S2. Multiple sequence alignment of the C-terminal CC domain of vertebrate TACC family members. The arrow indicates the conserved glycine residue used to separate and clone the TACC subdomains CC1 (aa 414-530) and CC2 (aa 530-630) of murine TACC3. The red box indicates the "coiled coil structure breaking region" separating the CC1 and CC2 regions of the TACC domain from each other. Evolutionary, CC1 displays a lower degree of sequence homology when compared to CC2.

FIGURE S3. Domain organization of murine TACC3 deletion variants and fragments analyzed in this study. N specifies the conserved ~100 amino acid residues from the N-terminus of all vertebrate TACC3 isoforms. r1 to r7 denotes the central region in TACC3 consisting of seven serin-proline-rich repeats. CC1 and CC2 indicate two coiled-coil regions in the C-terminus separated by a break region. The internal thrombin cleavage site close to the CC-domain is indicated.

FIGURE S4. Murine TACC3 deletion variants and fragments overexpressed and purified in this study. *A* to *E*, purified proteins as listed in Fig. S3 were analyzed on Coomassie Brilliant Blue stained SDS-PAGE gels. Molecular weights: TACC3, 70.5 kDa; TACC3-ΔR, 52.3 kDa; TACC3-ΔN, 57.2 kDa; TACC3-ΔNΔR, 39.1 kDa; 7R, 22.0 kDa; CC, 25.2 kDa; CC1, 14.4 kDa; CC2, 11.7 kDa. Note that the abnormal migration of TACC3 in SDS-PAGE gels (~125 kDa; theoretical molecular weight: 70 kDa) is associated with the presence of the seven repeat (7R) region, as its deletion normalizes gel migration to the expected molecular weight.

FIGURE S5. C-terminal chTOG fragments overexpressed and purified in this study. (*A*) Domain organization of murine chTOG and outline of C-terminal fragments analyzed for TACC3 binding. The TOG domains 1 to 5 are implicated in microtubule interaction (1). Fragment A covers also an additional and putative TOG domain (TOG6) that was recently identified (2). (*B,C*) C-terminal fragments of murine chTOG were purified after bacterial expression and analyzed on Coomassie Blue stained SDS-PAGE gels. Calculated molecular weights: chTOG-Cterm, 51.9 kDa; chTOG-A, 29.9 kDa; and chTOG-B, 23.2 kDa. The identity of the chTOG fragments A and B was verified by immunoblotting using αchTOG

antibodies which either recognize only fragment B (αchTOG, #34032 from QED Bioscience/Acris, raised against a peptide of 14 a.a. at the very C-terminus of human chTOG) or both fragments A and B (αchTOG #NB500-182, Novus Biologicals, raised against the C-terminal 301 a.a. of human chTOG) (data not shown). CBB, Commassie Brilliant Blue.

FIGURE S6. Experimental controls for the ITC experiments performed in this study. Control experiments done in the context of Fig. 3E and 4E included titration of CC1 (485 µM) over buffer (*A*), buffer on CC2 (40 µM) (*B*), 7R (450 µM) over buffer (*C*), and CC2 (160 µM) over buffer (D). The heat release detected in the latter case may indicate changes in the oligomeric behavior of CC2 upon dilution.

FIGURE S7. Lack of interaction between CC1 and CC2 under aSEC conditions points to a parallel coiled-coil structure of the TACC domain. Potential binding of the purified TACC domain fragments CC1 and CC2 to each other was analyzed by analytical size exclusion chromatography (aSEC) followed by SDS-PAGE and CBB staining of the respective peak fractions. The observation that CC1 and CC2 do not interact indicates that the TACC domain of murine TACC3 displays a parallel coiled-coil structure.

FIGURE S8. MLN8237 – mediated inhibition of Aurora-A kinase impairs colocalization of TACC3 and chTOG to spindle microtubules and poles, but does not completely abolish centrosomal TACC3-chTOG colocalization despite centrosomal fragmentation. HeLa cells were treated with DMSO or 0.5 µM MLN8237 for 2 h. Thereafter, colocalization of the centrosomal marker γ-Tubulin and Aurora-A kinase (autophosphorylated at T288) was analyzed in the absence or presence of the Aurora-A kinase inhibitor MLN8237 (*A*). (*B*) and (*C*) depict confocal section analyses of TACC3 (green)-chTOG (red) colocalization (yellow to orange) at centrosomes and spindles in the absence or presence of MLN8237, respectively. Antibodies against α-Tubulin were used to stain the mitotic spindle apparatus. (*D*) Magnifications (3.2-fold) of representative confocal pictures depicted in (B) and (C).

FIGURE S9. Binding of TACC3 to chTOG occurs *in vivo* in an Aurora-A – independent manner. HEK293 cells were transfected with expression constructs for TACC3 or the indicated C-terminal deletion mutants all fused C-terminally to GFP. Following 48 h, cells were treated with the Aurora-A inhibitor MLN8237 (0.5 µM) for 2h. Thereafter, totel cell lysates were prepared and subjected to co-immunoprecipitation analysis using a GFP-specific antibody followed by SDS-PAGE and detection of chTOG in the immunoprecipitates.

FIGURE S10. The chTOG-B fragment, but not chTOG-A, interacts with the CC1 subdomain of TACC3. Binding of chTOG-A (*A*) or chTOG-B (*B*) (Fig. S5) to the CC1 subdomain of TACC3 was analyzed using analytical size exclusion chromatography (aSEC) followed by SDS-PAGE and CBB staining of the respective peak fractions. A significant peak shift due to complex formation was observed for chTOG-B – CC1, but not for chTOG-A – CC1.

FIGURE S11. Biophysical characterization of purified murine TACC3. *A*, Thrombin cleavage of TACC3 did not impair it's α-helical content and secondary structure as revealed by circular dichroism (CD) measurements. *B*, Multi Angle Light Scattering (MALS) analysis reveals a polydisperse/oligomeric nature of TACC3 with a molecular mass of ~420 kDa at the maximum UV_{280} absorbance. In contrast, upon thrombin cleavage, TACC3 appears monodisperse with a molecular mass of ~72 kDa that is very close to the monomeric mass of murine TACC3 (70 kDa). *C*, analytical ultracentrifugation sedimentation velocity experiments analyzing the molecular weight of TACC3 in solution before and after thrombin cleavage (results summarized in Table S1).

SUPPLEMENTARY REFERENCES

1.   Al-Bassam, J., and Chang, F. (2011) *Trends Cell Biol* **21**, 604-614
2.   Hood, F. E., Williams, S. J., Burgess, S. G., Richards, M. W., Roth, D., Straube, A., Pfuhl, M., Bayliss, R., and Royle, S. J. (2013) *J Cell Biol* **202**, 463-478

Table S1. Biophysical parameters obtained from two independent AUC-SV experiments analyzing murine TACC3 *vs.* thrombin-cleaved TACC3.

Constructs		Amount (%)	MW (kDa)	$S_{10,w}$ (S)	f/f0
TACC3	*Species 1*	*87.71*	108.91 (108.03, 109.87)	3.12 (3.12, 3.12)	2.55 (2.53, 2.57)
	Species 2	12.29	57.40 (57.10, 58.20)	4.72 (4.68, 4.77)	1.10 (1.09, 1.12)
TACC3 + Thrombin	*Species 1*	*62.30*	52.55 (52.17, 52.92)	2.20 (2.19, 2.21)	2.22 (2.21, 2.24)
	Species 2	*29.32*	61.92 (60.98, 62.86)	1.28 (1.22, 1.27)	4.26 (4.24, 4.29)
	Species 3	8.63	66.09 (63.68, 68.50)	3.78 (3.77, 3.80)	1.51 (1.47, 1.55)

Abbrevations: AUC-SV, analytical ultracentrifugation – sedimentation velocity; MW-molecular weight; $S_{10,w}$ (S), sedimentation rate at 10 ˚C; f/f0, frictional coefficient.

TABLE S1

Figure S1

B

*Mm*TACC3

CC1   CC2

*Mm*TACC2

*Mm*TACC1

*Hs*TACC3

*Hs*TACC2

*Hs*TACC1

score

number of amino acid residue

0   50   100   150   200   250
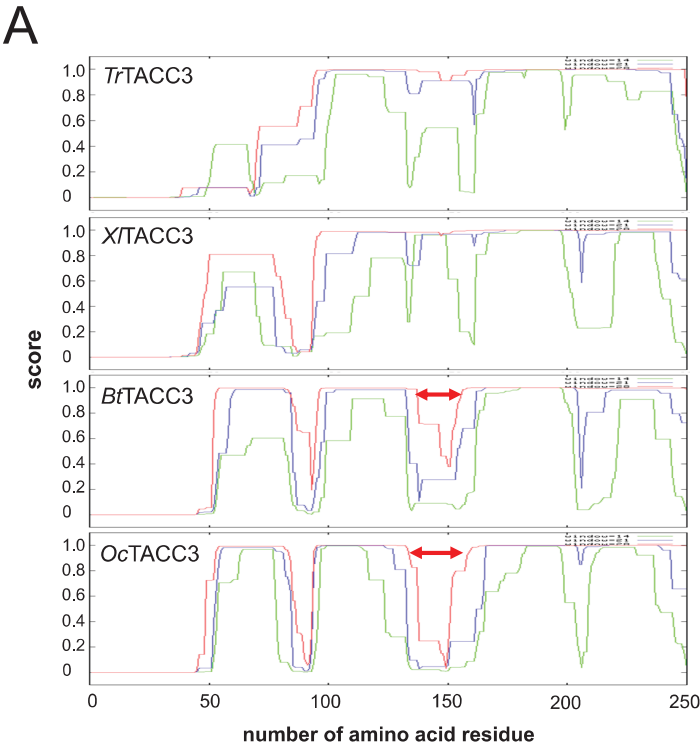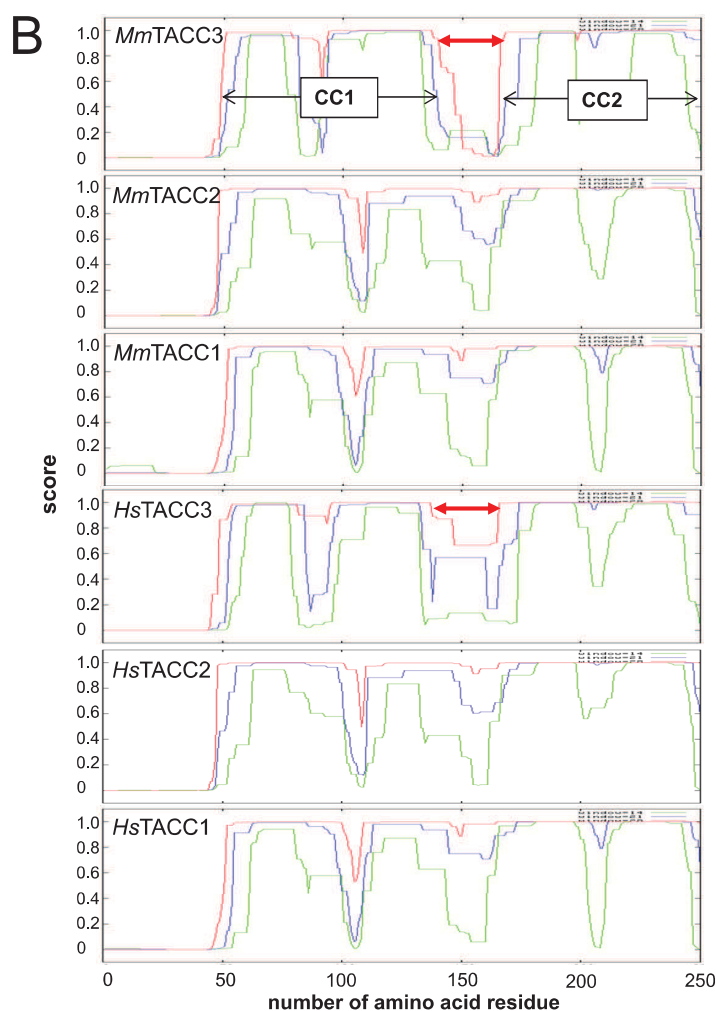
Figure S1

MmTACC3	- RGLLPAEP IVDVLKYSQKDLDAVVNVMQQEN - - - - - - LELKSKYEDLNTKYLEMGKSVDE	467
HsTACC3	- GGPPLSTGP IVDLLQYSQKDLDAVVKATQEEN - - - - - - RELRSRCEELHGKNLELGKIMDR	678
OcTACC3	- ILEPSCPPLPVGP IVDVLRYSQRDLDAAVQAAQQEN - - - - - - LELRSRCEELHTKNLEMGKIMDG	576
BtTACC3	- GAPLLPVGP IVDVLQYSQKDLDSAVEATQKEN - - - - - - EVLRGKCAALQERLLEMGKIMDS	650
XlTACC3	- NPFLSTSDAI VEMLKYSQKDMDAAIEAVRLEVQEKDLEVLEVKTKHEKLYLEYVEMGKIIAE	771
TrTACC3	- QTAHVEESII IEVLKYSQKDMDAAIAKVQAEVEKD - - - NCWSAYKKLLEDGQEMRKIIAE	718
MmTACC2	SRSRQDTKREAAHPPDVSISKTALYSRIGSTEVEKPPGLLFQQPDLDSALQVARAEVIAKEREVSEWRDKYEESRREVVEMRKIVAE	986
HsTACC2	SRSHQDAKREAAHPTDVSISKTALYSRIGTAEVEKPAGLLFQQPDLDSALQIARAEIITKEREVSEWDKYEESRREVMEMRKIVAE	866
MmTACC1	- - - - - - - - - - - - - - - - - - - ESPLDGICLSEADKTAVLTLIREEIITKEIEANEWKKKYEETREEVLEMRKIVAE	615
HsTACC1	- - - - - - - - - - - - - - - - - - - ESPLDGICLSESDKTAVLTLIREEIITKEIEANEWKKKYEETRQEVLEMRKIVAE	644

MmTACC3	FEKIAYKSLEEAEKQRELKEIAEDKIQKVLKERDQLNADLNSMEKSFSDLFKRFEKRKEVIEGYQKNEESLKKYVGECIVKIEKEGQ	554
HsTACC3	FEEVVYQAMEEVKQ - - - KELSKAEIVDLNSMEKSFSDLFKRFEKQKEVIEGYRKNEESLKKCVEDYLARITQEGQ	762
OcTACC3	FEGIVYQAMEEVQRQ - - - KEAARAEVQKVLKDREQLAADLSSTEKSFSDLFKRFEKQKEVIGGYRKNEESLKKCVEDYAARVEKEAQ	660
BtTACC3	FEGTVYQVMEESQKQ - - - KELTKAEMQKVLKEKAQLTADLHSMEKSFSDLFKRFEKQKEVIEGYRTNEESLKKCVEDYIERVEKEAQ	734
XlTACC3	FEGTITQILEDSQRQ - - - KETAKLELNKVLQEKQQVQDLNSMETSFSELFKRLEKQKEALEGYRKNEEALKKCVEDYLVRIKKEEQ	855
TrTACC3	FESMIAQMMADQEKQ - - - TEESQKQLNEALSEKEQVASDLNAMERSFSDLFKRLEKYKEVVQGYKKNEETLKACAQDYLARIKKEEQ	802
MmTACC2	YEKTIAQMIEDEQRE - - - KSISHQTVQQLVLEKEQALADLNSVEKSLADLFRRYEKMKEVLEGFRKNEEVLKKCAQEYLSRVKKEEQ	1070
HsTACC2	YEKTIAQMIEDEQRE - - - KSVSHQTVQQLVLEKEQALADLNSVEKSLADLFRRYEKMKEVLEGFRKNEEVLKKCAQEYLSRVKKEEQ	950
MmTACC1	YEKTIAQMIEDEQRT - - - SMSSQKSFQQLTMEKEQALADLNSVERSLSDLFRRYENLKGVLEGFKKNEEALKKCAQDYLARVKQEEQ	699
HsTACC1	YEKTIAQMIEDEQRT - - - SMTSQKSFQQLTMEKEQALADLNSVERSLSDLFRRYENLKGVLEGFKKNEEALKKCAQDYLARVKQEEQ	728

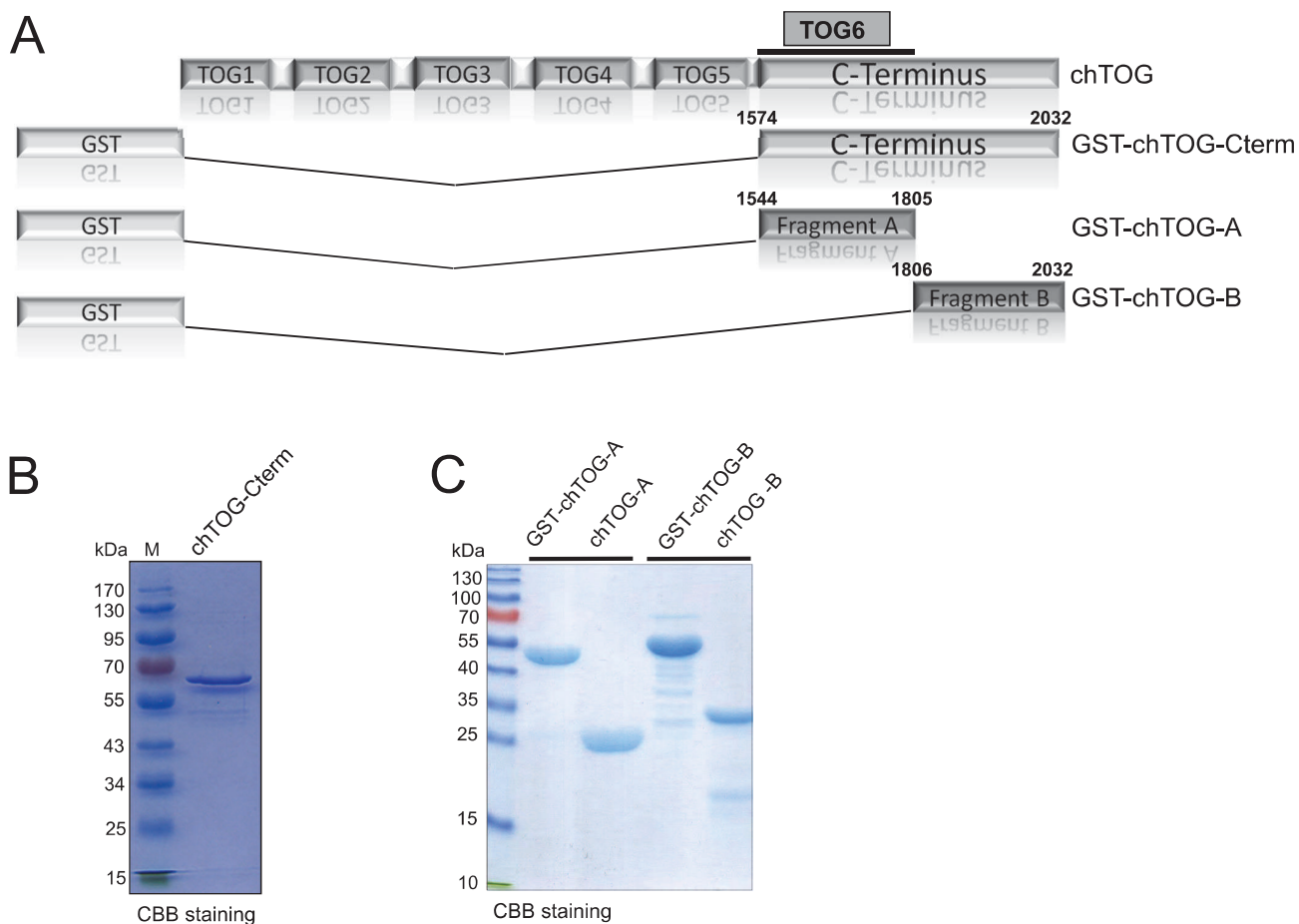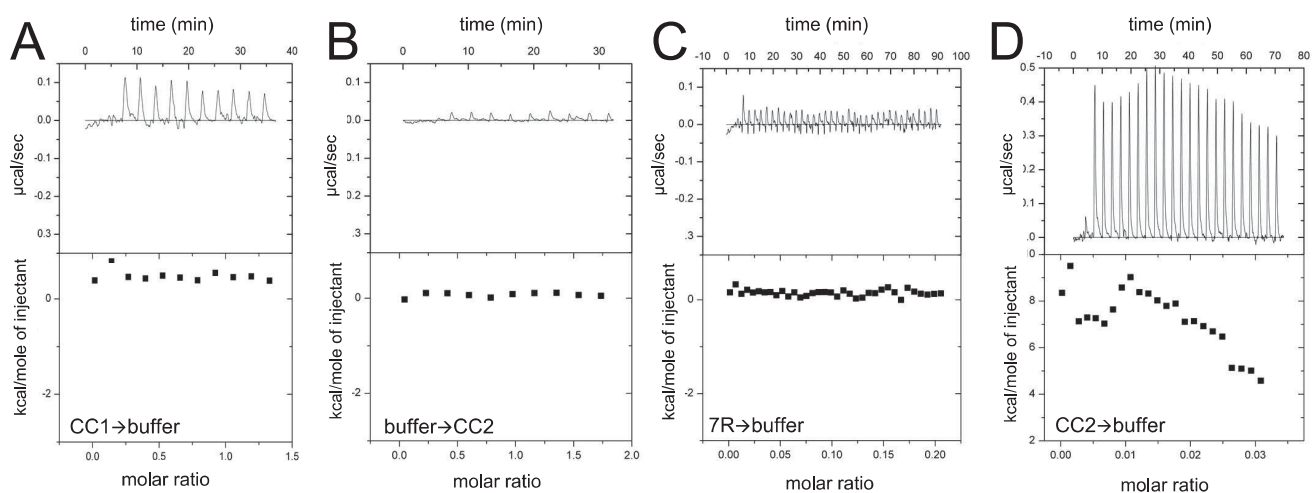|		
MmTACC3	RYQALKIHAEEKLRLANEEIAQVHSKAQAEVLALQASLRKADMQNHSLEMTLEQKTKEIDELTRICDDLISKMEKI-	630
HsTACC3	RYQALKAHAEEKLQLANEEIAQVRSKAQAEALALQASLRKEQMRIQSLEKTVEQKTKENEELTRICDDLISKMEKI-	838
OcTACC3	RYQALKAHAEEKLKLASEEIAQVRSKAQAEALAFQASMRKADMQIQSLEKTVEQKVKENEELTRICDDLISKMEKI-	736
BtTACC3	KYQALKAQAEEKLRQASEEIAQVRSKAQTDALALQAVLRKEQMRVHSLEKVVEQKTKENDELTRICDDLISKMKRI-	810
XlTACC3	RYQALKAHAEEKLNRANEEIAQVRSKAKSEATALQATLRKEQKIQSLERSLEQKSKENDELTKICDDFILKMEKI-	931
TrTACC3	RYQALKAHAEEKIAQANGEIAEVRSKNKAELSALQAQLRREQLKAQSLEKSLDQKGKEAAEELTKLCDELITKVQKG-	878
MmTACC2	RYQALKVHAEEKLDRANAEIAQVRGKAQQEQAAYQASLRKEQLRVDALERTLEQKNKEIEELTKICDELIAKMGKS-	1146
HsTACC2	RYQALKVHAEEKLDRANAEIAQVRGKAQQEQAAHQASLRKEQLRVDALERTLEQKNKEIEELTKICDELIAKMGKS-	1026
MmTACC1	RYQALKVHAEEKLDRANEEIAQVRSKAKAESAALHAGLRKEQMKVESLERALQQKNQEIEELTKICDELIAKLGKTD	776
HsTACC1	RYQALKIHAEEKLDKANEEIAQVRTKAAESAALHAGLRKEQMKVESLERALQQKNQEIEELTKICDELIAKLGKTD	805

Figure S2

Thrombin cleavage site (LEPR/GL)

repeats (7R)   Coiled Coil (CC)
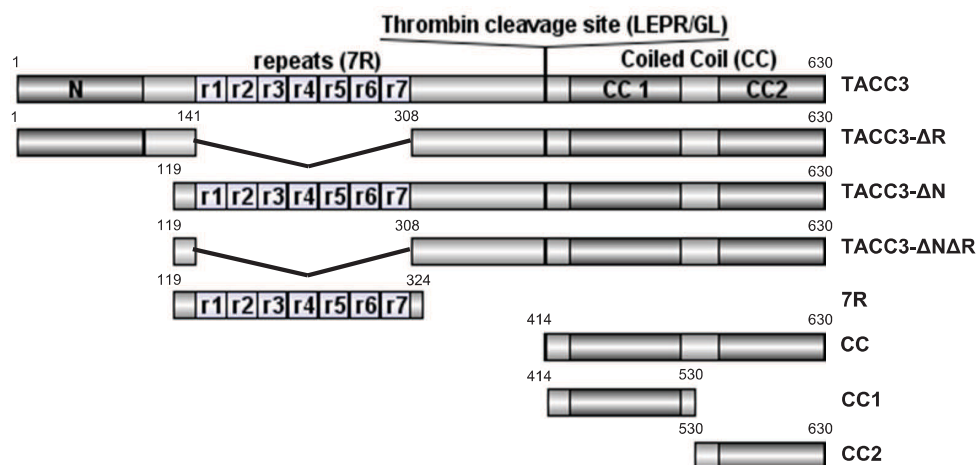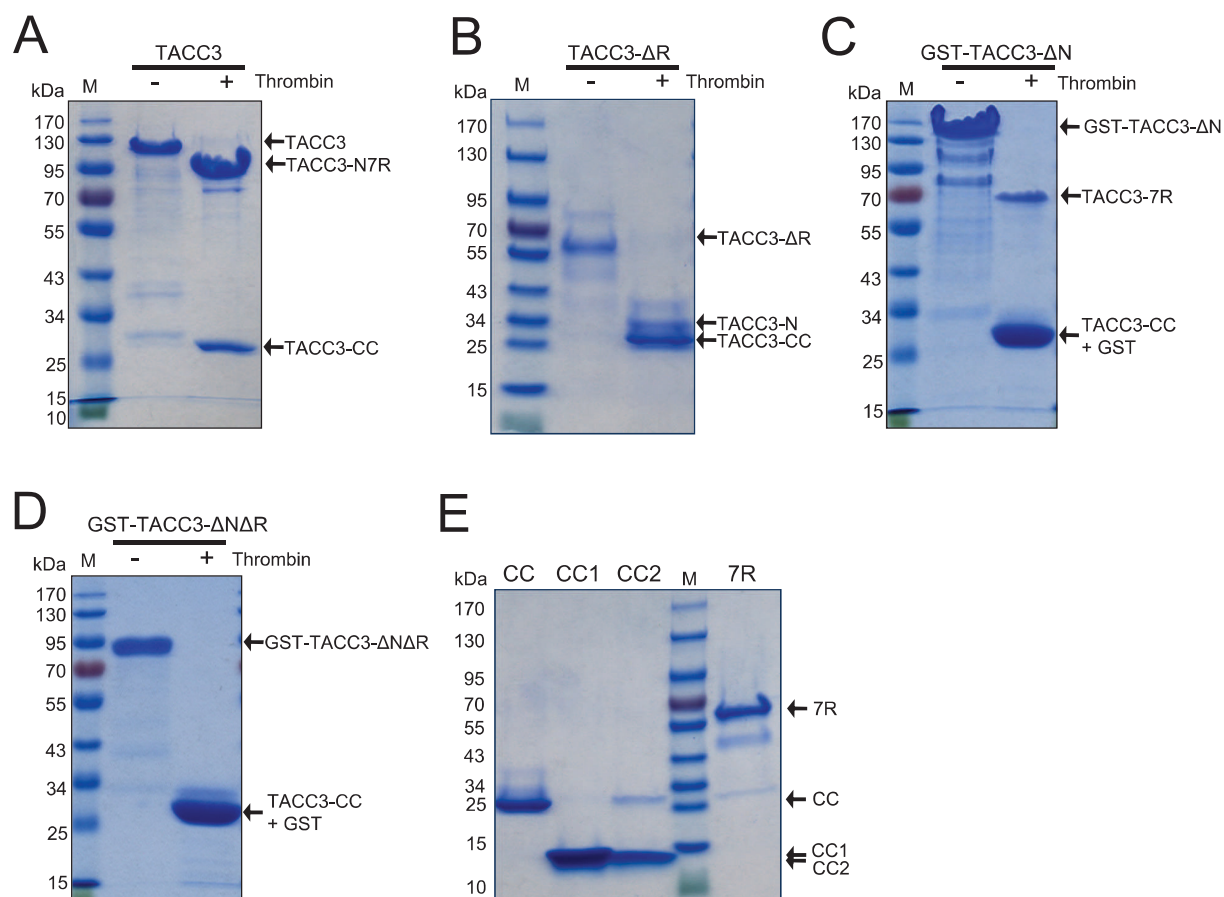
Figure S3

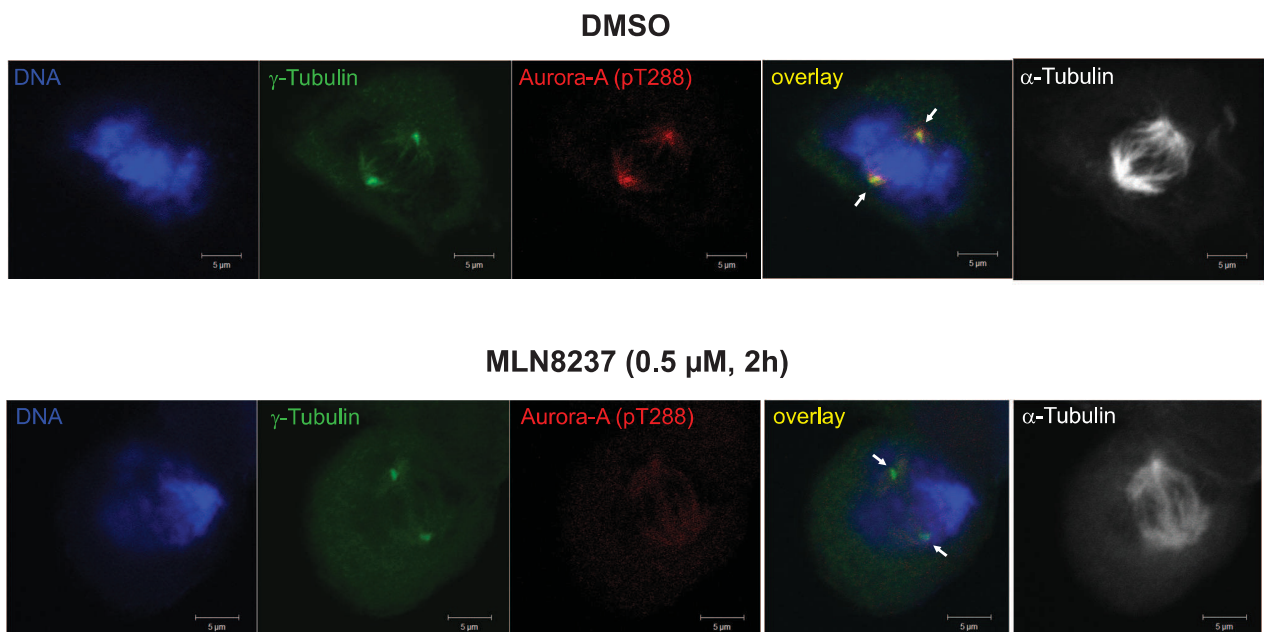**Figure S4**
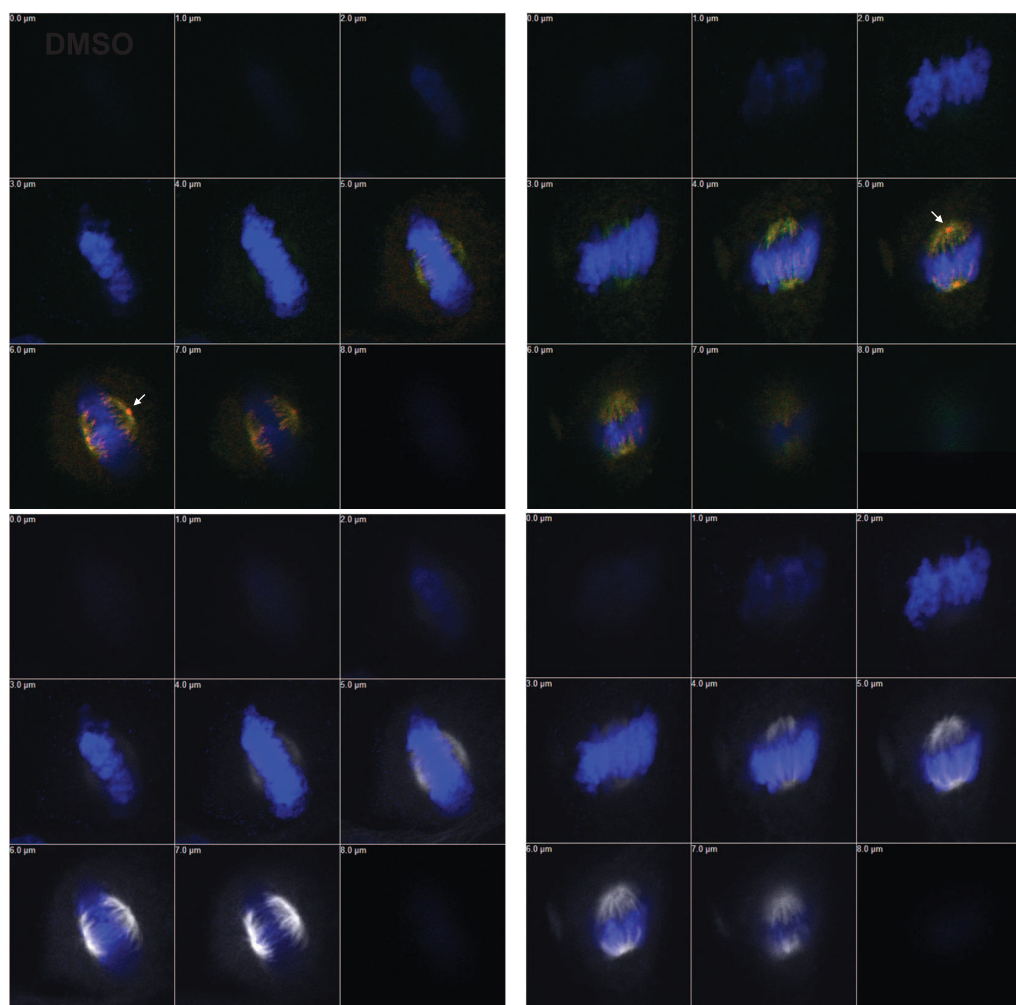
Figure S5

Figure S6

Figure S7

A

DMSO

| DNA | γ-Tubulin | Aurora-A (pT288) | overlay | α-Tubulin |

MLN8237 (0.5 µM, 2h)

| DNA | γ-Tubulin | Aurora-A (pT288) | overlay | α-Tubulin |

Figure S8

B

DMSO

TACC3
chTOG
DNA

DMSO

α-Tubulin

Figure S8

C

TACC3
chTOG
DNA

MLN8237
(0.5 μM, 2h)

α-Tubulin

Figure S8

D

DMSO	MLN8237
DMSO	MLN8237

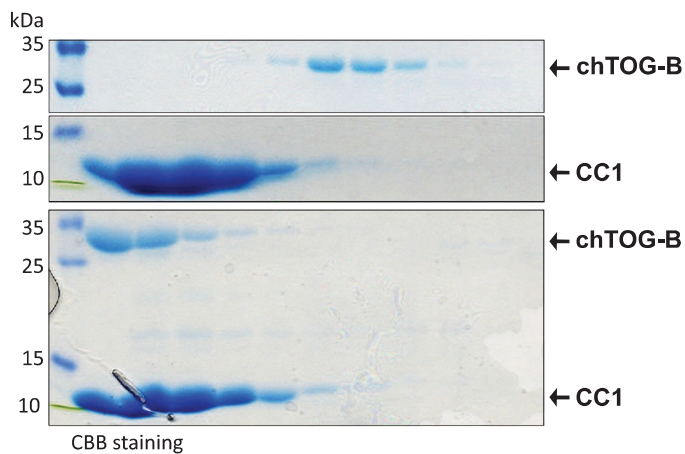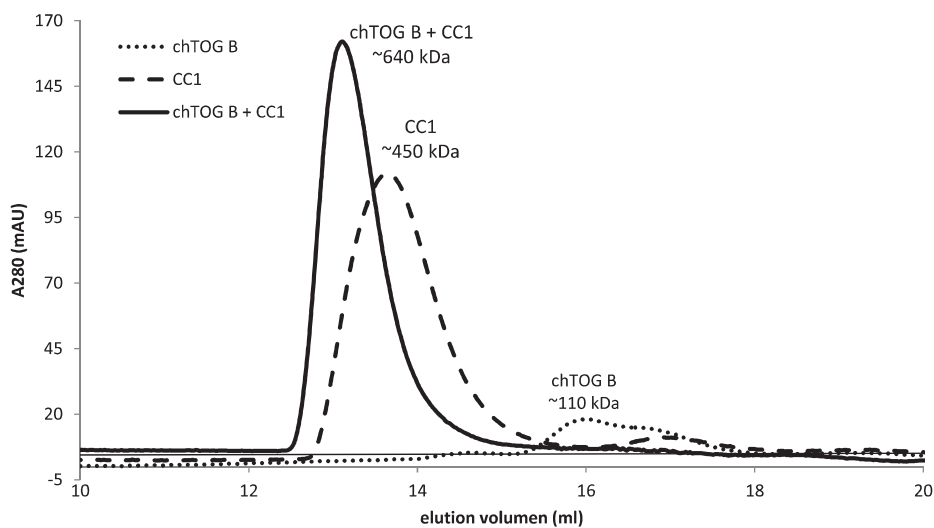**TACC3**
chTOG
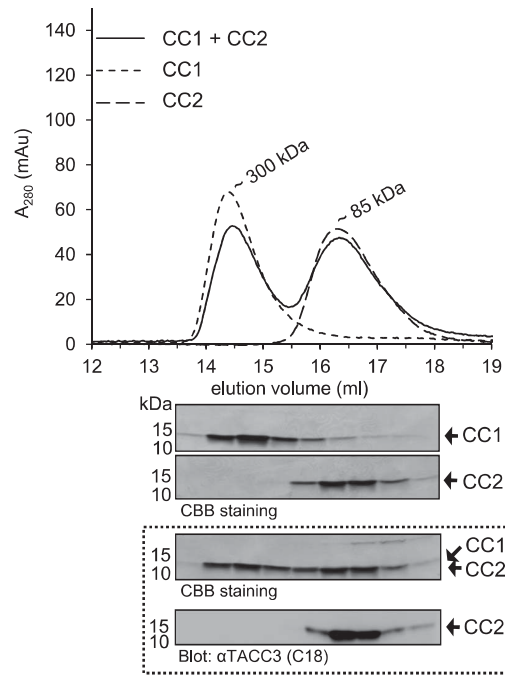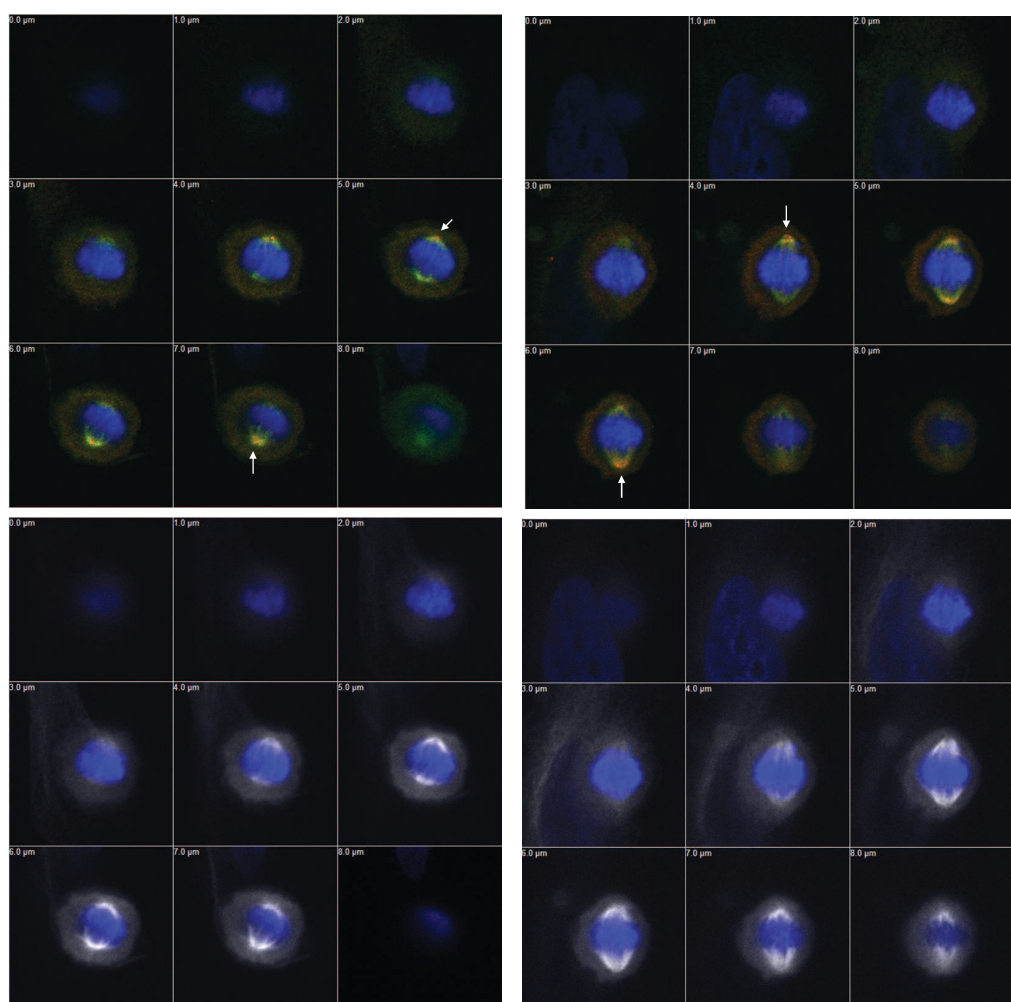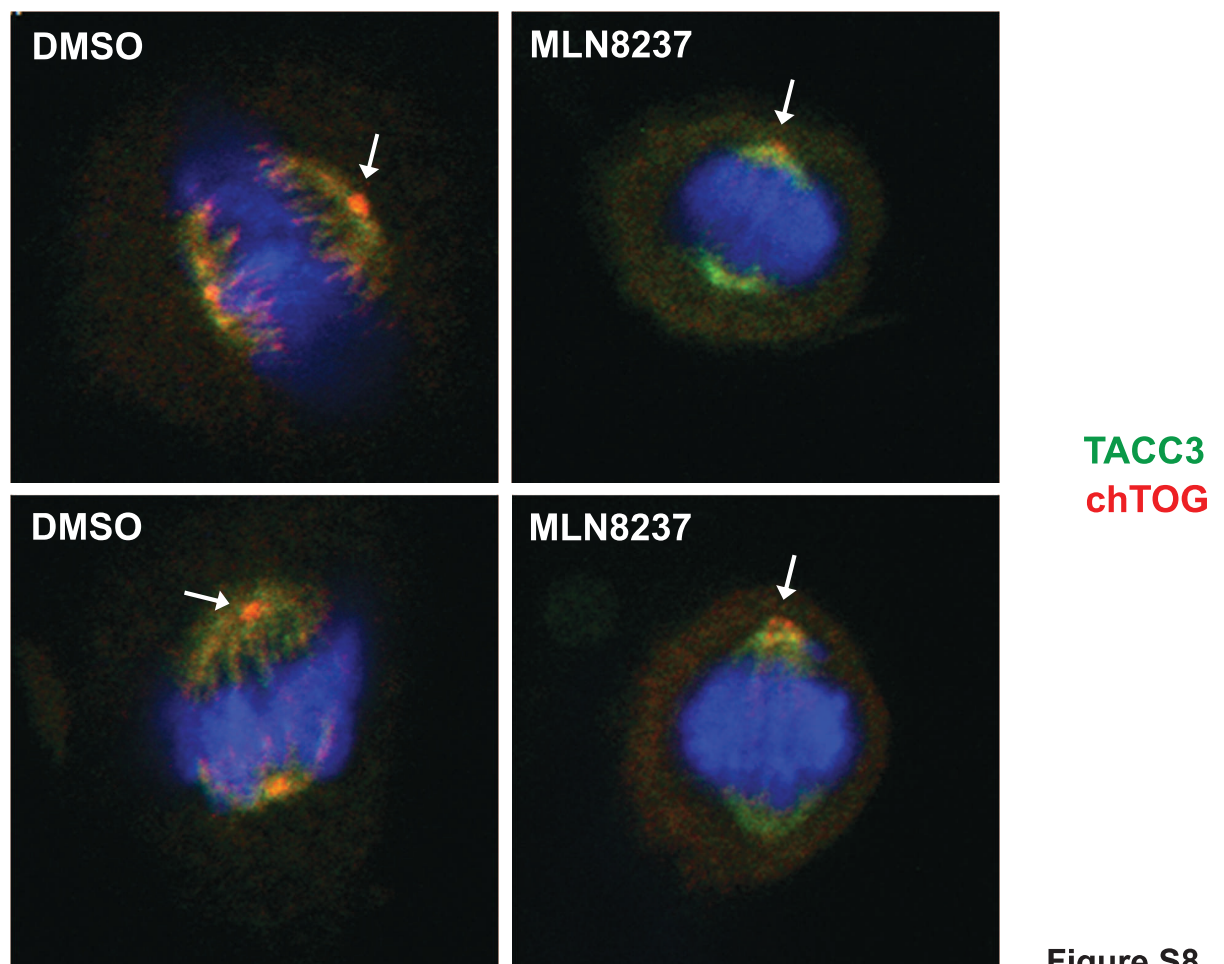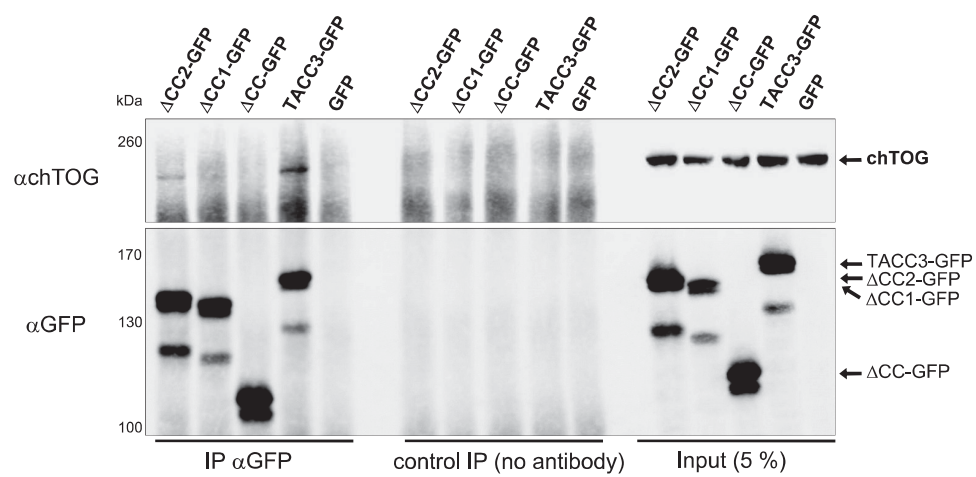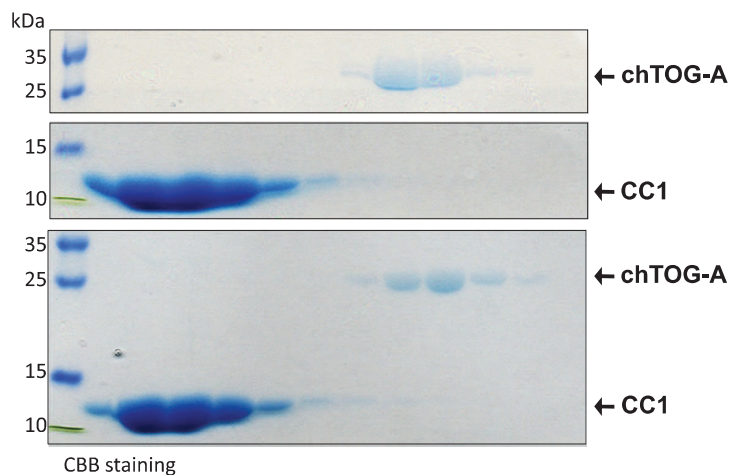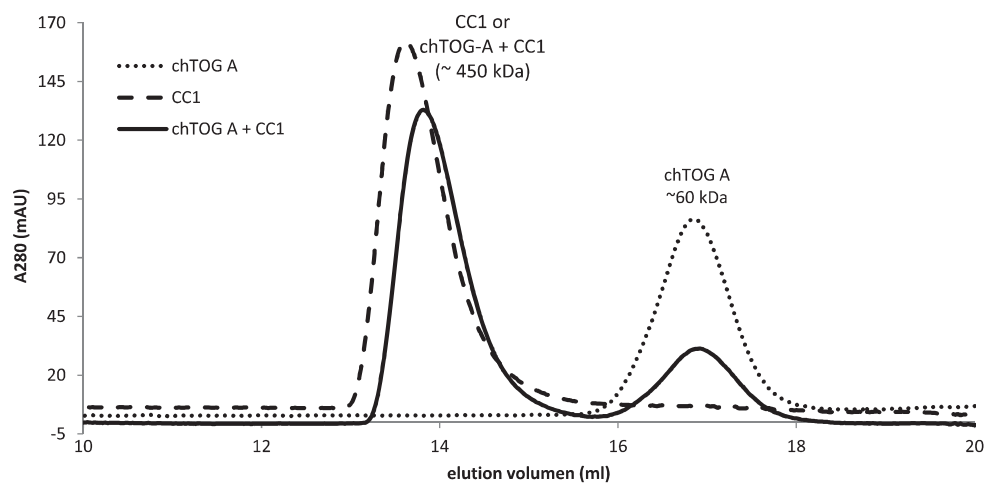
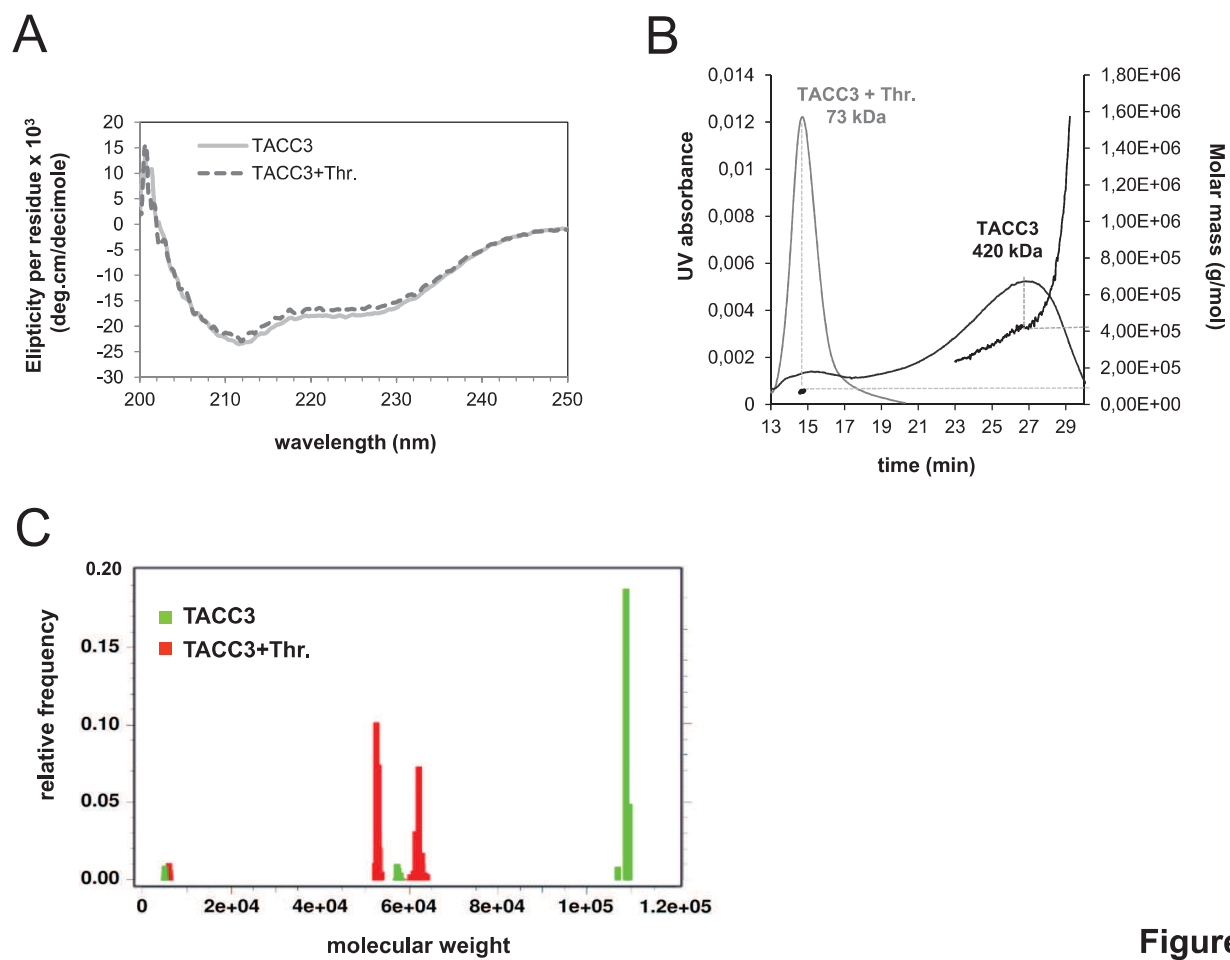**Figure S8**

Figure S9

Figure S10

Figure S11

The centrosome and mitotic spindle apparatus in cancer and senescence

Stephan Schmidt,[1] Frank Essmann,[6] Ion C. Cirstea,[1] Fabian Kuck,[1] Harish C. Thakur,[1] Madhurendra Singh,[1] Anja Kletke,[1] Reiner U. Jänicke,[2] Constanze Wiek,[3] Helmut Hanenberg,[3,4] M. Reza Ahmadian,[1] Klaus Schulze-Osthoff,[6] Bernd Nürnberg[5] and Roland P. Piekorz[1,*]

[1]Institut für Biochemie und Molekularbiologie II; [2]Klinik für Strahlentherapie und Radioonkologie; [3]Klinik für Kinder-Onkologie; Hämatologie und Klinische Immunologie; Universitätsklinikum der Heinrich-Heine-Universität; Düsseldorf, Germany; [4]Department of Pediatrics; Wells Center for Pediatric Research; Riley Hospital for Children; Indiana University School of Medicine; Indianapolis, IN USA; [5]Institut für Experimentelle & Klinische Pharmakologie & Toxikologie und Interfakultäres Zentrum für Pharmakogenomik & Arzneimittelforschung (ICePhA); Klinikum der Eberhard Karls Universität; [6]Abteilung für Molekulare Medizin; Interfakultäres Institut für Biochemie (IFIB); Eberhard Karls Universität; Tübingen, Germany

Altered cell division is associated with overproliferation and tumorigenesis, however, mitotic aberrations can also trigger antiproliferative responses leading to postmitotic cell cycle exit. Here, we focus on the role of the centrosome and in particular of centrosomal TACC (transforming acidic coiled coil) proteins in tumorigenesis and cellular senescence. We have compiled recent evidence that inhibition or depletion of various mitotic proteins which take over key roles in centrosome and kinetochore integrity and mitotic checkpoint function is sufficient to activate a p53-p21[WAF] driven premature senescence phenotype. These findings have direct implications for proliferative tissue homeostasis as well as for cellular and organismal aging.

Role of the Centrosome in Normal and Malignant Proliferation

Mitotic cell division is a prerequisite for development, proliferative homeostasis and tissue regeneration. During mitosis the bipolar spindle is organized by centrosomes to ensure faithful separation of chromosomes to both daughter cells.[1] Spindle poles, kinetochores and various microtubule-associated proteins are involved in the regulation of microtubule dynamics. On the one hand, the assembly of the mitotic spindle apparatus is a highly complex and dynamic process and tightly regulated by cell cycle components and in particular by the kinetochore attachment checkpoint.[2] On the other hand, anomalities in centrosome and mitotic spindle architecture and functions have profound consequences for cell cycle progression and can lead to chromosomal instability, aneuploidy/tetraploidy and cell death.[1,3,4]

Cancer cells often display genetic instability and centrosomal anomalies, thus implying chromosomal missegregation and aneuploidy as driving forces in tumorigenesis. Interestingly, this concept was already proposed almost 100 years ago by the pioneering work of Theodor Boveri.[5] However, the role of the centrosome and its amplification in generating genomic instability, and as a consequence cancer, is debated as amplified centrosomes can form clusters and assemble a bipolar rather than a multipolar spindle resulting in normal cell division.[6] Moreover, analysis of mice with reduced expression of the centromere-linked motor protein CENP-E (Centromere protein E) unexpectedly revealed that increased aneuploidy can act both in an oncogenic way (in the case of spontaneous tumors) and as a tumor suppressor (in the case of induced tumor formation).[7]

An alternative and intriguing concept linking centrosomal amplification to tumorigenesis was recently proposed and successfully tested in the fruit fly model. The authors demonstrated that symmetric (abnormal), rather than asymmetric (normal) cell division of neuroblasts, but not genomic instability, led to their overproliferation resulting in a transplantable
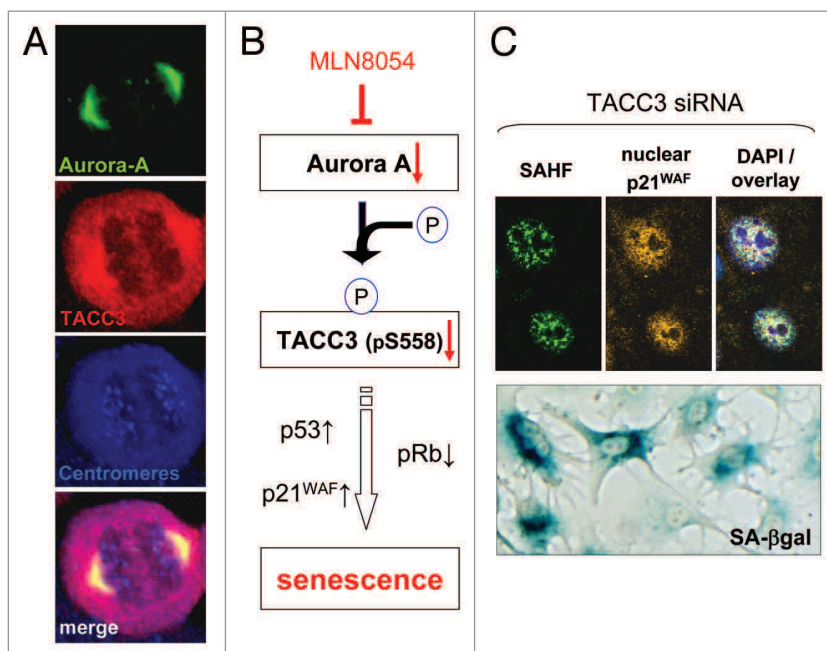
Figure 1. Inhibition of the Aurora-A-TACC3 function triggers premature senescence. (A) Confocal microscopic analysis of Aurora-A kinase colocalized with its substrate TACC3 during cell division. Centromeric regions were visualized by the CREST autoimmune serum. (B) Inhibition of Aurora-A activity by the small molecule inhibitor MLN8054, siRNA-mediated Aurora-A depletion or knock-down of its downstream target TACC3 all trigger comparable effector pathways and a premature senescence phenotype. (C) Senescence upon TACC3 depletion is characterized by the occurrence of HP1γ (pS83)-positive senescence-associated heterochromatic foci (SAHF), nuclear accumulation of the cell cycle inhibitor p21^{WAF}, and increased SA-β-Gal activity (blue staining). (B and C) modified from ref. 44.

cancer-like phenotype.[8,9] Given these provocative findings it is important to determine to which extent centrosomal aberrations occur in human cancer stem cells[10] and whether these defects affect an early stem cell balance between the symmetric (cancer promoting) and asymmetric (cancer suppressing) division mode.[11]

Centrosomal TACC Proteins and their Link to Cancer

The mammalian transforming acidic coiled coil (TACC) family of centrosomal proteins consists of three members (TACC1, 2, 3) which are important structural components of the mitotic spindle apparatus contributing to its dynamics.[12,13] TACC proteins are evolutionary conserved from yeast to man[12-16] and share a 200 amino acid coiled coil motif at their C-terminus, but have only limited homology in the N-terminal part. During mitosis, TACCs regulate centrosome integrity, centrosome-dependent assembly

of microtubules and spindle stability.[17-20] TACC3 is predominantly expressed during the G_2/M phase of the cell cycle where it localizes in an Aurora-A phosphorylation and clathrin heavy chain-dependent manner to centrosomes and mitotic spindles (**Fig. 1A**; refs. 21–24). TACC3, but not the related isoform TACC2 which is rather found in postmitotic tissues, is required for efficient cell expansion and survival as indicated by its crucial and non-redundant role(s) during embryogenesis and stem cell function.[20,25]

TACC genes have been originally discovered in genomic regions that are amplified in cancer.[26,27] Mutations of TACC3 as well as altered expression of TACC1 or TACC3 have been subsequently linked to the etiology of breast, ovarian, bladder and non-small cell lung cancer.[28-31] Interestingly, in gliomas, the TACC3 gene, localized at 4p16, is amplified. This is accompanied by a grade-specific upregulation of TACC3 expression which is highest in grade IV gliomas (glioblastoma

multiforme, GBM) which have a very poor prognosis.[32] Despite of these findings, the relevance of TACC3 for the pathogenesis of GBM or other cancer types needs to be substantiated and additional functional data are required to establish TACC3 as a "driver" in tumor development and hence as a potential therapeutic target.

Irrespective of the obvious connection between centrosomal aberrations, over-proliferation and tumorigenesis, alterations in the mitotic machinery can also act as potent triggers for postmitotic cell cycle exit and permanent growth arrest. Interestingly, as we discuss below and summarize in **Table 1,** various recent reports link centrosome and kinetochore dysfunction to the induction of cellular senescence.

Cellular Senescence— Causes and Characteristics

The phenomenon of cellular senescence was first described almost 50 years ago. Hayflick and Moorhead noted in their classical work that normal diploid fibroblasts exhibit in culture only a limited proliferative capacity and following a finite number of cell divisions undergo a state of cell cycle arrest, known as replicative senescence.[33] In human cells this intrinsic type of senescence is typically elicited by progressive erosion of telomeres.[34] Senescence represents a major cellular stress and self-defense response with tumor suppressor function. As such it is elicited by extrinsic factors, including strong mitogenic stimuli like oncogenic Ras(G12V) (referred to as oncogene-induced senescence), DNA damage, various cytotoxic drugs and oxidative stress.[35,36] These forms of senescence represent rapid antiproliferative reponses and are generally referred to as stress-induced premature senescence (SIPS).

Senescent cells exhibit characteristic features such as growth arrest, apoptosis resistance and altered gene expression.[36] The cells display several features which distinguish them from quiescent cells reversibly arrested in the G_1 phase of the cell cycle.[34,37] In particular, senescent cells adopt (1 morphological changes, i.e., they become larger and flattened and display an increased granularity, (2) changes in nuclear architecture characterized by

Table 1. Proteins of the mitotic spindle apparatus linked to premature senescence

Protein(s)	Localization & function	Mode of targeting function/ expression	Effector mechanisms & senescence markers	References
Aurora-A	mitotic kinase	small drugs, siRNA	p53, p21^{WAF}, pRb, SA-β-Gal	45, 48
TACC3	CT, MT dynamics	siRNA	p53, p21^{WAF}, pRb, SAHF, SA-β-Gal	44
PCM1	CT integrity	siRNA	P53, p21^{WAF}, pRb, SA-β-Gal	61, 62
Pericentrin	CT integrity	siRNA	p53, p21^{WAF}, pRb, SA-β-Gal	61, 62
p31^{Comet}	SAC	overexpression	p53, p21^{WAF}, SA-β-Gal, PAI-1	60
CENP-A	KT organisation	OIS, RS, siRNA	p16^{INK4a}, p53, p21^{WAF}, SAHF, SA-β-Gal	51
Bub1	KT/SAC	RS, siRNA	p53, p21^{WAF}	50
Bub3/Rae1	KT/SAC	haploinsufficiency (in vivo)	p16^{INK4a}, p53, p21^{WAF}, SA-β-Gal	53
BubR1	KT/SAC	hypomorphic alleles (in vivo)	p16^{INK4a}, p53, p21^{WAF}, SA-β-Gal	52
Mad2	KT/SAC	siRNA	p53, p21^{WAF}, SA-β-Gal, SASP	59

This table lists proteins of the mitotic spindle apparatus whose functional inhibition and/or the indicated changes in expression result in p53 activation and a cellular senescence response. Abbreviations: Bub, budding uninhibited by benzimidazoles; CENP, centromere protein; CT, centrosomal; Mad, mitotic arrest deficient; KT, kinetochore; MT, microtubule; OIS, oncogene induced senescence; PAI, plasminogen activator inhibitor; PCM, pericentriolar material; pRb, phosphorylated Retinoblastoma protein; RS, replicative senescence; SAC, spindle assembly checkpoint; SAHF, senescence associated heterochromatic foci; SASP, senescence associated secretory phenotype; TACC, transforming acidic coiled coil.

the formation of senescence associated heterochromatic foci (SAHF) linked to the repression of proliferative genes and (3) biochemical changes including an expansion of the lysosomal compartment with increased SA-β-galactosidase expression and lack of BrdU incorporation and DNA synthesis. Lastly, the cell cycle regulators p53, p21^{WAF1} and p16^{INK4a}, as well as the mTOR (mammalian Target of Rapamycin) pathway play crucial roles in the induction and maintenance of the senescent phenotype.[34,38,39] In this regard, recent findings underline a new and key function of mTOR in determining the choice between senescence and quiescence upon p53-p21^{WAF} mediated cell cycle arrest.[40,41]

Centrosomal and Kinetochore Proteins are Linked to Cellular Senescence via the Tumor Suppressor p53

Targeting TACC3 by gene inactivation in mice or RNA interference in cells causes centrosomal dysfunction and mitotic spindle stress with cellular consequences that are determined by the status of the postmitotic and p53-p21^{WAF}-controlled G$_1$ checkpoint.[25,42,43] Whereas checkpoint-compromised human cancer cells rapidly succumb to polyploidization and mitotic catastrophe,[19] checkpoint-proficient cells primarily activate a senescence program. This response is usually characterized

by an increase in p53 and p21^{WAF} levels, downregulation of phosphorylated and hence inactive retinoblastoma protein (pRb) preventing S phase entry, formation of SAHFs, and increased SA-β-Gal positivity (**Fig. 1**).[44] Interestingly, a similar premature senescence phenotype was observed in p53 proficient tumor cells when Aurora-A kinase, the upstream regulator of TACC3, was either pharmacologically inhibited or depleted.[45] These findings provide evidence that the centrosomal Aurora A-TACC3 axis (**Fig. 1**) affects the commitment of mitotic cells to cellular senescence. Given that p53 levels rise during prolonged mitosis ("mitotic clock function of p53"; reviewed in ref. 42), and that Aurora-A phosphorylates p53 at Ser315 thereby sensitizing p53 for degradation,[46] it is conceivable that elevated mitotic p53 levels per se link spindle stress to cellular senescence via transcriptional induction of p21^{WAF} in G$_1$. In this model, Aurora-A plays an inhibitory role during normal cell division, as it keeps p53 levels below a critical threshold, whereas upon prolonged mitotic arrest Aurora-A independent mechanisms may intervene to increase p53 concentrations necessary for G$_1$ arrest. Possible candidates for those positive p53 regulators would be the ataxia telangiectasia mutated (ATM) kinase and the cyclin-dependent kinase inhibitor p19^{ARF} that both prevent p53 degradation by the ubiquitin ligase MDM2.[47,48] However, a deficiency of either ATM or

p19^{ARF} did not prevent embryonic lethality caused by TACC3 deficiency (Piekorz et al., unpublished results). Nevertheless, the lethality of TACC3 deficient embryos (being probably secondary to a growth arrest phenotype) could be partially rescued by genetically reducing p53 expression.[25] Moreover, Vogel et al. observed that increase of p53 levels during transient mitotic arrest occurs independently of ATM, ATR, Chk1 and Chk2.[49] Thus, during prolonged mitosis, p53 levels may simply accumulate due to the lack of Mdm2-mediated degradation, as Mdm2 levels are dependent on transcription which is absent in mitosis and only resumes in G$_1$.[42]

As summarized in **Table 1**, altered expression of various proteins required for centrosomal integrity, kinetochore organisation or mitotic checkpoint function has now been linked to p53 activation and premature senescence. For instance, silencing of the mitotic spindle checkpoint kinase Bub1 or the centromere-localized histone H3 variant CENP-A activates a stress response characterized by the appearance of typical senescence markers. Consistent with these findings, downregulation of Bub1 and CENP-A has been observed under conditions of oncogenic stress and during replicative senescence.[50,51] Lastly, mouse models with a genetic insufficiency for BubR1 or a haploinsufficiency for both Bub3 and Rae1 display progressive aneuploidy, premature
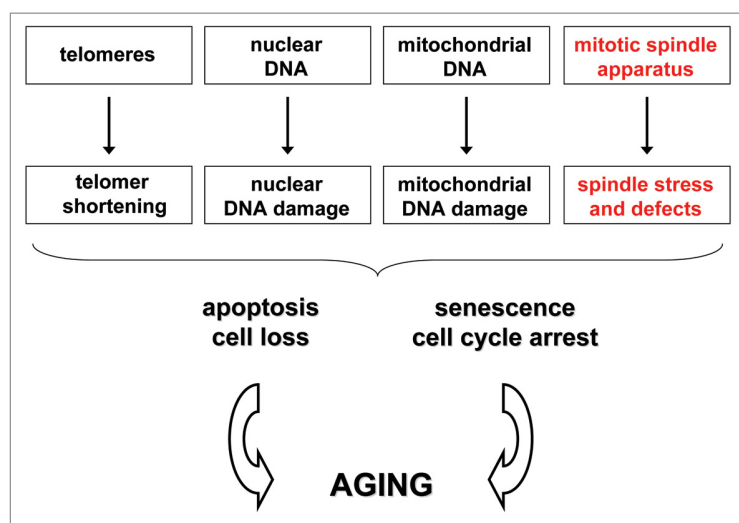
Figure 2. Cellular structures and macromolecules linked to senescence and aging. Degeneration of telomeres and nuclear or mitochondrial DNA damage are major causes for the induction of either apoptotic cell death or cellular senescence. Recent findings indicate that a functional impairment of the centrosome and mitotic spindle apparatus is as well sufficient to provoke a complete loss of proliferative capacity and induction of a cellular senescence program (**Table 1**). Thus, like telomeres, centrosomes and kinetochores may take over a crucial role in regulating commitment of mitotic cells to premature senescence.

senescence and pathological phenotypes typical for accelerated aging.[52,53] Taken together, these data uncovered a particular role of mitotic checkpoint proteins in the regulation of senescence and organismal aging.[54] However, it remains to be determined whether altered expression of the proteins summarized in **Table 1** regulates not only the onset of the postmitotic senescence response but also modulates its severity. Interestingly, whereas the proliferation arrest upon treatment with the Aurora-A kinase inhibitor MLN8054 was irreversible,[45] we observed indications for a reversible nature of the senescence phenotype caused by TACC3 depletion.[44]

Perspective—Exogenous Noxae, Mitotic Spindle Stress and Aging

Genomic and mitochondrial DNAs are classical cellular targets for the detrimental and senescence inducing effects of various intrinsic and extrinsic noxae, including ROS, ionizing radiation and UV light (**Fig. 2**). In contrast to these cellular macromolecules, surprisingly little is known about DNA damage-independent molecular effects and protein targets of exogenous insults targeting the centrosome and spindle apparatus during

mitosis. Mitotic dysfunction has a major impact on proliferative homeostasis and tissue regeneration, processes, which are progressively impaired during normal aging and characterized by the accumulation of senescent cells in proliferative tissues from aged primates.[55,56] Moreover, tetraploidy and polyploidy are biomarkers of aging, as for instance polyploid vascular smooth muscle cells with a senescent phenotype accumulate during aging.[57] Taken these observations into consideration it is conceivable that altered expression and/or functional inhibition of proteins of the mitotic spindle apparatus through the influence of intrinsic or extrinsic noxae contribute to aberrant mitosis and cytokinesis, tetraploidy and cellular senescence, and lastly dysfunction of major proliferative organs. Hence, the proteins listed in **Table 1** represent bona fide candidates for decisive stress sensors that may be redox sensitive and that are able to regulate the commitment of dividing cells to undergo premature senescence.

References

1. Nigg EA. Origins and consequences of centrosome aberrations in human cancers. Int J Cancer 2006; 119:2717-23.
2. Khodjakov A, Rieder CL. The nature of cell cycle checkpoints: Facts and fallacies. J Biol 2009; 8:88.
3. Doxsey S, Zimmerman W, Mikule K. Centrosome control of the cell cycle. Trends Cell Biol 2005; 15:303-11.
4. Sluder G. Two-way traffic: Centrosomes and the cell cycle. Nat Rev Mol Cell Biol 2005; 6:743-8.
5. Boveri T. Zur Frage der Entstehung maligner Tumoren. Jena, Germany:Gustav Fischer Verlag, 1914.
6. Gergely F, Basto R. Multiple centrosomes: Together they stand, divided they fall. Genes Dev 2008; 22:2291-6.
7. Weaver BA, Silk AD, Montagna C, Verdier-Pinard P, Cleveland DW. Aneuploidy acts both oncogenically and as a tumor suppressor. Cancer Cell 2007; 11:25-36.
8. Basto R, Brunk K, Vinadogrova T, Peel N, Franz A, Khodjakov A, et al. Centrosome amplification can initiate tumorigenesis in flies. Cell 2008; 133:1032-42.
9. Castellanos E, Dominguez P, Gonzalez C. Centrosome dysfunction in Drosophila neural stem cells causes tumors that are not due to genome instability. Curr Biol 2008; 18:1209-14.
10. Klonisch T, Wiechec E, Hombach-Klonisch S, Ande SR, Wesselborg S, Schulze-Osthoff K, et al. Cancer stem cell markers in common cancers: Therapeutic implications. Trends Mol Med 2008; 14:450-60.
11. Zyss D, Gergely F. Centrosome function in cancer: guilty or innocent? Trends Cell Biol 2009; 19:334-46.
12. Gergely F. Centrosomal TACCtics. Bioessays 2002; 24:915-25.
13. Peset I, Vernos I. The TACC proteins: TACC-ling microtubule dynamics and centrosome function. Trends Cell Biol 2008; 18:379-88.
14. Gomez-Baldo L, Schmidt S, Maxwell CA, Bonifaci N, Gabaldon T, Vidalain PO, et al. TACC3-TSC2 maintains nuclear envelope structure and controls cell division. Cell Cycle 2010; 9:1143-55.
15. Samereier M, Baumann O, Meyer I, Graf R. Analysis of Dictyostelium TACC reveals differential interactions with CP224 and unusual dynamics of Dictyostelium microtubules. Cell Mol Life Sci 2010; 68:275-87.
16. Still IH, Vettaikkorumakankauv AK, DiMatteo A, Liang P. Structure-function evolution of the transforming acidic coiled coil genes revealed by analysis of phylogenetically diverse organisms. BMC Evol Biol 2004; 4:16.
17. Cassimeris L, Morabito J. TOGp, the human homolog of XMAP215/Dis1, is required for centrosome integrity, spindle pole organization and bipolar spindle assembly. Mol Biol Cell 2004; 15:1580-90.
18. Gergely F, Draviam VM, Raff JW. The ch-TOG/XMAP215 protein is essential for spindle pole organization in human somatic cells. Genes Dev 2003; 17:336-41.
19. Schneider L, Essmann F, Kletke A, Rio P, Hanenberg H, Wetzel W, et al. The transforming acidic coiled coil 3 protein is essential for spindle-dependent chromosome alignment and mitotic survival. J Biol Chem 2007; 282:29273-83.
20. Yao R, Natsume Y, Noda T. TACC3 is required for the proper mitosis of sclerotome mesenchymal cells during formation of the axial skeleton. Cancer Sci 2007; 98:555-62.
21. Hubner NC, Bird AW, Cox J, Splettstoesser B, Bandilla P, Poser I, et al. Quantitative proteomics combined with BAC TransgeneOmics reveals in vivo protein interactions. J Cell Biol 189:739-54.

22. Kinoshita K, Noetzel TL, Pelletier L, Mechtler K, Drechsel DN, Schwager A, et al. Aurora A phosphorylation of TACC3/maskin is required for centrosome-dependent microtubule assembly in mitosis. J Cell Biol 2005; 170:1047-55.

23. LeRoy PJ, Hunter JJ, Hoar KM, Burke KE, Shinde V, Ruan J, et al. Localization of human TACC3 to mitotic spindles is mediated by phosphorylation on Ser558 by Aurora A: a novel pharmacodynamic method for measuring Aurora A activity. Cancer Res 2007; 67:5362-70.

24. Lin CH, Hu CK, Shih HM. Clathrin heavy chain mediates TACC3 targeting to mitotic spindles to ensure spindle stability. J Cell Biol 189:1097-105.

25. Piekorz RP, Hoffmeyer A, Duntsch CD, McKay C, Nakajima H, Sexl V, et al. The centrosomal protein TACC3 is essential for hematopoietic stem cell function and genetically interfaces with p53-regulated apoptosis. EMBO J 2002; 21:653-64.

26. Still IH, Hamilton M, Vince P, Wolfman A, Cowell JK. Cloning of TACC1, an embryonically expressed, potentially transforming coiled coil containing gene, from the 8p11 breast cancer amplicon. Oncogene 1999; 18:4032-8.

27. Still IH, Vince P, Cowell JK. The third member of the transforming acidic coiled coil-containing gene family, TACC3, maps in 4p16, close to translocation breakpoints in multiple myeloma, and is upregulated in various cancer cell lines. Genomics 1999; 58:165-70.

28. Cully M, Shiu J, Piekorz RP, Muller WJ, Done SJ, Mak TW. Transforming acidic coiled coil 1 promotes transformation and mammary tumorigenesis. Cancer Res 2005; 65:10363-70.

29. Jung CK, Jung JH, Park GS, Lee A, Kang CS, Lee KY. Expression of transforming acidic coiled-coil containing protein 3 is a novel independent prognostic marker in non-small cell lung cancer. Pathol Int 2006; 56:503-9.

30. Kiemeney LA, Sulem P, Besenbacher S, Vermeulen SH, Sigurdsson A, Thorleifsson G, et al. A sequence variant at 4p16.3 confers susceptibility to urinary bladder cancer. Nat Genet 2010; 42:415-9.

31. Lauffart B, Vaughan MM, Eddy R, Chervinsky D, DiCioccio RA, Black JD, et al. Aberrations of TACC1 and TACC3 are associated with ovarian cancer. BMC Womens Health 2005; 5:8.

32. Duncan CG, Killela PJ, Payne CA, Lampson B, Chen WC, et al. Integrated genomic analyses identify ERRFl1 and TACC3 as glioblastoma-targeted genes. Oncotarget 2010; 1:265-77.

33. Hayflick L, Moorhead PS. The serial cultivation of human diploid cell strains. Exp Cell Res 1961; 25:585-621.

34. Campisi J, d'Adda di Fagagna F. Cellular senescence: when bad things happen to good cells. Nat Rev Mol Cell Biol 2007; 8:729-40.

35. Ben-Porath I, Weinberg RA. The signals and pathways activating cellular senescence. Int J Biochem Cell Biol 2005; 37:961-76.

36. Collado M, Serrano M. The power and the promise of oncogene-induced senescence markers. Nat Rev Cancer 2006; 6:472-6.

37. Chuaire-Noack L, et al. The dual role of senescence in tumorigenesis. Int J Morphol 2010; 28:37-50.

38. Demidenko ZN, Blagosklonny MV. Growth stimulation leads to cellular senescence when the cell cycle is blocked. Cell Cycle 2008; 7:3355-61.

39. Demidenko ZN, Zubova SG, Bukreeva EI, Pospelov VA, Pospelova TV, Blagosklonny MV. Rapamycin decelerates cellular senescence. Cell Cycle 2009; 8:1888-95.

40. Korotchkina LG, Leontieva OV, Bukreeva EI, Demidenko ZN, Gudkov AV, Blagosklonny MV. The choice between p53-induced senescence and quiescence is determined in part by the mTOR pathway. Aging (Albany NY) 2:344-52.

41. Demidenko ZN, Korotchkina LG, Gudkov AV, Blagosklonny MV. Paradoxical suppression of cellular senescence by p53. Proc Natl Acad Sci USA 107:9660-4.

42. Blagosklonny MV. Prolonged mitosis versus tetraploid checkpoint: how p53 measures the duration of mitosis. Cell Cycle 2006; 5:971-5.

43. Schneider L, Essmann F, Kletke A, Rio P, Hanenberg H, Schulze-Osthoff K, et al. TACC3 depletion sensitizes to paclitaxel-induced cell death and overrides p21(WAF)-mediated cell cycle arrest. Oncogene 2008; 27:116-25.

44. Schmidt S, Schneider L, Essmann F, Cirstea IC, Kuck F, Kletke A, et al. The centrosomal protein TACC3 controls paclitaxel sensitivity by modulating a premature senescence program. Oncogene 2010; 29:6184-92; DOI:10.1038/onc.2010.354.

45. Huck JJ, Zhang M, McDonald A, Bowman D, Hoar KM, Stringer B, et al. MLN8054, an inhibitor of Aurora A kinase, induces senescence in human tumor cells both in vitro and in vivo. Mol Cancer Res 2010; 8:373-84.

46. Katayama H, Sasai K, Kawai H, Yuan ZM, Bondaruk J, Suzuki F, et al. Phosphorylation by aurora kinase A induces Mdm2-mediated destabilization and inhibition of p53. Nat Genet 2004; 36:55-62.

47. Dominguez-Brauer C, Brauer PM, Chen YJ, Pimkina J, Raychaudhuri P. Tumor suppression by ARF: Gatekeeper and caretaker. Cell Cycle 9:86-9.

48. Tritarelli A, Oricchio E, Ciciarello M, Mangiacasale R, Palena A, Lavia P, et al. p53 localization at centrosomes during mitosis and postmitotic checkpoint are ATM-dependent and require serine 15 phosphorylation. Mol Biol Cell 2004; 15:3751-7.

49. Vogel C, Kienitz A, Hofmann I, Muller R, Bastians H. Crosstalk of the mitotic spindle assembly checkpoint with p53 to prevent polyploidy. Oncogene 2004; 23:6845-53.

50. Gjoerup OV, Wu J, Chandler-Militello D, Williams GL, Zhao J, Schaffhausen B, et al. Surveillance mechanism linking Bub1 loss to the p53 pathway. Proc Natl Acad Sci USA 2007; 104:8334-9.

51. Maehara K, Takahashi K, Saitoh S. CENP-A reduction induces a p53-dependent cellular senescence response to protect cells from executing defective mitoses. Mol Cell Biol 2010; 30:2090-104.

52. Baker DJ, Jeganathan KB, Cameron JD, Thompson M, Juneja S, Kopecka A, et al. BubR1 insufficiency causes early onset of aging-associated phenotypes and infertility in mice. Nat Genet 2004; 36:744-9.

53. Baker DJ, Jeganathan KB, Malureanu L, Perez-Terzic C, Terzic A, van Deursen JM. Early aging-associated phenotypes in Bub3/Rae1 haploinsufficient mice. J Cell Biol 2006; 172:529-40.

54. Baker DJ, Chen J, van Deursen JM. The mitotic checkpoint in cancer and aging: What have mice taught us? Curr Opin Cell Biol 2005; 17:583-9.

55. Campisi J, Sedivy J. How does proliferative homeostasis change with age? What causes it and how does it contribute to aging? J Gerontol A Biol Sci Med Sci 2009; 64:164-6.

56. Jeyapalan JC, Ferreira M, Sedivy JM, Herbig U. Accumulation of senescent cells in mitotic tissue of aging primates. Mech Ageing Dev 2007; 128:36-44.

57. Yang D, McCrann DJ, Nguyen H, St. Hilaire C, DePinho RA, Jones MR, et al. Increased polyploidy in aortic vascular smooth muscle cells during aging is marked by cellular senescence. Aging Cell 2007; 6:257-60.

58. Görgün G, Calabrese E, Hideshima T, Ecsedy J, Perrone G, Mani M, et al. A novel Aurora-A kinase inhibitor MLN8237 induces cytotoxicity and cell cycle arrest in multiple myeloma. Blood 2010; 115:5202-13.

59. Prencipe M, Fitzpatrick P, Gorman S, Tosetto M, Klinger R, Furlong F, et al. Cellular senescence induced by aberrant MAD2 levels impacts on paclitaxel responsiveness in vitro. Br J Cancer 2009; 101:1900-8.

60. Yun M, Han YH, Yoon SH, Kim HY, Kim BY, Ju YJ, et al. p31comet Induces cellular senescence through p21 accumulation and Mad2 disruption. Mol Cancer Res 2009; 7:371-82.

61. Mikule K, Delaval B, Kaldis P, Jurcyzk A, Hergert P, Doxsey S. Loss of centrosome integrity induces p38-p53-p21-dependent G_1-S arrest. Nat Cell Biol 2007; 9:160-70.

62. Srsen V, Gnadt N, Dammermann A, Merdes A. Inhibition of centrosome protein assembly leads to p53-dependent exit from the cell cycle. J Cell Biol 2006; 174:625-30.

cell death (**Fig. 1**). This was remarkably different from the cellular pathways mediated by ATP or nigericin, which triggered significant IL-1β release, caspase-1-dependent pyroptosis and no protein degradation. Importantly, in cells treated with ATP or nigericin, lysosome rupture occurred only after caspase-1 activation and induction of pyroptosis, suggesting that lysosome dysfunction is not required for inflammasome activation. Based on these results, the authors conclude that upstream signals, such as potassium efflux, are likely more effective stress signals for NLRP3 activation than lysosome disruption. Taken together, their findings confirm that complete lysosome rupture is a catastrophic event leading to necrotic cell death; this cell death is independent of NLRP3 signaling and distinct from pyroptosis triggered by inflammasome-inducers, and can therefore explain the different immune response associated with these compounds. These observations complement another recent article published by the same group, where the authors showed that alum and LLOMe trigger cathepsin-mediated, caspase-1 and RIP-1-independent necrosis that is essential for their function as immunologic adjuvants.[5] Together these papers provide insight into the mechanism by which the cell death phenotype of lysosome-disrupting agents contributes to the unique immunologic response generated by these compounds when used as adjuvants. More broadly, these studies provide strong proof for a danger theory of adjuvancy suggesting that our immune system has evolved to respond to agents that trigger cytotoxic events.

References
1. Guicciardi ME, et al. Oncogene 2004; 23:2881-90; PMID:15077151; http://dx.doi.org/10.1038/sj.onc.1207512
2. Repnik U, et al. Biochim Biophys Acta 2012; 1824:22-33; PMID:21914490; http://dx.doi.org/10.1016/j.bbapap.2011.08.016
3. Brennan MA, et al. Mol Microbiol 2000; 38:31-40; PMID:11029688; http://dx.doi.org/10.1046/j.1365-2958.2000.02103.x
4. Lima H Jr., et al. Cell Cycle 2013; 12; PMID:23708522
5. Jacobson LS, et al. J Biol Chem 2013; 288:7481-91; PMID:23297415; http://dx.doi.org/10.1074/jbc.M112.400655
6. Bruchard M, et al. Nat Med 2013; 19:57-64; PMID:23202296; http://dx.doi.org/10.1038/nm.2999

Senescence-associated lysosomal α-L-fucosidase (SA-α-Fuc): A sensitive and more robust biomarker for cellular senescence beyond SA-β-Gal

Comment on: Hildebrand DG, et al. Cell Cycle 2013; 12:1922–7; PMID:23673343; http://dx.doi.org/10.4161/cc.24944

Madhurendra Singh and Roland P. Piekorz*; Institut für Biochemie und Molekularbiologie II; Universitätsklinikum der Heinrich-Heine-Universität Düsseldorf; Düsseldorf, Germany; *Email: Roland.Piekorz@uni-duesseldorf.de; http://dx.doi.org/10.4161/cc.25318

Discovery and Origin of Cellular Senescence
Classical work by Hayflick and Moorhead[1] uncovered more than 50 y ago the biological and evolutionarily conserved phenomenon of cellular senescence. The authors demonstrated that primary fibroblasts exhibit only a finite proliferative capacity in culture, before they exit the cell cycle in a state known as replicative senescence ("Hayflick phenomenon").[1] This type of senescence is caused by progressive telomeric erosion associated with the accumulation of DNA damage. Alternatively, several stress factors, including hypermitogenic stimuli like oncogenic Ras, reactive oxygen species and cytotoxic drugs that cause DNA damage, as well as mitotic spindle dysfunction and aneuploidy can trigger an accelerated antiproliferative response, known as stress-induced, premature senescence (SIPS).[2]

(Patho)biological Role of Senescence
Senescence comes along as a (patho)biologically relevant, but two-edged, cellular stress response. On one hand, a protective and tumor-suppressive role of cellular senescence has been demonstrated at the pre-malignant level.[3] On the other hand, senescence exhibits detrimental effects at the cellular and organ level, including proliferative exhaustion of progenitor and stem cells or promotion of inflammatory processes linked to the so-called senescence-associated secretory phenotype (SASP) (**Fig. 1**).[4] Interestingly, elimination of accumulating senescent cells in vivo in the mouse effectively delays aging-associated disorders, thereby corroborating the causative link between cellular senescence and tissue dysfunction in age-related phenotypes.[5] Thus, cellular senescence seems to be ultimately connected to health and lifespan regulation during organismal aging.

Characteristics and Markers of Senescent Cells
In order to detect senescent cells in culture, and clearly more challenging under in vivo and in situ conditions, several markers with varying robustness are being used beyond the typical flattened cellular morphology and increased cell surface (**Fig. 1**). Overall, proliferative arrest, apoptosis resistance and altered gene expression and miRNA profiles (**Fig. 1**) represent general features of senescent cells.[2] At the nuclear architecture level, formation of DNA-SCARS (DNA segments with chromatin alterations reinforcing senescence) and senescence-associated heterochromatic foci (SAHF)[4] mirror the repression of proliferative genes and therefore the lack of DNA synthesis as detected by a lack of BrdU incorporation and G_1 arrest. At the molecular checkpoint level, the p53-p21[WAF1] pathway and the tumor suppressor p16INK4a, as well as rapamycin-sensitive mTOR (mammalian Target of Rapamycin) signaling take over synergistic roles in the induction and maintenance of the senescent phenotype (**Fig. 1**).[2,6] Lastly, at the biochemical and enzymatic level, a considerable expansion of the lysosomal compartment and, hence, increased granularity is typically observed in cells undergoing senescence. That is demonstrated by an increased senescence-associated β-galactosidase activity (SA-β-Gal; measured at pH 6), the classical marker that is widely used to detect senescent cells.[7]

**Senescence-Associated Lysosomal α-L-Fucosidase (SA-α-Fuc): A new and Robust Senescence Marker**
Several of the markers described above may work in a cell type- and senescence stimulus-dependent manner and are therefore not always reliable. For example, p16[INK4a] increases during replicative aging. However, p16[INK4a] is either not expressed or inactivated in certain tumor cells, which, however, are still prone to SIPS due to an intact p53 pathway.

Moreover, solely determining SA-β-Gal activity can potentially result in both wrong positive results (increased SA-β-Gal activity due to hyper-dense cell cultures), or wrong negative results, where SA-β-Gal is not or only weakly induced and therefore not sensitively enough detected upon cellular senescence. Taking in particular the latter observation into account, Hildebrand et al. investigated comprehensively several lysosomal hydrolases, besides SA-β-Gal, for their suitability as senescence markers.[8] Interestingly, the authors identified α-L-fucosidase, a glycosidase involved in the metabolism of certain glycolipids and glycoproteins, as a novel and promising biomarker for cellular senescence. Hildebrand et al. tested senescence-associated α-fucosidase activity (SA-α-Fuc) in various senescence models in cell culture, including replicative and oncogene-induced senescence, as well as SIPS. Unequivocally, both at the transcriptional and the enzymatic level SA-α-Fuc turned out as an at least equivalent, and in most cases an even more reliable, marker for the detection of cellular senescence as compared with SA-β-Gal.

Taken together, SA-α-Fuc represents a convenient, sensitive and robust senescence marker in cell culture experiments employing both rodent and human senescence models. Further characterization of SA-α-Fuc expression and activity under stringent in vivo and in situ settings could include the detection of rather sparsely occurring senescent cells at the cancer stem and progenitor level, as well as the analysis of senescent cells during tissue aging.
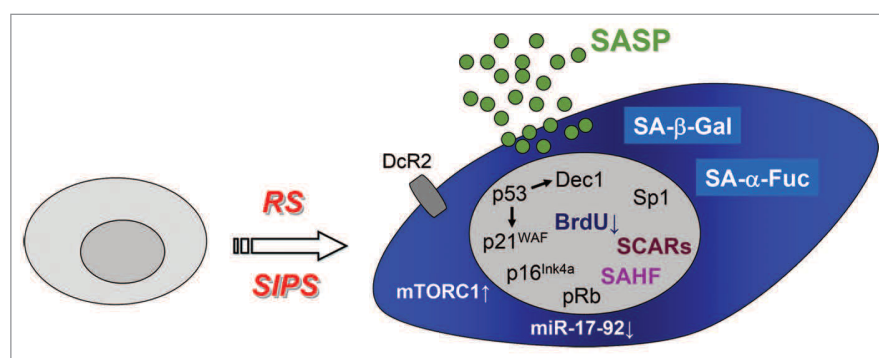
Figure 1. Characteristic features of senescent cells. Cells undergoing replicative senescence (RS) or stress-induced premature senescence (SIPS) are distinguished by an enlarged and flattened morphology and several molecular and subcellular changes, including activation of tumor suppressor pathways (p53-p21^{WAF}, p53-Dec1, p16^{Ink4a}), chromatin alterations (DNA-SCARS, DNA segments with chromatin alterations reinforcing senescence; SAHF, senescence-associated heterochromatic foci) and activation of certain transcription factors (Sp1) as well as production of secreted factors (SASP, senescence-associated secretory phenotype). Moreover, cell surface expression of decoy receptor 2 (DcR2) typically increases during senescence. Lastly, the lysosomal compartment expands considerably in cells undergoing cellular senescence. Here, as demonstrated by Hildebrand et al.,[8] the classical and widely used senescence-associated β-galactosidase activity (SA-β-Gal)[7] is now joined by a novel and more robust lysosomal (bio)marker for cellular senescence, SA-α-Fuc (senescence-associated α-fucosidase activity).

References
1. Hayflick L, et al. Exp Cell Res 1961; 25:585-621; PMID:13905658; http://dx.doi.org/10.1016/0014-4827(61)90192-6
2. Collado M, et al. Nat Rev Cancer 2006; 6:472-6; PMID:16723993; http://dx.doi.org/10.1038/nrc1884
3. Kang TW, et al. Nature 2011; 479:547-51; PMID:22080947; http://dx.doi.org/10.1038/nature10599
4. Rodier F, et al. J Cell Biol 2011; 192:547-56; PMID:21321098; http://dx.doi.org/10.1083/jcb.201009094
5. Baker DJ, et al. Nature 2011; 479:232-6; PMID:22048312; http://dx.doi.org/10.1038/nature10600
6. Demidenko ZN, et al. Cell Cycle 2009; 8:1888-95; PMID:19471117; http://dx.doi.org/10.4161/cc.8.12.8606
7. Dimri GP, et al. Proc Natl Acad Sci USA 1995; 92:9363-7; PMID:7568133; http://dx.doi.org/10.1073/pnas.92.20.9363
8. Hildebrand DG, et al. Cell Cycle 2013; 12: In press; PMID:23673343.v

INK4a/ARF-dependent senescence upon persistent replication stress

Comment on: Monasor A, et al. Cell Cycle 2013; 12: In press; PMID:23676215

Mark O'Driscoll; Human DNA Damage Response Disorders Group; Genome Damage & Stability Centre; University of Sussex; Brighton, UK; Email: m.o-driscoll@sussex.ac.uk; http://dx.doi.org/10.4161/cc.25319

One outcome of persistent activation of the DNA damage response (DDR) is cellular senescence; a programmed, permanent, cell cycle exit. DDR activation serves as a block to malignant transformation with senescence as a core feature of this effect. Diverse conditions that induce senescence, for example ionizing radiation, oncogene activation and telomere attrition, themselves induce DDR activation. In virtually all of these instances, senescence can be rescued by ablation of p53 function, thereby allowing the cells to re-enter the cell cycle in the presence of DNA damage. In this issue, Monasor and colleagues provide new evidence suggesting that the well-known tumor suppressor INK4a/ARF enables replicative stress (RS)-induced senescence.[1] This is notable, since, in contrast to p53, INK4a/ARF has generally been thought not to play a role in DNA damage-induced senescence. Loss of the *INK4a/ARF* locus on chromosome 9p21 is one of the most frequent abnormalities observed in human tumors, second only to loss and/or mutation of *TP53* (p53). The *INK4a/ARF* locus encodes two proteins, p16(INK4a) and ARF (p16^{Ink4A} and p19^{ARF} in mice), which regulate the Retinoblastoma and p53 pathways respectively.[2] In normal cells, INK4a/ARF levels are usually barely detectable. Monasor and colleagues report that persistent RS is also associated with elevated INK4a/ARF expression, and that INK4a/ARF deficient cells can sustain growth in the presence of substantial levels of RS. Furthermore, upon interrogation of the Cancer Cell Line Encyclopaedia Project (http://www.broadinstitute.org/ccle/home), they found a correlation between copy number variation (CNV) and p16^{INK4A} levels; cell lines with high levels of CNVs (RS has been shown to cause CNV[3]) exhibited low levels of p16^{INK4A}. The authors consequently propose INK4a/ARF as a bona fide RS-checkpoint activator.[1]